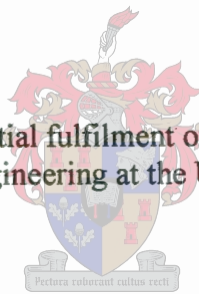# MODELLING OF DRAGLINE DYNAMICS

Pieter Gobregts Crous

Thesis project presented in partial fulfilment of the requirements for the degree
Master of Science in Engineering at the University of Stellenbosch.

Thesis Supervisor: Mr. D.N.J. Els

Department of Mechanical Engineering

March 2000

DECLARATION

I the undersigned hereby declare that the work contained in this thesis project is my own original work and has not previously in its entirety or in part been submitted at any university for a degree.

Signature: Date:

ABSTRACT

The utilisation of Draglines to remove overburden in surface mining operations is often the process that determines the output of these operations. The bucket and its rigging have been identified as important components where design changes can improve the efficiency of the dragline. It is necessary to create a method to predict the dynamic behaviour of the bucket when various design changes are made to the rigging and the bucket. A rigid multibody dynamic method is formulated that can be used to predict the behaviour of any physical system that can be modelled as a set of connected rigid bodies. This multibody method is verified with analytic test problems and an experiment. A description is given how to use this rigid multibody dynamic method to model the dragline and predict the behaviour of the bucket during an operational cycle.

OPSOMMING

Sleepgrawe word gebruik in oppervlakmynbouaktiwiteite om die mineraal neerslae wat ontgin word te ontbloot. Hierdie proses bepaal baie keer die produksie van die mynbou aktiwiteit. Die sleepgraaf se bak en die takelwerk van die bak het 'n groot invloed op die sleepgraaf se werksverrigting. Om die bak se werksverrigting te verbeter is 'n metode nodig om die dinamiese gedrag van die bak te voorspel. In hierdie dokument word 'n metode beskryf waarmee die dinamiese gedrag van enige stelsel bepaal kan word, wat as 'n stelsel van onderling-verbinde onbuigbare liggame beskryf kan word. Die korrektheid van hierdie metode is getoets met behulp van analitiese sowel as eksperimentele metodes. Daar word ook 'n beskrywing gegee hoe hierdie metode gebruik kan word om die beweging van die bak tydens 'n tipiese werksiklus te voorspel.

TABLE OF CONTENTS

LIST OF FIGURES

NOMENCLATURE

The mathematical notation used in this document is based on the Matrix Tensor Notation proposed by Hassenpflug (1993, 1995). A description of the notation is given in Appendix A.

Tensors and Vectors

$\overline{\overline{\mathbf{A}}}$ Second order tensor

$\overline{\mathbf{A}}$ Initial value of set of differential equations

$\overline{\mathbf{a}}$ Vector pointing from the centre of mass of a body to the position of a connecting joint with an outboard body.

a Component of second order tensor

$\overline{\overline{\mathbf{C_q}}}$ Jacobian matrix of constraint equations

$\overline{\overline{\mathbf{C}}}$ Vector of constraint equations

$\overline{\mathbf{d}}$ Vector pointing from a body's centre of mass to the position of the connecting joint with the inboard body.

$\vec{\overline{\mathbf{E}}}$ Cartesian base

$\overline{\overline{\mathbf{E}}}$ Transformation matrix

$\overline{\mathbf{e}}$ Base vector

$\overline{\mathbf{F}}$ Force vector

$\overline{\mathbf{f}}$ Force vector, Vector of functions, Right hand side vector of the governing equation.

$\overline{\overline{\mathbf{Fa}}}$ Applied Force

$\overline{\mathbf{Fe}}$ Force vector of a force element

$Fe = \left\| \overline{\mathbf{Fe}} \right\|$	Force exerted by a force element
$\overline{\mathbf{Fi}}$	Inertial Force
$\underline{\overline{\mathbf{G}}}$	Transformation Matrix between first time derivative of orientation coordinates and angular velocity vector
$\overline{\mathbf{g}}$	Gravitational acceleration vector
$g = \left\| \overline{\mathbf{g}} \right\|$	Gravitational acceleration
$\underline{\overline{\mathbf{H}}}$	Jacobian matrix of a spherical joint of a body.
$\overline{\mathbf{h}}$	Angular momentum vector, Vector of Coriolis and centripetal acceleration in governing dynamic equation.
$\underline{\overline{\mathbf{I}}}$	Identity matrix
$\underline{\overline{\mathbf{J}}}$	Inertial matrix
J	Element of inertial matrix
$\overline{\mathbf{k}}$	Vector of numeric result of differential equations at different time values
$\underline{\overline{\mathbf{M}}}$	Mass matrix of system
$\overline{\mathbf{N}}$	Moment vector of a force
$\overline{\mathbf{n}}$	Unit vector
$\overline{\mathbf{Na}}$	Applied Moment
$\overline{\mathbf{Ni}}$	Inertial moment
$\overline{\mathbf{p}}$	Linear momentum vector, Position vector of a point in a rigid body, Vector along joint axis of a revolute joint.
$\overline{\mathbf{Q}}$	Generalised force vector
$\overline{\mathbf{q}}$	Generalised coordinate vector
$\overline{\mathbf{Qa}}$	Generalised applied force vector
$\overline{\mathbf{Qc}}$	Generalised constraint force vector
$\overline{\mathbf{Qd}}$	Vector of first generalised coordinate derivatives
$\overline{\mathbf{Qi}}$	Generalised inertial force vector
$\underline{\overline{\mathbf{R}}}$	Rotation tensor

$\overline{\mathbf{R}}$	Position vector of particle system's centre of mass.
$\overline{\mathbf{r}}$	Position vector of a the centre of mass of a particle/body
$\overline{\mathbf{s}}$	Unit vector
$\overline{\mathbf{t}}$	Unit vector
$\overline{\mathbf{u}}$	Position vector of a point in a rigid body, Eigenvector
$\underline{\overline{\mathbf{V}}}$	Partial velocity array
$\overline{\mathbf{v}}$	Cartesian vector, velocity vector
$v = \left\| \overline{\mathbf{v}} \right\|$	Velocity
$\overline{\mathbf{v}}_t$	Cartesian vector
$\overline{\mathbf{x}}$	Coordinate vector
$\overline{\mathbf{y}}$	Vector of generalised speeds
$\overline{\mathbf{z}}$	State vector
$\overline{\varepsilon}$	Vector of Euler parameters
ε	Euler parameter
$\underline{\overline{\Gamma}}$	Second order tensor
$\overline{\lambda}$	Vector of Lagrange multipliers
λ	Element of the vector of Lagrange multipliers
$\overline{\theta}$	Orientation Coordinate vector
$\overline{\rho}$	Position vector
$\overline{\rho}$	Relative joint displacement vector
$\underline{\overline{\Omega}}$	Skew symmetric matrix of the components of the angular velocity vector
$\overline{\omega}$	Angular Velocity vector
$\omega = \left\| \overline{\omega} \right\|$	Angular velocity
$\overline{\xi}$	Relative displacement vector
$\xi = \left\| \overline{\xi} \right\|$	Relative displacement

Scalars

a	Components of second order tensor, Lower boundary of time interval
b	Higher boundary of time interval
c	Viscous Damping constant (N m^{-1} s)
E	Modulus of Elastisity (Pa)
e	coefficient of restitution
f	Function
h	Integration step size
J	Moment of inertia (kg m^2)
k	Spring stiffness (N/m)
l	Length (m)
M	Total mass of system (kg)
m	Mass of particle/body (kg)
n	Counter
r	Root of characteristic polynomial
T	Kinetic Energy (J)
t	Time (seconds)
V	Potential energy (J)
W	Work (J)
Wa	Work of applied forces (J)
Wc	Work of constraint forces (J).
Wi	Work of inertial forces (J)
α	Angle
Δ	Difference
δ	Virtual difference
δ	Kronecker delta

γ	Shear-damping constant
ϑ	Local rounding error
ϕ	Angle of rotation
λ	Eigenvalue
μ	Friction Coefficient
θ	Angle
ρ	Pulley radius (m)
υ	Poison ratio
Ψ	Hertz contact constant

Subscripts and Superscripts

av	Average
b	Name of Cartesian Base
C	Centre of mass
d	Dynamic
dep	Dependent coordinates
f	Final condition
i	Index of matrix or vector, Body/Particle number, Initial condition
in	Independent coordinates
j	Index of matrix or vector, Body/Particle number
k	Index of matrix or vector, Body/Particle number
l	Index of matrix or vector, Body/Particle number
n	Normal to surface
O	Origin of coordinate system
s	Static, Shear
s	Name of Cartesian Base

r Name of Cartesian Base

Mathematical Symbols

T Transpose of matrix/vector

$\cdot$ First time derivative of component

$\cdot\cdot$ Second time derivative of component

$\rightarrow$ Physical vector

$\bar{\ }$ Column vector

          Row vector

$\doubleunderline{\ }$ Matrix

$\simeq$ Skew symmetric matrix of the vector

$()$ Body index

CHAPTER 1

INTRODUCTION

Surface mining is the most economical method of unearthing mineral deposits close to the earth's surface. The costliest stage of this type of mining operation is the process of removing the waste rock (overburden). Increasing the effectiveness of this process will increase the economic viability of the mining operation as a whole. Many types of large earthmoving machinery and auxiliary equipment have been developed. Each of these systems has its advantages and disadvantages. The optimum equipment selection for each mining operation is different.

Different machines are used for the removal of the overburden and the removal of the mineral deposits. Machines normally used for overburden removal are: draglines, bucket wheel excavators and shovel/truck systems (Van Leyen, 1991). Overburden removal includes an excavation process and a transportation process. Most systems use separate specialised machines for the excavation and the transportation, but with draglines the whole process is done in a single operation. This is one of the biggest advantages of the use of draglines in surface mining.

Rowlands (1991) states that draglines existed since 1912. The bucket sizes of the first machines were less than 10 m^3. They were used in normal excavation operations. During the 1930s, they were employed in surface mining operations and the need to increase production arose. Building larger machines capable of handling larger buckets increased the excavation capacity. The largest machine built has a bucket capacity of 170 m^3. These increases in the size of the machines were however found to be uneconomical and other productivity improvements were initiated. The primary focus of studies is the design and utilisation of the machines (Rowlands, 1991).

Draglines are used in a variety of mining activities, from the removal of overburden in coal mining to unique applications such as phosphate mining in Florida (USA) and oil sand mining in Alberta (USA) (Golosinski, 1994). In South Africa, the majority of draglines are used in coal mining applications, but a unique application can be found in the mining of diamonds at Kleinzee. In the coal mining industry it is generally accepted that a 1% improvement in the efficiency of a dragline will result in a R1 million increase in the annual production of a dragline (Esterhuyse, 1997).

This project focuses on the creation of a dynamic model of the bucket of a dragline. This model is necessary for the optimisation of the rigging of the bucket and the design of new buckets. A multibody method with all the building blocks needed to create a multibody dynamic model of a dragline is formulated and a method to model a dragline is stated. It was unfortunately not possible to implement and verify this model on a full size dragline using the computer hardware that was available.

Figure 1.1 shows a dragline in a mining operation.
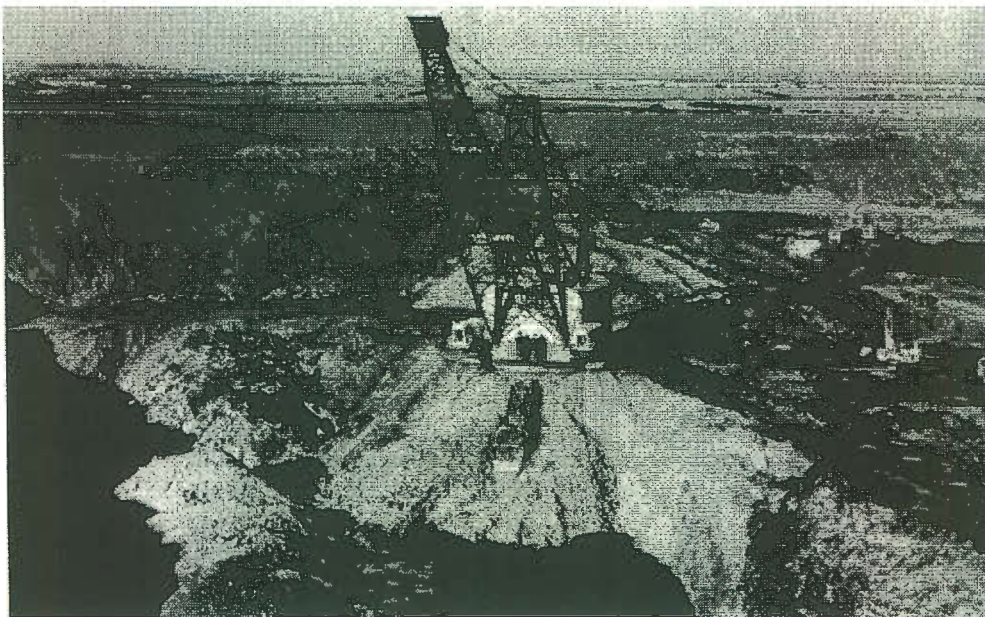
Figure 1.1 *A dragline in a mining operation.*

CHAPTER 2

DRAGLINES

A dragline is a machine similar to a crane, with the difference that an open mouth bucket is suspended beneath the boom. The bucket is used to excavate and carry material to a dumping location. The bucket is filled with material by dragging it over the ground towards the machine. When it is filled, it is hoisted from the ground and the machine is rotated. During this action, the bucket is positioned so that it can dump at the correct location.

Draglines are grouped into three classes determined by their method of propulsion (Shand, 1970):

(i) Truck mounted draglines

The machines in this group have the smallest capacity. The motorised chassis limits the size of the unit. Outriggers are fitted to the chassis to increase stability during side loading. This group has the highest mobility.

(ii) Crawler mounted

As implied by the name, these machines are mounted on crawler tracks. The long side tracks reduce bearing pressure and increase stability. These machines could work on surfaces too soft for wheel type machines.

(iii) Walking dragline

The machines in this group are physically the largest. The weight of the machine makes it impossible to mount on crawler tracks or wheels; it is mounted on a tub. The tub carries the weight of the machine over a large area. Because of this, the bearing pressure of the machine is very low for its size, enabling the machine to operate near the face of the excavation. Propulsion is with two gigantic

pads. These machines are usually powered by electricity. They are the largest mobile land based excavators used. Figure (2.1) shows a typical walking dragline.

The volume of material that must be removed in some surface mining activities could only be achieved by walking draglines, although crawler mounted draglines are also used (Adams, 1990, Rutten *et al.,* 1994). Any improvement in productivity would have a significant economical benefit.

Figure 2.1   *A typical walking dragline.*

2.1 Description

Walking draglines are large machines and can have a weight of between 3000 and 5000 tonnes. Figure 2.2 shows the components of a typical dragline.

The machine has a long, fixed boom, which extends from the machinery house. The boom is of a lattice construction. A support structure and support ropes hold the boom at a

constant angle to the horizontal. The support structure is also mounted to the machinery house. The boom is typically 100 meter long and makes an angle of approximately 38 degrees with the horizontal. The length and angle of the boom determine the width and depth of the mining pit. Increasing the boom length makes it possible to develop wider and deeper pits, which reduce the amount of rehandling (Rowlands, 1991). Unfortunately, a longer boom has disadvantages. It increases the rotating inertia of the machine, causing the need for more powerful swinging motors, and it requires more strength to counter the large bending and torsion stresses developed (Rowlands, 1991).
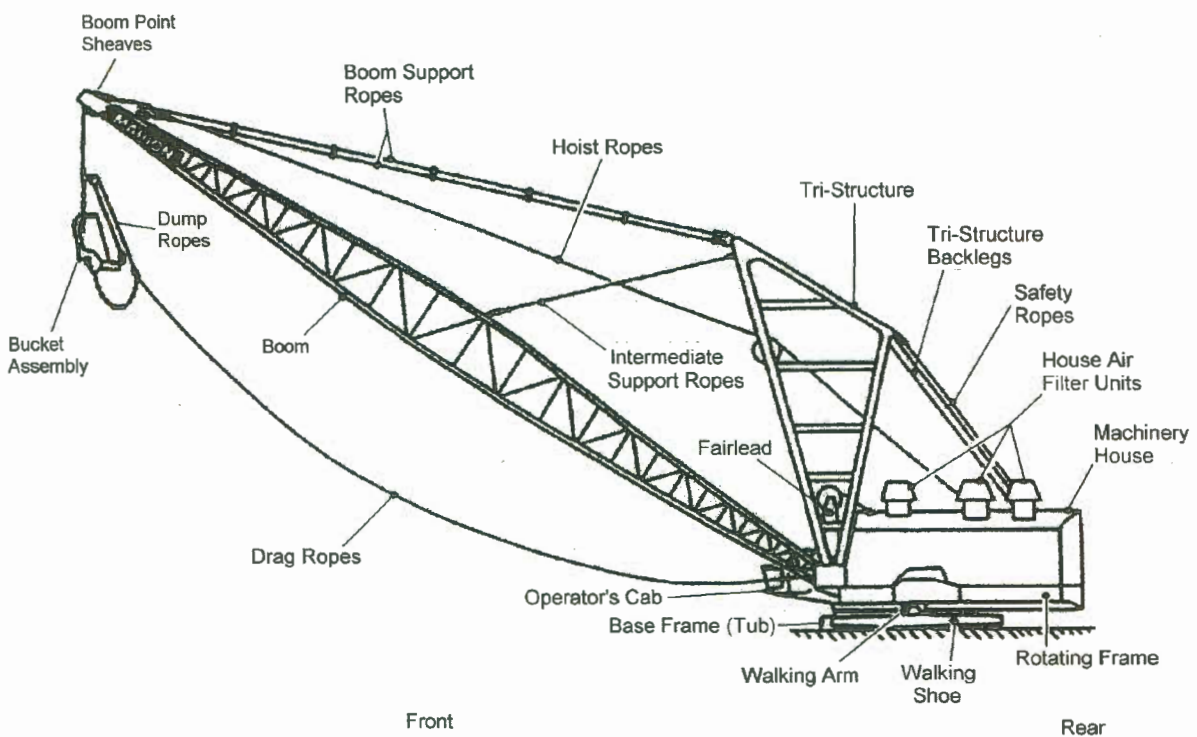
Figure 2.2   *The components of a dragline.*

An open-topped bucket is suspended beneath the boom by two sets of metal ropes, called the hoist and drag ropes. These ropes are connected to electric winches in the machinery house. The hoist rope runs over the boom point and is used to lift the bucket. The drag rope runs from the base of the boom and is used to pull the bucket towards the machine. The length of the hoist and drag ropes determines the position of the bucket. The attitude of the bucket is determined by the system of chains and cables called the rigging that connects the bucket to the hoist and drag ropes.

The machinery house houses the electric supplies system, the drag and hoist motors and winches, the swing motors and the propulsion mechanism.

Beneath the machinery house is a squat circular structure called the tub. This is the base of the machine and supports it during digging. Between the tub and machinery house is a bearing surface, which allows the machine to rotate about the centre of the tub. A large diameter ring gear is fixed to the tub and the machinery house is rotated by a number of pinions driven by motors in the machinery house.

The tub is dragged along the ground by means of large eccentrically driven walking shoes at each side of the machine.
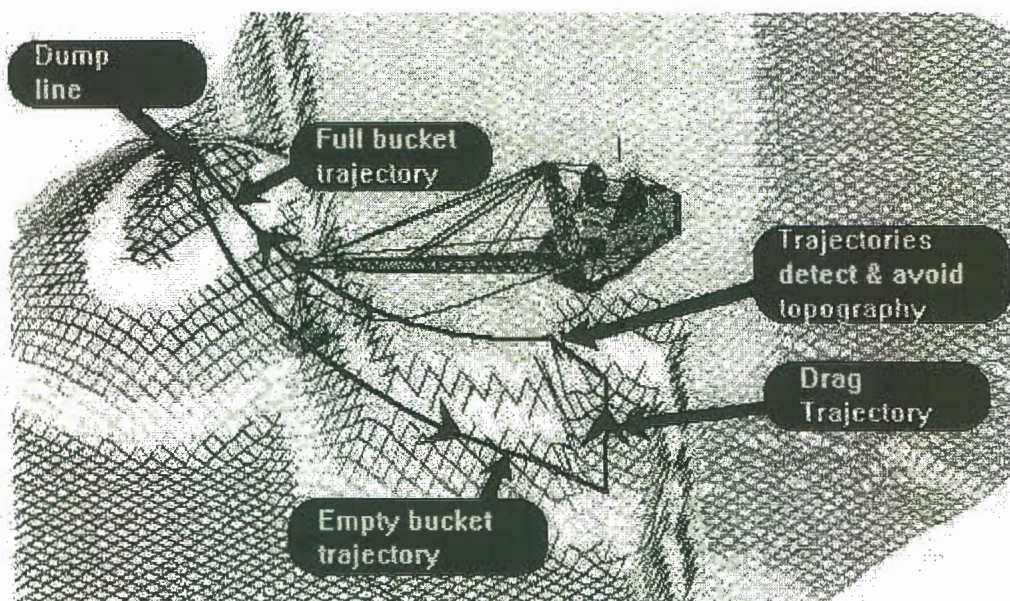
Figure 2.3   *The movement of the machine during an operation cycle.*

2.2 Operation cycle

The dragline cycle can be divided into the following steps (Rowlands, 1991):

(i) Bucket spotting

Position the bucket at the correct location to remove material.

(ii) Filling

When the bucket rests on the ground, the hoist cable is slackened slightly and tension is applied to the drag cable. This pulls the bucket towards the machine over the working face bank or drag slope. The front end of the bucket begins to dig into the ground and pile material into the bucket. A row of teeth on the front of the bucket assists with these processes. During this operation, the drag rope is subjected to the maximum tension force. Normally the dump rope is slack. If the bucket encounters very large resistive loads however, some tension to the hoist rope may be necessary to prevent the bucket from digging in. This tightens the dump rope, which lifts the front of the bucket and allows the digging to continue. A slight tension force must always be applied to the hoist rope to keep it tight. If the hoist rope becomes too slack, the hoist chains, the dump block and the spreader bar would slump into the bucket.
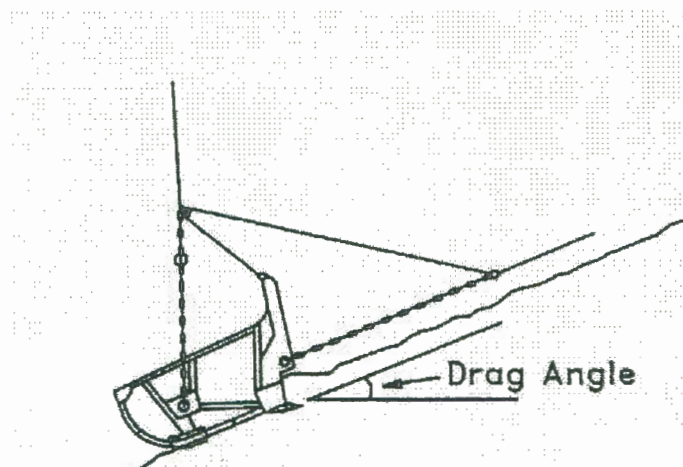
Figure 2.4   *The bucket during the filling operation.*

Stellenbosch University http://scholar.sun.ac.za

(iii) Disengage, hoist and swing

When the bucket is filled, tension is applied to the hoist rope and the bucket is lifted off the ground. This tightens the dump rope, which lifts the front of the bucket. The bucket assumes an angle, called the carry angle (Figure 2.5). This angle depends on the position of the bucket relative to the boom. The swing is started as soon as the bucket is off the ground. The bucket is moved to the dumping position by swinging, hoisting and paying out the dumping rope simultaneously. During the swing, the drag rope is paid out but not disengaged. The carry angle decreases as the drag rope is let out to position the bucket for dumping.
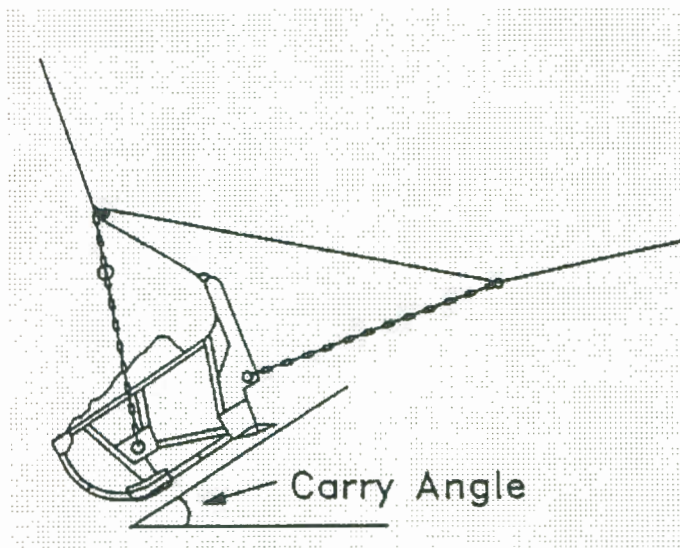
Figure 2.5   *The carry angle.*

(iv) Dumping

The content of the bucket is normally dumped beneath the boom point. As the spoiling position is approached, the drag ropes are released. This allows the dump rope to slack and causes the bucket to tip forward and dump its load. Dumping usually occurs over an arc and not at a distinct point. The length of the drag cable determines the position where the dumping will occur. A longer dump cable will cause the bucket to dump further away from the boom point.

(v) Return swing

While the bucket is dumping its content, the swing direction is reversed. This

allows for a smooth transition into the return swing. The hoist rope is lowered and the drag rope is pulled in to position the bucket for the next cycle.

2.3 Bucket Rigging

The rigging of a dragline bucket is critical to its performance. The rigging arrangement affects all the phases of the dragline cycle and has a major impact on productivity. It is most obvious once the bucket has disengaged from the bank after filling and has begun its swing. Normally material is lost during the disengaging and swinging operations. Figure 2.6 shows a typical rigging set-up.
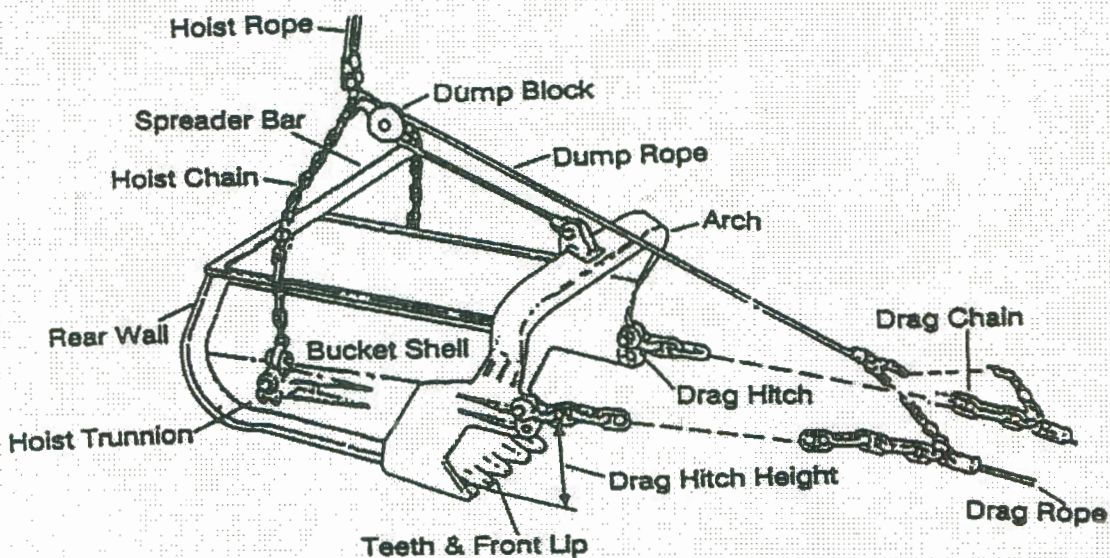
Figure 2.6   *A dragline bucket with a typical rigging set-up.*

Normally the balanced carry angle of the bucket is different from the drag angle. When the bucket disengages, a large quantity of material falls from the front of the bucket. This causes the centre of gravity of the filled bucket to move towards the rear. The carry angle increases and the remaining load is retained. If the initial carry angle could be increased, the material loss would be reduced.

During the swinging cycle, the bucket is hoisted and played out to a position beneath the boom point. After disengagement, the bucket's carry angle is fairly steep, but it flattens as the bucket moves further out along the boom. A steep carry angle has the tendency to spill material out of the rear of the bucket. A flat carry angle allows material to fall from the front of the bucket. If this change in carry angle could be reduced, the amount of material lost can be reduced and the overall efficiency improved.

The basic dragline bucket rigging consists of four different sections: the drag assembly, the dump assembly, the lower hoist assembly and the upper hoist assembly (Lumley and O'Beirne, 1997).

(i) Drag Assembly

Most draglines use two drag cables connected to each side of the bucket. During the filling cycle, the sections closest to the bucket can be dragged through the dirt. This causes significant wear to these sections. They are replaced with chains, which have a better resistance to the abrasive wear. The drag assembly includes all the components that transfer the drag force from the drag ropes to the bucket.

(ii) Lower hoist assembly

The lower hoist assembly extends from the hoist trunnion of the bucket to the spreader bar.

(iii) Upper hoist assembly

The upper hoist assembly forms the connection between the lower hoist assembly and the hoist rope. The spreader bar prevents contact between the bucket sides and the lower hoist chains. Without the bar, the lower hoist chains would continuously rub against the sides of the bucket.

(iv) Dump assembly

The dump assembly consists of the dump rope, the dump block and the dump chains. The dump rope is attached to the dump chains, runs over the dump block

and terminates at the centre of the bucket's arch. At the other side, the dump chains are connected to the connecting point of the drag rope and drag chain.

Of all the rigging components, the dump assembly has the biggest influence on the bucket's performance.

2.3.1 Influence of the rigging

Lumley and O'Beirne (1997) did a rigging study on several scale-size buckets and came to the following conclusions.

- The lengths of the dump rope, the drag chains, the hoist chains and the dump chains determine the carry angle and dumping performance of the bucket. Within reasonable limits, the lengths of the hoist chain and drag chain will not affect the productivity of the bucket to a high extend, provided that the bucket is set up at its optimum carry angle by changing the length of the dump rope. A long hoist assembly will lower the spoil height of the dragline.

- The position of the hoist trunnion, the position of the dump ropes anchor bracket on the arch, the position of the bucket's centre of mass and the position of the payload's centre of mass determine:

    1. The carry angle of the bucket.
    2. The dumping characteristics of the bucket.
    3. How easy it is to lift the bucket from the drag slope.

2.4   Mining Method and Mine Planning

Typical surface mining operations involve a variety of operations from the start of excavation to the end of the restoration process.

The mining operation starts with the removal of the topsoil and subsoil by motor scrapers. These soils are stored separately in baffle mounds at the site perimeter and will be used later in the restoration process. The baffle mounds form visual and environmental barriers.

When a sufficient amount of top- and subsoil has been removed, the initial box cut is started. Overburden is removed by a large face shovel and dump truck operation. This material is stored on a large mound. Once the mineral deposit is uncovered, it is removed by a small shovel and truck operation. The overburden above the mineral deposit is removed and dumped in an area where the minerals have been removed previously. Draglines, bucket wheel excavators with conveyors/spreaders systems or shovel/truck systems are normally used for this operation. This sequence is repeated until the mineral deposit has been extracted.

The overburden mound from the initial box cut is placed in the final void. The restoration of the site is then started. The spoil pile is formed in acceptable contours and the subsoil and topsoil are replaced. The site restoration is often done progressively as the excavation advances.

Although the basic concept of an open pit is quite simple, the planning required to develop a large deposit for surface mining is very complex. The objective of mine design is to maximise mineral uncovering rate subject to the constraints of pit stability, machine size and scheduling. Due to the complex nature of dragline operations, a large number of digging methods is used. The mining methods are dictated by mine geometry, which includes geological structure, pit width and strip length. In any strip mining operation the volume of material that has to be rehandled must be minimised. Correct mine planning will achieve improvement in productivity.
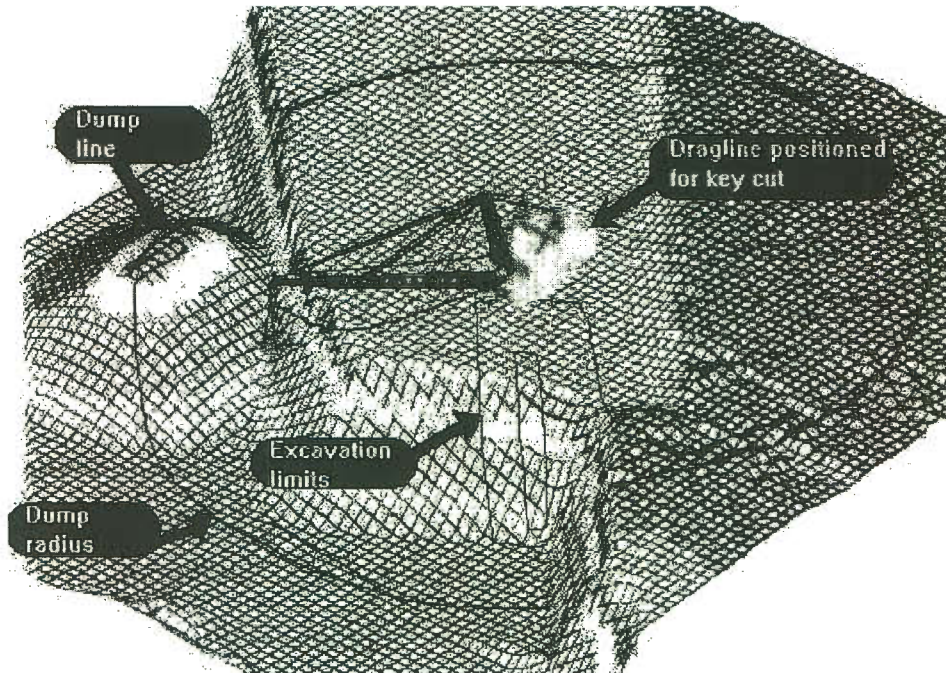
Figure 2.7   *Side casting mining method.*

The simplest and most widely used mining method is side casting. Thin strips of overburden are removed from the area that is mined. The machine is situated on the bank and is able to strip material to a considerable depth below the bank depending on the boom length and the digging slope angle. The bank on which the dragline stands is systematically cut away by the bucket and the material is cast to the side using a swing of 90 degrees (Figure 2.7). The overburden is dumped in an adjacent, previously mined strip. The dragline moves backward along the mining strip.

The design and optimisation of complex mining systems are simplified with the use of computer based simulation models. The first computer simulators used a trigonometric approach to carry out the required calculations (Baafi and Mirabediny, 1997). The spoil pile was built geometrically and accurate interactions between spoil and topography were difficult to predict. Recent simulators use more complex calculations and can predict the behaviour of the spoiling material more successfully. The new simulators are CAD-oriented products that can quickly and efficiently test the dragline excavation and casting methods in three dimensions on real pit models. Spoiling strategies for the given equipment could be optimised. Reports on prime and rehandled material are generated and the productivity of the mining operation can be estimated.

CHAPTER 3

MULTIBODY DYNAMICS

The operator determines the ultimate performance of the dragline operation. During an operation cycle, he must decide where to position the bucket for filling, where to dump the material and how to control the bucket's swinging dynamics. Constructing the spoil pile at an unsuitable location or dumping material at an incorrect spot on the spoil pile, could increase the percentage of the soil that will have to be rehandled. The swing cycle consumes approximately 80% of the total cycle time. During the cycle, the operator must concentrate on keeping the bucket at the correct carry angle. With the correct rigging set-up, this task will be easier and the operator will be able to concentrate on the correct positioning of the bucket for dumping or filling.

The rigging and bucket interaction is complex. Traditionally the design of rigging has rested on previous experience, educated guesses and testing. In research, static calculations (Knights and Shanks, 1992) or model testing was used to determine the attitude of the bucket during swinging for a specific rigging set-up. These models identified some trends, but it was difficult to predict the behaviour of full-size models. It is difficult to calculate component loads accurately. Because of competition, research done by rigging manufacturers is not published. By accurately predicting the bucket's attitude and the forces on the rigging, effective dragline operation and reduced rigging design time can be achieved. A model, which could predict the dynamic behaviour of the rigging, is necessary to accomplish this.

3.1 Objective

The dynamic model must be able to calculate the dynamic behaviour of the bucket. The shifting of the payload's centre of gravity due to movement of the payload during the

14

swinging cycle and the loss of payload due to the change in carry angle must be taken into account. The behaviour of the bucket during dumping must be included, because some components are subjected to high impulse loads during this operation. The model must be able to predict the loads that the components are subjected to at any bucket position.

During the design of the bucket, especially when the filling performance is evaluated, the modelling of the bucket's motion and attitude is crucial. The modelling method must be able to model the dynamics of the bucket during the bucket-ground interaction phase.

Because of the complexity of the system, a numeric multibody dynamic approach is used. This modelling method has the advantage that the governing dynamic equations are in the same form as the governing equations of general granular flow (that is used to model the dynamic behaviour of the ground) as described by Cundall and Strack (1979). A further advantage is that many of the modelling principles are the same. It would therefore be easy to combine the dynamic model of the bucket and the rigging with a granular description of the soil during the bucket-ground interaction phase.

It is possible to develop simpler methods that can give an approximation of the dynamic behaviour of the bucket during an operation cycle. The motion of the bucket during the filling and dumping are very complex and any method simpler that the method that is developed in this chapter will give highly inaccurate results during the named steps of an operation cycle. The accurate calculation of the dynamic behaviour of the bucket during these cycles is crucial for the optimisation of the bucket and the rigging.

3.2 Fundamental Principles

The study of multibody dynamics considers the motion of a system of connected material bodies. The study includes an examination of the motions, inertia and forces of the system, as well as the development of the governing equations of motion. The governing equations are based on a number of principles describing the dynamic behaviour of physical systems. If the system that is studied is non-relativistic and macroscopic, the principles of classical and analytical mechanics may be used.

3.2.1 Newton's Laws and Systems of Particles

The three laws of motion that Sir Isaac Newton stated in his *Philosophiae Naturalis Principia Mathematica* (1687) form the basis of classical mechanics. The laws are formulated for single particles in an inertial or *Galilean* system of reference. An inertial system is defined as being at rest or moving with uniform velocity relative to an average position of the distant "fixed stars". It may be reasonable to regard other reference systems as inertial, providing that the accelerations resulting from the motion of the coordinate system are negligible compared with the acceleration of the body under consideration. A coordinate system moving through space with the solar system, or a system whose origin coincides with the centre of the earth, or a system that is attached to the earth's surface may be regarded as inertial systems. The motion (displacement, velocity, acceleration and time) of the body under consideration determines which system may be regarded as inertial.

Newton's laws of motion can be stated as follow:

First Law   *In the absence of forces applied to a particle, the particle will remain at rest or it will move along a straight line at constant velocity.*

Second Law *The time rate of change of linear momentum of a particle is proportional to the force acting upon it and occurs in the direction in which the force acts.*

Third Law *When two particles exert a force upon each other, the respective force are equal in magnitude and in opposite in direction. (To every action there is an equal and opposite reaction.)*

These laws provide a complete formulation of the dynamic problem associated with a single free particle. They can be extended to systems of particles and bodies of finite dimension. (A particle is defined mathematically as a mass point that does not have volume.)
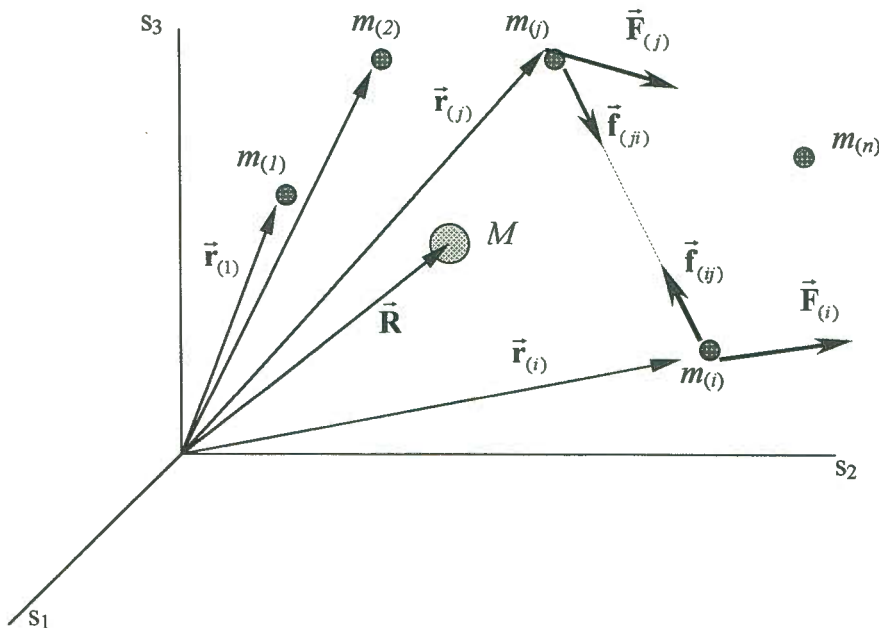
Figure 3.1 *A system of particles with applied and internal force in an inertial system s.*

Consider a system of n particles of mass m_j ($j = 1, 2, \ldots, n$) as shown in Figure 3.1. The forces applied to a particle can be classified as external or internal forces. External forces are due to sources outside the system and internal forces are due to interactions among the

17

particles. Let $\vec{\mathbf{F}}_{(j)}$ be the external force acting upon particle j and let $\vec{\mathbf{f}}_{(ji)}$ be the internal force representing the action of particle i upon j. The internal force of the action of particle j upon i can be obtained by applying Newton's third law.

$$\vec{\mathbf{f}}_{(ji)} = -\vec{\mathbf{f}}_{(ij)} \tag{3.2.1}$$

The position of the centre of mass of the system is defined by

$$\vec{\mathbf{R}} = \frac{1}{M} \sum_{j=1}^{n} m_{(j)} \vec{\mathbf{r}}_{(j)}, \tag{3.2.2}$$

where M^{1} is the total mass of the system. In a uniform gravitational field, the centre of mass of a system coincides with the centre of gravity.

Newton's second law for the j'th particle is

$$\vec{\mathbf{F}}_{(j)} + \sum_{i=1}^{n} \delta_{ji}^{*} \vec{\mathbf{f}}_{(ji)} = m_{(j)} \ddot{\vec{\mathbf{r}}}_{(j)}, \tag{3.2.3}$$

where δ_{ji}^{*} is a complementary Kronecker delta defined by

$$\delta_{ji}^{*} = 1 - \delta_{ji} = \begin{cases} 0 & \text{if } j = k \\ 1 & \text{if } j \neq k \end{cases}, \tag{3.2.4}$$

where δ_{ji} is the ordinary Kronecker delta. The complementary Kronecker delta symbol is used in equation (3.2.2) to take into account that there are no internal interacting forces acting between a particle and itself. Summing the forces over the entire system of particles we obtain

---

[1] $M = \sum_{j=1}^{n} m_{(j)}$

$$\sum_{j=1}^{n} \vec{\mathbf{F}}_{(j)} + \sum_{j=1}^{n}\sum_{i=1}^{n} \delta_{ji}^{*} \vec{\mathbf{f}}_{(ji)} = \sum_{j=1}^{n} m_{(j)} \ddot{\vec{\mathbf{r}}}_{(j)} . \tag{3.2.5}$$

When equation (3.2.1) is introduced into equation (3.2.5), the double sum reduces to zero. By letting $\vec{\mathbf{F}}$ be the resultant of the external forces acting on the system

$$\vec{\mathbf{F}} = \sum_{j=1}^{n} \vec{\mathbf{F}}_{(j)} , \tag{3.2.6}$$

and by taking the second time derivative of equation (3.2.2), equation (3.2.5) simplifies to

$$\vec{\mathbf{F}} = M\ddot{\vec{\mathbf{R}}} = \dot{\vec{\mathbf{p}}} , \tag{3.2.7}$$

where

$$\dot{\vec{\mathbf{p}}} = M\dot{\vec{\mathbf{R}}} \tag{3.2.8}$$

is the linear momentum vector of the system of particles.

Equation (3.2.7) indicates that the motion of the centre of mass of the system is the same as the motion of an imaginary particle, equal in mass to the total mass of the system, located at the centre of mass and acted upon by the resultant of all the applied forces. It is assumed that the total mass of the system does not change in time. The motion of the particle system's centre of mass is unaffected by the internal forces.

The particles may also have a rotational motion around the system's centre of mass. To describe this motion we need to look at the angular momentum of the system. Figure 3.2 shows a single particle with mass m in an inertial system s.
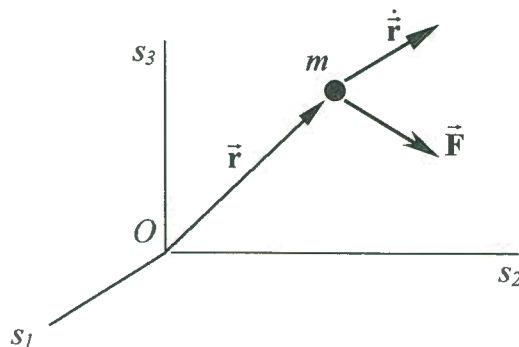
Figure 3.2   *A single particle in an inertial system.*

The angular momentum or moment of momentum of a particle with mass m, with respect to the origin of the inertial system O is defined as

$$\vec{h}_O = \vec{r} \times m\dot{\vec{r}} \qquad (3.2.9)$$

If the mass of the particle is constant, the rate of change of the angular momentum is

$$\dot{\vec{h}}_O = \dot{\vec{r}} \times m\dot{\vec{r}} + \vec{r} \times m\ddot{\vec{r}}$$
$$= \vec{r} \times m\ddot{\vec{r}} \qquad (3.2.10)$$

The moment of a force, with respect to point O is defined as

$$\vec{N}_O = \vec{r} \times \vec{F} \qquad (3.2.11)$$

Introducing Newton's second law, one can write equation (3.2.11) as

$$\vec{N}_O = \vec{r} \times m\ddot{\vec{r}} \qquad (3.2.12)$$
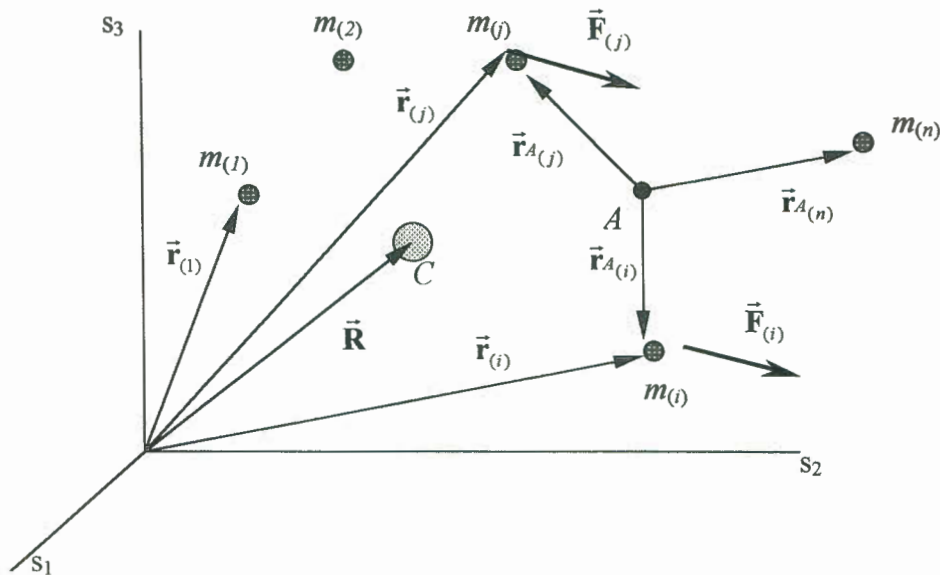
Figure 3.3 *A system of particles with applied force in an inertial system s. C is the system's centre of mass and A is an arbitrary moving point.*

It can be seen that the moment of the inertial force is equal to the rate of change of the angular momentum. Thus, one obtains the relation

$$\vec{N}_O = \dot{\vec{h}}_O \tag{3.2.13}$$

The equations of the angular momentum of a single particle can also be extended to describe a system of particles. Consider a system of particles with centre of mass C, shown in Figure (3.3).

The angular momentum of a system of particles with respect to any moving point A is defined as

$$\vec{h}_A = \sum_{j=1}^{n} \vec{h}_{A_{(j)}} = \sum_{j=1}^{n} \vec{r}_{A_{(j)}} \times m_{(j)} \dot{\vec{r}}_{(j)} \tag{3.2.14}$$

Assuming that the masses $m_{(j)}$ of the particles and the number of particles do not vary with time, the time rate of change of the angular momentum can be obtained as:

$$\dot{\vec{h}}_A = \sum_{j=1}^{n} \dot{\vec{r}}_{A_{(j)}} \times m_{(j)} \dot{\vec{r}}_{(j)} + \sum_{j=1}^{n} \vec{r}_{A_{(j)}} \times m_{(j)} \ddot{\vec{r}}_{(j)} \tag{3.2.15}$$

Choosing point A to coincide with the moving centre of mass C, and applying Newton's second law of motion and the definition of the centre of mass, equation (3.2.15) becomes

$$\dot{\vec{h}}_C = \sum_{j=1}^{n} \vec{N}_{C_{(j)}} = \vec{N}_C \tag{3.2.16}$$

Hence, the time rate of change of the angular momentum with respect to the centre of mass is equal to the resultant of the external torques about the centre of mass.

3.3 The Motion of a Rigid Body

In the previous section, we have developed equations to describe the motion of a particle and systems of particles. In this section the equations of motion of a non-deformable or rigid body with distributed mass will be developed. A body with distributed mass may be regarded as a conglomeration of an infinite number of particles. If the body is non-deformable, the distance between any pair of particles is constant. This statement enables the description of the motion of a rigid body by using only six coordinates. Three translational and three rotational coordinates are normally used.

We will use the same principles that have been used to derive the equations of a system of particles to obtain the equations of motion for a rigid body. Many of the relations that have been developed for a system of particles can be applied directly to a rigid body. Before we can derive the equations of motion, we must define some kinematic relations of a rigid body.

3.3.1 Kinematic Relations

To describe the motion of a rigid body in a multibody system, we assign a coordinate system to each body. The origin of this coordinate system is rigidly attached to a point on the body. This causes it to experience the same motion as the body. Sometimes it is more convenient to describe the geometric and inertial properties of the body in terms of the body's fixed coordinate system. Figure (3.4) shows an inertial system s (fixed in space) and a body coordinate system b. The body has an angular velocity of $\vec{\omega}$ as shown. The vector $\vec{u}_{(i)}$ is fixed in the body reference system and experiences the same motion as the body.

Referring to Figure (3.4) the position of any point in the rigid body can be written as:

$$\vec{\rho}_{(i)} = \vec{r}_0 + \vec{u}_{(i)} \qquad (3.3.1)$$

This equation can be stated in orthogonal base notation respect to base $\underline{\vec{E}}_s$ as

$$\overline{\rho}_{(i)}^{s} = \overline{r}_{0}^{s} + \overline{u}_{(i)}^{s} \qquad\qquad (3.3.2)$$
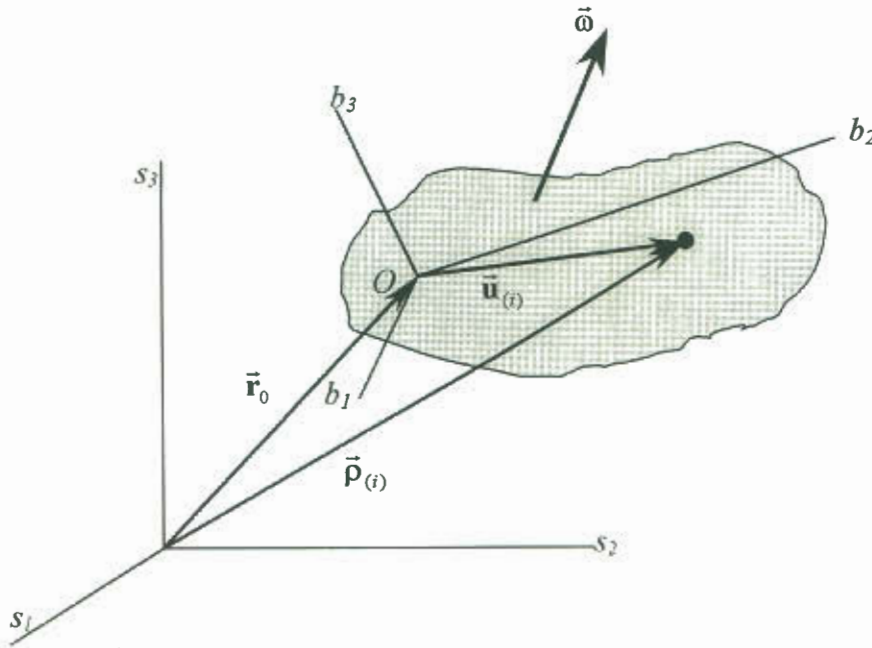
Figure 3.4   *A rigid body, with a body coordinate system b and an inertial frame of reference s.*

Taking the first and second time derivative of equation (3.3.2), one obtains the velocity and acceleration relations as:

$$\dot{\overline{\rho}}_{(i)}^{s} = \dot{\overline{r}}_{0}^{s} + \dot{\overline{u}}_{(i)}^{s} \qquad\qquad (3.3.3)$$

$$\ddot{\overline{\rho}}_{(i)}^{s} = \ddot{\overline{r}}_{0}^{s} + \ddot{\overline{u}}_{(i)}^{s} \qquad\qquad (3.3.4)$$

The vector $\overline{u}_{(i)}$ is fixed to the body and will remain constant with respect to the body reference system during any motion of the body. This implies that with respect to the body reference system

$$\dot{\bar{\mathbf{u}}}_{(i)}^{b} = \ddot{\bar{\mathbf{u}}}_{(i)}^{b} = \overline{\mathbf{0}}^{b} \tag{3.3.5}$$

The relationship between the descriptions of the vector $\ddot{\mathbf{u}}_{(i)}$ relative to the two reference systems s and b is

$$\overline{\mathbf{u}}_{(i)}^{s} = \underline{\overline{\mathbf{E}}}_{b}^{s} \overline{\mathbf{u}}_{(i)}^{b} \tag{3.3.6}$$

with $\underline{\overline{\mathbf{E}}}_{b}^{s}$ the transformation matrix between the two reference systems.

By taking the time derivative of equation (3.3.6), one obtains:

$$\begin{aligned}
\dot{\bar{\mathbf{u}}}_{(i)}^{s} &= \underline{\overline{\mathbf{E}}}_{b}^{s} \dot{\bar{\mathbf{u}}}_{(i)}^{b} + \underline{\dot{\overline{\mathbf{E}}}}_{b}^{s} \overline{\mathbf{u}}_{(i)}^{b} \\
&= \underline{\dot{\overline{\mathbf{E}}}}_{b}^{s} \underline{\overline{\mathbf{E}}}_{s}^{b} \overline{\mathbf{u}}_{(i)}^{s} \\
&= \underline{\widetilde{\overline{\omega}}}_{s}^{s} \overline{\mathbf{u}}_{(i)}^{s}
\end{aligned} \tag{3.3.7}$$

where $\underline{\widetilde{\overline{\omega}}}_{s}^{s}$ is the cross product tensor of the angular velocity vector with respect to s. The acceleration relation can be obtained by taking the time derivative of equation (3.3.7)

$$\begin{aligned}
\ddot{\bar{\mathbf{u}}}_{(i)}^{s} &= \underline{\dot{\widetilde{\overline{\omega}}}}_{s}^{s} \overline{\mathbf{u}}_{(i)}^{s} + \underline{\widetilde{\overline{\omega}}}_{s}^{s} \dot{\bar{\mathbf{u}}}_{(i)}^{s} \\
&= \underline{\dot{\widetilde{\overline{\omega}}}}_{s}^{s} \overline{\mathbf{u}}_{(i)}^{s} + \underline{\widetilde{\overline{\omega}}}_{s}^{s} \underline{\widetilde{\overline{\omega}}}_{s}^{s} \overline{\mathbf{u}}_{(i)}^{s}
\end{aligned} \tag{3.3.8}$$

The velocity and acceleration can also be written in the following forms, which are used in the derivation of the momentum equations.

$$\dot{\bar{\mathbf{u}}}_{(i)}^{s} = \overline{\omega}^{s} \times \overline{\mathbf{u}}_{(i)}^{s} \tag{3.3.9}$$

$$\ddot{\bar{\mathbf{u}}}_{(i)}^{s} = \dot{\overline{\omega}}^{s} \times \overline{\mathbf{u}}_{(i)}^{s} + \overline{\omega}^{s} \times \left(\overline{\omega}^{s} \times \overline{\mathbf{u}}_{(i)}^{s} \right) \tag{3.3.10}$$

With these relations, we can rewrite the velocity and acceleration relations of equation (3.3.3) and (3.3.4) as:

$$\dot{\overline{\rho}}_{(i)}^{s} = \dot{\overline{\mathbf{r}}}_{o}^{s} + \overline{\boldsymbol{\omega}}^{s} \times \overline{\mathbf{u}}_{(i)}^{s} \tag{3.3.11}$$

$$\ddot{\overline{\rho}}_{(i)}^{s} = \ddot{\overline{\mathbf{r}}}_{0}^{s} + \dot{\overline{\boldsymbol{\omega}}}^{s} \times \overline{\mathbf{u}}_{(i)}^{s} + \overline{\boldsymbol{\omega}}^{s} \times \left(\overline{\boldsymbol{\omega}}^{s} \times \overline{\mathbf{u}}_{(i)}^{s}\right) \tag{3.3.12}$$

These equations can be expressed in terms of physical vectors as:

$$\dot{\vec{\rho}}_{(i)} = \dot{\vec{\mathbf{r}}}_{0} + \vec{\omega} \times \vec{\mathbf{u}}_{(i)} \tag{3.3.13}$$

$$\ddot{\vec{\rho}}_{(i)} = \ddot{\vec{\mathbf{r}}}_{0} + \dot{\vec{\omega}} \times \vec{\mathbf{u}}_{(i)} + \vec{\omega} \times \left(\vec{\omega} \times \vec{\mathbf{u}}_{(i)}\right) \tag{3.3.14}$$

The velocity and acceleration of any point in a rigid body can be described in terms of the translation of the origin of a body reference system and the rotation of the reference system about the origin.

3.3.2 Linear and Angular Momentum of a Rigid Body

Consider a rigid body of total mass m and a set of body axes denoted by the base b with origin O as shown in Figure (3.5). We defined a rigid body as a conglomeration of a large number of particles with mass $m_{(i)}$, where the distance between any two particles is constant. An alternative representation is that at every point in the body a solid continuum, with a differential element of mass, is defined. The linear and angular momentum definitions retain the same basic structure as for a system of particles. They can either be expressed in terms of a summation over the system of particles or in terms of an integral over the body.

The total mass of the body can be expressed mathematically as

$$m = \lim_{n \to \infty} \sum_{i=1}^{n} m_{(i)} = \int_{\text{Body}} dm \tag{3.3.15}$$

25
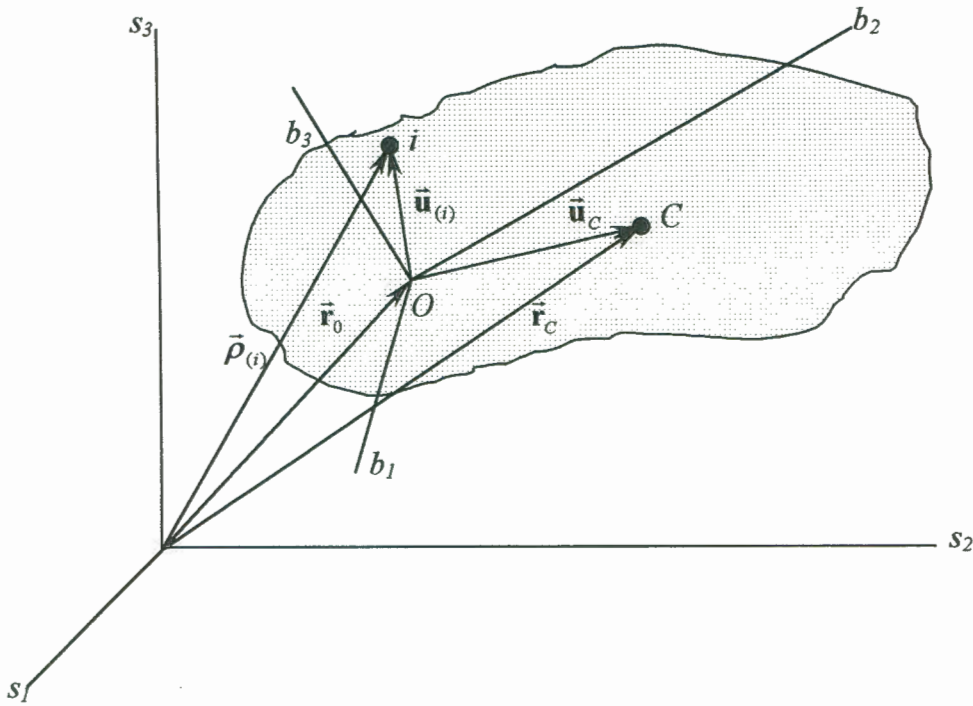
Figure 3.5   *A general rigid body with coordinate systems and vectors. Point i is the position of one of the particles or solid continuum in the conglomeration that forms the rigid body.*

The vector $\vec{\mathbf{u}}_C$ from the origin O of the body reference system to the center of mass C, is defined as

$$\vec{\mathbf{u}}_C = \lim_{n \to \infty} \frac{1}{m} \sum_{i=1}^{n} m_{(i)} \vec{\mathbf{u}}_{(i)} = \frac{1}{m} \int_{Body} \vec{\mathbf{u}}\, dm \qquad (3.3.16)$$

The expression for the linear momentum vector, $\vec{\mathbf{p}}$, of the rigid body has the same form as for a system of particles and can be stated as

$$\vec{\mathbf{p}} = \lim_{n \to \infty} \sum_{i=1}^{n} m_{(i)} \dot{\vec{\rho}}_{(i)} = \int_{Body} \dot{\vec{\rho}}\, dm \qquad (3.3.17)$$

From equation (3.3.11) we have seen that the velocity of any point in a rigid body can be expressed in terms of the velocity of the origin of the body reference system and the

26

rotation of the body reference system. Using this relation, the linear momentum equation becomes:

$$\vec{\mathbf{p}} = \lim_{n \to \infty} \sum_{i=1}^{n} m_{(i)} \left(\dot{\vec{\mathbf{r}}}_0 + \vec{\omega} \times \vec{\mathbf{u}}_{(i)} \right)$$

$$= m\dot{\vec{\mathbf{r}}}_0 + \lim_{n \to \infty} \left(\vec{\omega} \times \sum_{i=1}^{n} m_{(i)} \vec{\mathbf{u}}_{(i)} \right)$$

$$= m\left(\dot{\vec{\mathbf{r}}}_0 + \vec{\omega} \times \vec{\mathbf{u}}_c \right)$$

However, $\dot{\vec{\mathbf{r}}}_c = \dot{\vec{\mathbf{r}}}_0 + \vec{\omega} \times \vec{\mathbf{u}}_c$ is the velocity of the center of mass.

$$\vec{\mathbf{p}} = m\dot{\vec{\mathbf{r}}}_c \qquad\qquad (3.3.18)$$

Thus, the linear momentum of a rigid body is equal to the product of velocity of the centre of mass and the total mass of the body.

The angular momentum of the rigid body about the origin O is defined by:

$$\vec{\mathbf{h}}_0 = \lim_{n \to \infty} \sum_{i=1}^{n} \vec{\mathbf{u}}_{(i)} \times m_{(i)} \dot{\vec{\rho}}_{(i)} = \int_{Body} \vec{\mathbf{u}} \times \dot{\vec{\rho}}\, dm$$

$$= \int_{Body} \vec{\mathbf{u}} \times \left(\dot{\vec{\mathbf{r}}}_0 + \vec{\omega} \times \vec{\mathbf{u}} \right) dm$$

$$= \int_{Body} \left(\vec{\mathbf{u}} \times \dot{\vec{\mathbf{r}}}_0 \right) dm + \int_{Body} \vec{\mathbf{u}} \times \left(\vec{\omega} \times \vec{\mathbf{u}} \right) dm$$

$$= -\dot{\vec{\mathbf{r}}}_0 \times \int_{Body} \vec{\mathbf{u}}\, dm + \int_{Body} \vec{\mathbf{u}} \times \left(\vec{\omega} \times \vec{\mathbf{u}} \right) dm \qquad (3.3.19)$$

If O coincides with the centre of mass, it implies that $\int \vec{\mathbf{u}}\, dm = \vec{\mathbf{0}}$. This leads to the equation for the angular momentum of a body about the centre of mass C.

$$\vec{\mathbf{h}}_c = \int_{Body} \vec{\mathbf{u}} \times \left(\vec{\omega} \times \vec{\mathbf{u}} \right) dm \qquad\qquad (3.3.20)$$

27

By applying the relation for a triple cross product, equation (3.3.20) can be written as

$$\vec{h}_C = \int_{Body} [\vec{\omega}(\vec{u} \bullet \vec{u}) - \vec{u}(\vec{\omega} \bullet \vec{u})]\, dm \qquad (3.3.21)$$

This equation can be written in orthogonal base notation with respect to base *s* as

$$\overline{h}_C^s = \int_{Body} \left[\overline{\omega}^s(\overline{u}^s \bullet \overline{u}^s) - \overline{u}^s(\overline{\omega}^s \bullet \overline{u}^s)\right] dm \qquad (3.3.22)$$

Let $\overline{u}^s = \begin{bmatrix} u_{s1} & u_{s2} & u_{s3} \end{bmatrix}^T$ and $\overline{\omega}^s = \begin{bmatrix} \omega_{s1} & \omega_{s2} & \omega_{s3} \end{bmatrix}^T$ then after algebraic manipulations of equation (3.3.22), the angular momentum equation can be written in the form

$$
\overline{h}_C^s = \int_{Body}
\begin{bmatrix}
u_{s2}^2 + u_{s3}^2 & -u_{s1}u_{s2} & -u_{s1}u_{s3} \\
-u_{s2}u_{s1} & u_{s1}^2 + u_{s3}^2 & -u_{s2}u_{s3} \\
-u_{s3}u_{s1} & -u_{s3}u_{s2} & u_{s1}^2 + u_{s2}^2
\end{bmatrix}
\begin{bmatrix}
\omega_{s1} \\
\omega_{s2} \\
\omega_{s3}
\end{bmatrix} dm
$$

$$
=
\begin{bmatrix}
\int_{Body}\left(u_{s2}^2 + u_{s3}^2\right)dm & -\int_{Body}\left(u_{s1}u_{s2}\right)dm & -\int_{Body}\left(u_{s1}u_{s3}\right)dm \\
-\int_{Body}\left(u_{s2}u_{s1}\right)dm & \int_{Body}\left(u_{s1}^2 + u_{s3}^2\right)dm & -\int_{Body}\left(u_{s2}u_{s3}\right)dm \\
-\int_{Body}\left(u_{s3}u_{s1}\right)dm & -\int_{Body}\left(u_{s3}u_{s2}\right)dm & \int_{Body}\left(u_{s1}^2 + u_{s2}^2\right)dm
\end{bmatrix}
\begin{bmatrix}
\omega_{s1} \\
\omega_{s2} \\
\omega_{s3}
\end{bmatrix}
$$

$$
=
\begin{bmatrix}
J_{11} & J_{12} & J_{13} \\
J_{21} & J_{22} & J_{23} \\
J_{31} & J_{32} & J_{33}
\end{bmatrix}
\begin{bmatrix}
\omega_{s1} \\
\omega_{s2} \\
\omega_{s3}
\end{bmatrix}
$$

$$= \underline{\overline{J}}_s^s \overline{\omega}^s \qquad (3.3.23)$$

which can be written in terms of physical tensors as:

$$\vec{h}_C = \underline{\vec{J}}\vec{\omega} \qquad (3.3.24)$$

The symmetric tensor $\vec{\mathbf{J}}$ is a second rank Cartesian tensor called the *inertia tensor*. The diagonal elements are called *moments of inertia* and the negative non-diagonal elements are called *products of inertia*.

3.3.3 Equations of Motion

The equations of motion derived for a system of particles are perfectly valid for a rigid body, because the rigid body can be considered as a system of particles where the distance between any two particles remain constant. Certain mass distribution characteristics are expressed by means of the position of the centre of mass as well as the moments and products of inertia, with respect to a set of body axes. The relation between the force and linear momentum (equation 3.2.7) and the relation of the torque and angular momentum (equation 3.2.16) remain unchanged for rigid bodies.

The force equation follows directly from the equation (3.2.7) for a system of particles and the equation for the linear momentum (equation 3.3.18) for a rigid body.

$$
\begin{aligned}
\vec{\mathbf{F}} &= \dot{\vec{\mathbf{p}}} \\
&= \frac{d}{dt}(m\dot{\vec{\mathbf{r}}}_C) \\
&= m\ddot{\vec{\mathbf{r}}}_C
\end{aligned}
\tag{3.3.25}
$$

where $\vec{\mathbf{F}}$ is the resultant of the applied force and $\vec{\mathbf{r}}_C$ is the position of the body's centre of mass. Alternatively, equation (3.3.25) can be stated in orthogonal base notation with respect to the inertial system s as

$$
\overline{\mathbf{F}}^s = m\ddot{\overline{\mathbf{r}}}_C^s
\tag{3.3.26}
$$

The equations for the rotational motion about the centre of mass can be obtained from the relation between the applied torque and the angular momentum for a system of particles (equation 3.2.16).

$$\vec{N}_C = \dot{\vec{h}}_C$$

where $\vec{N}_C$ is the resultant of the applied moments and $\dot{\vec{h}}_C$ is the rate of change of the angular momentum, which is obtained by taking the time derivative of equation (3.3.20)

$$\dot{\vec{h}}_C = \frac{d}{dt} \int\limits_{Body} \vec{u} \times (\vec{\omega} \times \vec{u}) \, dm$$
$$= \int\limits_{Body} \left(\dot{\vec{u}} \times (\vec{\omega} \times \vec{u}) + \vec{u} \times (\dot{\vec{\omega}} \times \vec{u}) + \vec{u} \times (\vec{\omega} \times \dot{\vec{u}}) \right) dm \qquad (3.3.27)$$

By using the velocity relation of equation (3.3.9), we can write equation (3.3.27) as

$$\dot{\vec{h}}_C = \int\limits_{Body} (\vec{\omega} \times \vec{u}) \times (\vec{\omega} \times \vec{u}) \, dm + \int\limits_{Body} \vec{u} \times (\dot{\vec{\omega}} \times \vec{u}) \, dm + \int\limits_{Body} \vec{u} \times (\vec{\omega} \times (\vec{\omega} \times \vec{u})) \, dm$$
$$(3.3.28)$$

From the definition of the cross product tensor, it can be seen that the first integral in equation (3.3.28) is equal to zero. The second integral has the same form as equation (3.3.20) with the exception that the angular acceleration vector is used instead of the angular velocity vector. When the same method is used as in the previous section, the second term can be written as

$$\int\limits_{Body} \left(\vec{u} \times (\dot{\vec{\omega}} \times \vec{u}) \right) dm = \underline{\vec{J}} \dot{\vec{\omega}} \qquad (3.3.29)$$

The integrand of the third integral in equation (3.3.28) can be algebraically manipulated to obtain

$$\vec{u} \times [\vec{\omega} \times (\vec{\omega} \times \vec{u})] = \vec{\omega} \times [\vec{u} \times (\vec{\omega} \times \vec{u})] \qquad (3.3.30)$$

With this relation, we can write the third integral of equation (3.3.28) as

$$\int\limits_{Body} \vec{u} \times [\vec{\omega} \times (\vec{\omega} \times \vec{u})] \, dm = \int\limits_{Body} \vec{\omega} \times [\vec{u} \times (\vec{\omega} \times \vec{u})] \, dm$$
$$= \vec{\omega} \times \int\limits_{Body} [\vec{u} \times (\vec{\omega} \times \vec{u})] \, dm$$

30

$$= \vec{\omega} \times \underline{\underline{\mathbf{J}}}\vec{\omega} \qquad (3.3.31)$$

By using equation (3.3.29) and equation (3.3.31), we can write the moment equation as

$$\vec{\mathbf{N}}_C = \dot{\vec{\mathbf{h}}}_C = \underline{\underline{\mathbf{J}}}\dot{\vec{\omega}} + \vec{\omega} \times \underline{\underline{\mathbf{J}}}\vec{\omega} \qquad (3.3.32)$$

or in orthogonal base notation with respect to the inertial system *s* as

$$\dot{\mathbf{h}}_C^s = \overline{\mathbf{N}}_C^s = \underline{\overline{\mathbf{J}}}_s^s \dot{\overline{\omega}}^s + \overline{\omega}^s \times \underline{\overline{\mathbf{J}}}_s^s \overline{\omega}^s \qquad (3.3.33)$$

Equation (3.3.32) is known as *Euler's equation of motion*.

The equations of motion of a rigid body in space are given by equations (3.3.25) and (3.3.32). The combination of these equations is called the *Newton - Euler equations of motion* and they form the foundation of multibody dynamics.

3.3.4 Rigid Body Rotations

It can be shown that the rotation tensor, representing a general rotation of a rigid body, has an eigenvalue equal to unity. Thus, for the eigenvector problem of the rotation tensor

$$\underline{\underline{\vec{\mathbf{R}}}}\vec{\mathbf{u}} = \lambda\vec{\mathbf{u}} \qquad (3.3.34)$$

there exists one vector $\vec{\mathbf{u}}$, the eigenvector, that corresponds to the unity eigenvalue ($\lambda = 1$) that is unaffected by the rotation. This is only possible if it is a vector along the axis of rotation. This property of rigid body rotations is known as Euler's theorem:

> *The most general displacement of a rigid body with one point fixed is equivalent to a rotation about some axis.*

According to this theorem, any rigid body rotation can be defined by a single rotation about an axis. We can express the rotation tensor defining the orientation of a body by

using four parameters: the three components of the unit vector along the axis of rotation and the angle of rotation.

Kang (1993), for example, used the following method to define the rotation matrix: Consider a vector with initial orientation $\bar{\mathbf{v}}^s$ in a stationary base $\underline{\bar{\mathbf{E}}}_s$. The vector is rotated through an angle ϕ around an axis defined by the unit vector $\bar{\mathbf{n}}$. The final orientation of the vector after the rotation is $\bar{\mathbf{v}}_t^s$. From Figure (3.6) it is clear that

$$\bar{\mathbf{v}}_t^s = \bar{\mathbf{r}}_{OC}^s + \bar{\mathbf{r}}_{CB}^s$$

$$= \left| \bar{\mathbf{v}}_t^s \right| \cos(\alpha) \cdot \bar{\mathbf{n}}^s + \left| \bar{\mathbf{v}}_t^s \right| \sin(\alpha) \left[\bar{\mathbf{s}}^s \cos(\phi) + \bar{\mathbf{t}}^s \sin(\phi) \right] \qquad (3.3.35)$$
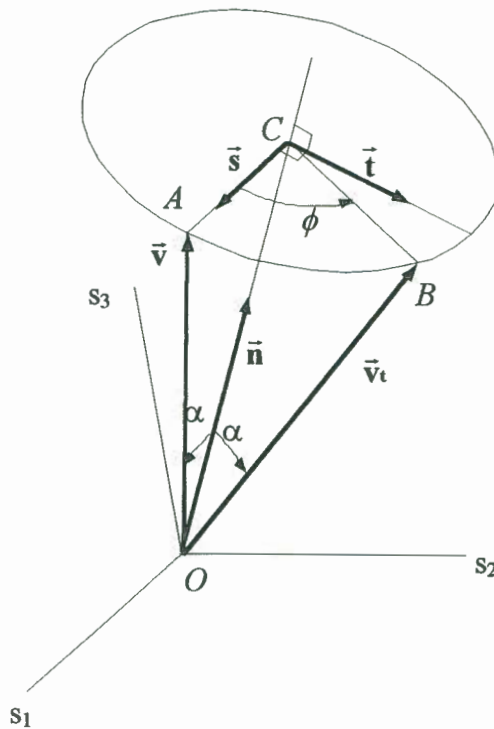
Figure 3.6   *The rotation of a vector about an axis.*

where $\bar{\mathbf{s}}^s$ and $\bar{\mathbf{t}}^s$ are unit vectors defined as

$$\bar{t}^s = \frac{\bar{n}^s \times \bar{v}^s}{\left| \bar{n}^s \times \bar{v}^s \right|} \tag{3.3.36}$$

and

$$\bar{s}^s = \bar{t}^s \times \bar{n}^s = \frac{(\bar{n}^s \times \bar{v}^s) \times \bar{n}^s}{\left| \bar{n}^s \times \bar{v}^s \right|} \tag{3.3.37}$$

The length of a vector is preserved during a rotation, hence we can write the scalar product

$$(\underline{n}_s \bar{v}^s) = (\underline{v}_s \bar{n}^s) = \left| \bar{v}^s \right| \cos(\alpha) = \left| \bar{v}_t^s \right| \cos(\alpha), \tag{3.3.38}$$

and the vector product

$$\left| \bar{n}^s \times \bar{v}^s \right| = \left| \bar{v}^s \right| \sin(\alpha) = \left| \bar{v}_t^s \right| \sin(\alpha). \tag{3.3.39}$$

By introducing the relations given above in equation (3.3.35), it becomes

$$\bar{v}_t^s = (\underline{v}_s \bar{n}^s)\bar{n}^s + (\bar{n}^s \times \bar{v}^s) \times \bar{n}^s \cos(\phi) + (\bar{n}^s \times \bar{v}^s) \sin(\phi) \tag{3.3.40}$$

It can be shown that the first term in equation (3.3.40) is equal to

$$(\underline{v}_s \bar{n}^s)\bar{n}^s = \bar{v}^s + \bar{n}^s \times (\bar{n}^s \times \bar{v}^s), \tag{3.3.41}$$

so that equation (3.3.40) can be written in the form

$$\bar{v}_t^s = \bar{v}^s - (\bar{n}^s \times \bar{v}^s) \times \bar{n}^s (1 - \cos(\phi)) + (\bar{n}^s \times \bar{v}^s) \sin(\phi). \tag{3.3.42}$$

By using the trigonometric relations for halve angles and the cross product tensor, we can write equation (3.3.42) as

$$\overline{\mathbf{v}}_{\mathbf{t}}{}^{s} = \left[\overline{\mathbf{\underline{I}}}_{s}^{s} + 2\sin(\phi/2)\cos(\phi/2)\widetilde{\overline{\mathbf{\underline{n}}}}_{s}^{s} + 2\sin^{2}(\phi/2)\widetilde{\overline{\mathbf{\underline{n}}}}_{s}^{s}\widetilde{\overline{\mathbf{\underline{n}}}}_{s}^{s} \right]\overline{\mathbf{v}}^{s} \qquad (3.3.43)$$

where $\widetilde{\overline{\mathbf{\underline{n}}}}_{s}^{s}$ is the cross product tensor of the unit vector $\overline{\mathbf{n}}^{s}$ and $\overline{\mathbf{\underline{I}}}_{s}^{s}$ is the 3×3 identity tensor. Equation (3.3.43) can also be written as a single matrix product

$$\overline{\mathbf{v}}_{\mathbf{t}}{}^{s} = \overline{\mathbf{\underline{R}}}_{s}^{s}\,\overline{\mathbf{v}}^{s} \qquad (3.3.44)$$

where $\overline{\mathbf{\underline{R}}}_{s}^{s}$ is the rotation tensor defined as

$$\overline{\mathbf{\underline{R}}}_{s}^{s} = \overline{\mathbf{\underline{I}}}_{s}^{s} + 2\sin(\phi/2)\cos(\phi/2)\widetilde{\overline{\mathbf{\underline{n}}}}_{s}^{s} + 2\sin^{2}(\phi/2)\widetilde{\overline{\mathbf{\underline{n}}}}_{s}^{s}\widetilde{\overline{\mathbf{\underline{n}}}}_{s}^{s} \qquad (3.3.45)$$

This equation is known as Rodrigues's formula.

Parameterisation of Rotations

The orientation of a body after two successive rotations stated by the rotation tensors $\overrightarrow{\underline{\mathbf{R}}_{1}}$ and $\overrightarrow{\underline{\mathbf{R}}_{2}}$ can be obtained from

$$\overrightarrow{\underline{\mathbf{R}}} = \overrightarrow{\underline{\mathbf{R}}_{1}} \cdot \overrightarrow{\underline{\mathbf{R}}_{2}} \qquad (3.3.46)$$

In general, matrix multiplication is not commutative and it is therefore important to specify the order in which the successive rotations are performed. For this reason finite rotations cannot be treated as vector quantities, neither can the components of a rigid body's angular velocity vector be integrated to obtain the orientation of the body in space. It is also impossible to find a set of three independent orientation coordinates with the components of the angular velocity as time derivatives.

The Euler angles are a set of coordinates commonly used to describe the orientation of a body. The orientation of the body is specified by three successive angular displacements about three non-orthogonal axes. The order of the rotations and the corresponding axes are

specified. Wertz, *et al.* (1978) lists 12 distinct representations of Euler angle rotations. It is possible to express the angular velocity of the body in terms of the angles and their time derivatives.

All the Euler angle systems are subjected to singular orientations for which two Euler angles are undefined. This situation occurs when the second rotation is such that the first and third rotations occur about the same axes with the same orientation in space. Only two degrees of freedom are then represented. This corresponds to a condition of gyroscopic suspension which is known as gimbal lock (Greenwood, 1988). An accurate computer representation of rigid body rotations near the singular orientation is difficult because small changes in the body orientation may result in large changes in the value of the Euler angles. The angular velocity of the body is trigonometric functions of the Euler angles and causes many computational operations if it is used in a computer procedure. For computer implementations, orientation parameters instead of orientation angles are used.

Robertson and Schwertassek (1988) state that Euler developed a parameterisation that involved four algebraic variables called the Euler parameters. The four parameters can be regarded as the components of a quaternion. The main advantage of the Euler parameters is that they do not contain singularities. If $\bar{\mathbf{n}}$ is the unit vector defining the rotation axis and ϕ is the rotation angle, then the four Euler parameters are defined as

$$
\begin{aligned}
\varepsilon_1 &= n_1 \sin(\phi/2) \\
\varepsilon_2 &= n_2 \sin(\phi/2) \\
\varepsilon_3 &= n_3 \sin(\phi/2) \\
\varepsilon_4 &= \cos(\phi/2)
\end{aligned}
\tag{3.3.47}
$$

It can be seen that the four parameters can be written as a vector with four components

$$
\bar{\varepsilon} = \begin{bmatrix} \bar{\mathbf{n}} \sin(\phi/2) \\ \cos(\phi/2) \end{bmatrix}
\tag{3.3.48}
$$

35

The four parameters are not independent and it can be seen from equation (3.3.47) that they follow the constraint

$$\varepsilon_1{}^2 + \varepsilon_2{}^2 + \varepsilon_3{}^2 + \varepsilon_4{}^2 = 1 \qquad (3.3.49)$$

The rotation tensor can be obtained with Rodrigues's formula as

$$\underline{\overline{\mathbf{R}}}_s^s = \underline{\overline{\mathbf{I}}}_s^s + 2\sin(\phi/2)\cos(\phi/2)\underline{\widetilde{\overline{\mathbf{n}}}}_s^s + 2\sin^2(\phi/2)\underline{\widetilde{\overline{\mathbf{n}}}}_s^s \underline{\widetilde{\overline{\mathbf{n}}}}_s^s \qquad (3.3.50)$$

By introducing the parameters defined in equation (3.3.48) in equation (3.3.49), we can write the rotation tensor as

$$\underline{\overline{\mathbf{R}}}_s^s = \underline{\overline{\mathbf{I}}}_s^s + 2\varepsilon_4 \underline{\overline{\mathbf{\Gamma}}}_s^s + 2\underline{\overline{\mathbf{\Gamma}}}_s^s \underline{\overline{\mathbf{\Gamma}}}_s^s, \qquad (3.3.51)$$

where $\underline{\overline{\mathbf{\Gamma}}}_s^s = \sin(\phi/2)\underline{\widetilde{\overline{\mathbf{n}}}}_s^s$. By performing the matrix multiplication and simplifying the equation, the rotation tensor can be written explicitly in terms of the Euler parameters.

$$\underline{\overline{\mathbf{R}}}_s^s = \begin{bmatrix} \left(\varepsilon_1{}^2 - \varepsilon_2{}^2 - \varepsilon_3{}^2 + \varepsilon_4{}^2\right) & 2\left(\varepsilon_1\varepsilon_2 - \varepsilon_3\varepsilon_4\right) & 2\left(\varepsilon_1\varepsilon_3 + \varepsilon_2\varepsilon_4\right) \\ 2\left(\varepsilon_1\varepsilon_2 + \varepsilon_3\varepsilon_4\right) & \left(-\varepsilon_1{}^2 + \varepsilon_2{}^2 - \varepsilon_3{}^2 + \varepsilon_4{}^2\right) & 2\left(\varepsilon_2\varepsilon_2 - \varepsilon_1\varepsilon_4\right) \\ 2\left(\varepsilon_1\varepsilon_3 - \varepsilon_2\varepsilon_4\right) & 2\left(\varepsilon_2\varepsilon_3 + \varepsilon_1\varepsilon_4\right) & \left(-\varepsilon_1{}^2 - \varepsilon_2{}^2 + \varepsilon_3{}^2 + \varepsilon_4{}^2\right) \end{bmatrix}$$

$$(3.3.52)$$

The transformation matrix between a coordinate system fixed to the body and the inertial system for this rotation of the body is

$$\underline{\overline{\mathbf{E}}}_b^s = \underline{\overline{\mathbf{R}}}_s^s \qquad (3.3.53)$$

The angular velocity can be expressed in terms of the Euler parameters and their time derivatives. Huston (1990) showed a method to obtain a set of four independent linear equations from the derivative of the transformation matrix and the derivative of the

constraint equation (3.3.49). After mathematical manipulations, the four linearly independent equations are

$$\omega_{s1} = 2\left(\varepsilon_4\dot{\varepsilon}_1 - \varepsilon_3\dot{\varepsilon}_2 + \varepsilon_2\dot{\varepsilon}_3 - \varepsilon_1\dot{\varepsilon}_4\right)$$
$$\omega_{s2} = 2\left(\varepsilon_3\dot{\varepsilon}_1 + \varepsilon_4\dot{\varepsilon}_2 - \varepsilon_1\dot{\varepsilon}_3 - \varepsilon_2\dot{\varepsilon}_4\right)$$
$$\omega_{s3} = 2\left(-\varepsilon_2\dot{\varepsilon}_1 + \varepsilon_1\dot{\varepsilon}_2 + \varepsilon_4\dot{\varepsilon}_3 - \varepsilon_3\dot{\varepsilon}_4\right)$$
$$0 = 2\left(\varepsilon_1\dot{\varepsilon}_1 + \varepsilon_2\dot{\varepsilon}_2 + \varepsilon_3\dot{\varepsilon}_3 + \varepsilon_4\dot{\varepsilon}_4\right) \tag{3.3.54}$$

These equations can be written as a single matrix equation

$$\begin{bmatrix} \omega_{s1} \\ \omega_{s2} \\ \omega_{s3} \\ 0 \end{bmatrix} = 2 \begin{bmatrix} \varepsilon_4 & -\varepsilon_3 & \varepsilon_2 & -\varepsilon_1 \\ \varepsilon_3 & \varepsilon_4 & -\varepsilon_1 & -\varepsilon_2 \\ -\varepsilon_2 & \varepsilon_1 & \varepsilon_4 & -\varepsilon_3 \\ \varepsilon_1 & \varepsilon_2 & \varepsilon_3 & \varepsilon_4 \end{bmatrix} \begin{bmatrix} \dot{\varepsilon}_1 \\ \dot{\varepsilon}_2 \\ \dot{\varepsilon}_3 \\ \dot{\varepsilon}_4 \end{bmatrix} \tag{3.3.55}$$

$$\begin{bmatrix} \overline{\omega}^s \\ 0 \end{bmatrix} = 2 \underline{\overline{A}}^s \dot{\overline{\varepsilon}} \tag{3.3.56}$$

The matrix $\underline{\overline{A}}^s$ is orthogonal, thus its inverse and its transpose are equal. From equation (3.3.56) we can obtain the derivatives of the Euler parameters as

$$\dot{\overline{\varepsilon}}^s = \tfrac{1}{2}\left[\underline{\overline{A}}^s\right]^T \begin{bmatrix} \overline{\omega}^s \\ 0 \end{bmatrix}. \tag{3.3.57}$$

If the terms in the matrix corresponding to the zero value are omitted, we can write

$$\overline{\omega}^s = 2 \begin{bmatrix} \varepsilon_4 & -\varepsilon_3 & \varepsilon_2 & -\varepsilon_1 \\ \varepsilon_3 & \varepsilon_4 & -\varepsilon_1 & -\varepsilon_2 \\ -\varepsilon_2 & \varepsilon_1 & \varepsilon_4 & -\varepsilon_3 \end{bmatrix} \dot{\overline{\varepsilon}} \tag{3.3.58}$$

and

$$\dot{\bar{\varepsilon}} = \frac{1}{2} \begin{bmatrix} \varepsilon_4 & \varepsilon_3 & -\varepsilon_2 \\ -\varepsilon_3 & \varepsilon_4 & \varepsilon_1 \\ \varepsilon_2 & -\varepsilon_1 & \varepsilon_4 \\ -\varepsilon_1 & -\varepsilon_2 & -\varepsilon_3 \end{bmatrix} \overline{\omega}^s \qquad (3.3.59)$$

This equation can be written in the form of a general coordinate transformation as

$$\overline{\omega}^s = \underline{\overline{\mathbf{G}}}^s \dot{\bar{\varepsilon}} \quad \text{and} \quad \dot{\bar{\varepsilon}} = \underline{\overline{\mathbf{G}^T}}_s \overline{\omega}^s \qquad (3.3.60)$$

It is also possible to obtain a relation between the Euler parameters and their time derivatives from equations (3.3.54)

$$\begin{bmatrix} \dot{\varepsilon}_1 \\ \dot{\varepsilon}_2 \\ \dot{\varepsilon}_2 \\ \dot{\varepsilon}_4 \end{bmatrix} = \frac{1}{2} \begin{bmatrix} 0 & \omega_{s3} & -\omega_{s2} & \omega_{s1} \\ -\omega_{s3} & 0 & \omega_{s1} & \omega_{s2} \\ \omega_{s2} & -\omega_{s1} & 0 & \omega_{s3} \\ -\omega_{s1} & -\omega_{s2} & -\omega_{s3} & 0 \end{bmatrix} \begin{bmatrix} \varepsilon_1 \\ \varepsilon_2 \\ \varepsilon_3 \\ \varepsilon_4 \end{bmatrix} \qquad (3.3.61)$$

$$\dot{\bar{\varepsilon}} = \tfrac{1}{2} \underline{\overline{\Omega}} \, \overline{\varepsilon} \qquad (3.3.62)$$

One of the disadvantages of the Euler parameters is the extra differential equation that has to be solved. During numerical integration, numerical round-off errors cause the parameters to violate the constraint equation and the rotation tensor becomes non-orthogonal. Normalising the parameters on a regular basis during the integration process can keep the rotation tensor orthogonal.

3.4 Multibody Dynamic Formulation

3.4.1 Generalised Coordinates

In the previous section, it has been shown that it is necessary to use six independent coordinates to describe the motion of a rigid body. If we want to describe the motion of N rigid bodies, six coordinates (three translations and three rotations) are needed for each body. Thus, a total of $6N$ coordinates are necessary to describe the motion of all the rigid bodies. If some of the bodies are connected, their motion is not independent and the coordinates are not independent. It may sometimes be advantageous to express the motion in a different set of coordinates. A general form of the coordinate transformation may be given for each body as (Greenwood, 1988:242, Meirovitch, 1970:73 and Shabana, 1994:184)

$$\overline{\mathbf{x}}_{(i)} = \overline{\mathbf{x}}_{(i)}(\overline{\mathbf{q}}, t), \qquad (i = 1, 2, \ldots, N) \qquad (3.4.1)$$

where $\overline{\mathbf{x}}_{(i)}$ is the vector of coordinates for a body describing the motion. The set of coordinates $\underline{\mathbf{q}} = [q_1 \quad q_2 \quad \ldots \quad q_n]$ is referred to as generalised coordinates. The number of degrees of freedom of a system coincides with the minimum number of independent coordinates necessary to describe the system uniquely. Physical constraints on the system may be interpreted as a restriction of the motion to a subspace of a corresponding smaller dimension, equal to the number of independent coordinates. It may not always be possible or advisable to eliminate the excess coordinates, making it necessary to work with a larger number of coordinates than the number of degrees of freedom would require. Auxiliary conditions equal in number to the number of coordinates exceeding the degrees of freedom must be included.

The set of generalised coordinates may not always have a physical meaning, nor is it unique, which implies that there may be more than one set of coordinates capable of describing the system. They must be finite, single-valued, continuous and differentiable with respect to time. Meirovitch (1970:48) describes the use of generalised coordinates as:

"... *shifting the emphasis from the physical world of vectorial mechanics to the more mathematical world of analytical mechanics.*"

By differentiating equation (3.4.1) with respect to time and by applying the chain rule of differentiation one obtains

$$\frac{d\overline{\mathbf{x}}_{(i)}}{dt} = \frac{\partial \overline{\mathbf{x}}_{(i)}}{\partial \overline{\mathbf{q}}} \frac{d\overline{\mathbf{q}}}{dt} + \frac{\partial \overline{\mathbf{x}}_{(i)}}{\partial t}$$
$$\Rightarrow \dot{\overline{\mathbf{x}}}_{(i)} = \frac{\partial \overline{\mathbf{x}}_{(i)}}{\partial \overline{\mathbf{q}}} \dot{\overline{\mathbf{q}}} + \frac{\partial \overline{\mathbf{x}}_{(i)}}{\partial t}$$

(3.4.2)

from which we can obtain the relation

$$\frac{\partial \dot{\overline{\mathbf{x}}}_{(i)}}{\partial \dot{\overline{\mathbf{q}}}} = \frac{\partial \overline{\mathbf{x}}_{(i)}}{\partial \overline{\mathbf{q}}}$$

(3.4.3)

3.4.2 Constraints

It has been said that the coordinates defining the motion of a system of bodies are not independent except for a system of free bodies, but are subject to certain auxiliary conditions or constraints. Consider a system described by n generalised coordinates. Suppose that there are m linearly independent constraint equations of the form

$$f_i(q_1, q_2, ..., q_n, t) = 0, \qquad\qquad (i = 1, 2, \ldots, m) \qquad (3.4.4)$$

The constraints restrict the motion of the system by applying additional reaction forces to the system. These reaction forces are called constraint forces. Reaction forces that are caused by friction are not included in the constraint forces, but are treated separately. The constraint equations can be expressed as the total differential of equation (3.4.4), namely,

$$df_i = \frac{\partial f_i}{\partial q_1} dq_1 + ... + \frac{\partial f_i}{\partial q_n} dq_n + \frac{\partial f_i}{\partial t} dt = 0, \quad (i = 1, 2, \ldots, m) \qquad (3.4.5)$$

The differential expression of equation (3.4.5) is said to be in Pfaffian form. The class of displacement with components dq_1, dq_2, . . . , dq_n , which the system may undergo in the time interval dt , is referred to as possible displacements. The actual displacement that the system undergoes is one of the totality of possible displacements. A more general form of constraint equations is

$$a_{i1}dq_1 + \ldots + a_{in}dq_n + a_{i0}dt = 0, \qquad (i = 1, 2, \ldots, m) \qquad (3.4.6)$$

If equation (3.4.6) is integrable, the integrated form of the equation would be the same as given by equation (3.4.4) and is classified as a holonomic constraint. If the equation is not integrable, the constraint is classified as a non-holonomic constraint. Constraints that restrict the position or geometry of a system are holonomic constraints. Those that restrict the motion or kinematics of the system are non-holonomic constraints (Huston, 1990).

We introduce another class of displacements, called virtual displacements. They are not true displacements, but infinitesimal changes in the coordinates consistent with the constraints. It is imagined that these displacements take place at the same time in a process that does not involve the time element. The virtual displacements satisfy the relations

$$\sum_{j=1}^{n} a_{ij}\delta q_j = 0, \qquad (i = 1, 2, \ldots, m) \qquad (3.4.7)$$

In general, virtual displacements are not possible displacements. It can be stated that the work performed by the constraint forces through the virtual displacements is zero if they are not friction forces. If Qc_j is the generalised constraint force corresponding to q_j then

$$\sum_{j=1}^{n} Qc_j \delta q_j = 0 \qquad (3.4.8)$$

for any set of virtual displacements satisfying equation (3.4.7).

By multiplying equation (3.4.7) by a factor λ_i, known as a Lagrange multiplier, and by writing an equation for each of the m constraints, we obtain

$$\lambda_i \sum_{j=1}^{n} a_{ij} \delta q_j = 0, \qquad\qquad (i = 1, 2, \ldots, m) \qquad\qquad (3.4.9)$$

By subtracting the sum of the m equations of (3.4.9) from (3.4.8) and interchanging the order of the summation, we obtain

$$\sum_{j=1}^{n} \left(Q_{C_j} - \sum_{i=1}^{m} \lambda_i a_{ij} \right) \delta q_j = 0, \qquad\qquad (3.4.10)$$

If we chose the λ's so that each of the coefficients of δq is zero in equation (3.4.10), then these equations will apply for all values of the δq, that is, they can be chosen arbitrarily. Hence we may assume that the λ's have values such that

$$Q_{C_j} = \sum_{i=1}^{m} \lambda_i a_{ij}, \qquad\qquad (j = 1, 2, \ldots, n) \qquad\qquad (3.4.11)$$

The constraint forces may vary with time, even for the case of fixed constraints. The λ's will in general be functions of time. The system with $n - m$ unknowns is replaced with one with $n + m$ unknowns, when the λ's are considered to be additional variables.

3.4.3 Absolute Coordinate Method

Generalised Coordinates

In this approach Cartesian coordinates are assigned to each body to define its location with respect to the inertial system, and orientation coordinates are assigned to define its attitude. The vector of the generalised coordinates for the body i'th in the system is defined as

$$\overline{\mathbf{q}}_{(i)} = \begin{bmatrix} \overline{\mathbf{r}}_{(i)}^{s} \\ \overline{\theta}_{(i)} \end{bmatrix} \qquad\qquad (3.4.12)$$

where $\overline{\mathbf{r}}_{(i)}^{s}$ is the vector defining the position of the body's centre of mass and $\overline{\theta}_{(i)}$ is the column vector of the components that describe the body's orientation. The components of the orientation can for example be the three Euler angles or the four Euler Parameters. The position vector is stated with respect to the inertial reference frame. We define the system's vector of generalised coordinates as the vector of the generalised body coordinates.

$$\overline{\mathbf{q}} = \begin{bmatrix} \overline{\mathbf{q}}_{(1)} \\ \overline{\mathbf{q}}_{(2)} \\ \vdots \\ \overline{\mathbf{q}}_{(N)} \end{bmatrix} \qquad\qquad (3.4.13)$$

The virtual displacement of the translation coordinates $\overline{\mathbf{r}}_{(i)}^{s}$ is given by $\delta\overline{\mathbf{r}}_{(i)}^{s}$ and can be stated in terms of the generalised coordinates as

$$\delta\overline{\mathbf{r}}_{(i)}^{s} = \frac{\partial\overline{\mathbf{r}}_{(i)}^{s}}{\partial\overline{\mathbf{q}}}\delta\overline{\mathbf{q}} = \frac{\partial\dot{\overline{\mathbf{r}}}_{(i)}^{s}}{\partial\dot{\overline{\mathbf{q}}}}\delta\overline{\mathbf{q}} \qquad\qquad (3.4.14)$$

Similarly, the virtual displacement of the orientation coordinates, stated in terms of the generalised coordinates is

$$\delta\overline{\theta}_{(i)} = \frac{\partial\overline{\theta}_{(i)}}{\partial\overline{\mathbf{q}}}\delta\overline{\mathbf{q}} = \frac{\partial\dot{\overline{\theta}}_{(i)}}{\partial\dot{\overline{\mathbf{q}}}}\delta\overline{\mathbf{q}} \qquad\qquad (3.4.15)$$

Coordinate Partitioning

It has been stated that if some of the bodies in the multibody system are connected to one another, components of the vector of generalised coordinates of equation (3.4.13) is not

independent. The auxiliary conditions or constraint conditions describing these connections are given by equation (3.4.4) and can be stated in Matrix Tensor Notation as

$$\overline{\mathbf{C}}(\overline{\mathbf{q}}, t) = \overline{\mathbf{0}} \qquad (3.4.16)$$

where $\overline{\mathbf{C}}$ is the vector of the m scalar constraint functions. A virtual change in the system coordinates is given by equation (3.4.7), which can be written as a matrix equation

$$\underline{\overline{\mathbf{C_q}}}\ \delta\overline{\mathbf{q}}\ = \overline{\mathbf{0}} \qquad (3.4.17)$$

The matrix $\underline{\overline{\mathbf{C_q}}} = \partial\overline{\mathbf{C}}/\partial\overline{\mathbf{q}}$ is the constraint Jacobian matrix.

The coordinate partitioning is used to arrange the order of the elements of the generalised coordinate vector that it can be grouped in two vectors: the m dimensional vector of dependent coordinates, $\overline{\mathbf{q}}_{dep}$ and the $n - m$ dimensional vector of independent coordinates, $\overline{\mathbf{q}}_{in}$. The vector of generalised coordinates can be written in the partitioned form

$$\overline{\mathbf{q}} = \begin{bmatrix} \overline{\mathbf{q}}_{dep} \\ \overline{\mathbf{q}}_{in} \end{bmatrix} \qquad (3.4.18)$$

By applying this coordinate partitioning to equation (3.4.17), one can write

$$\begin{bmatrix} \left[\underline{\overline{\mathbf{C_q}}}\right]_{dep} & \left[\underline{\overline{\mathbf{C_q}}}\right]_{in} \end{bmatrix} \begin{bmatrix} \delta\overline{\mathbf{q}}_{dep} \\ \delta\overline{\mathbf{q}}_{in} \end{bmatrix} = \overline{\mathbf{0}}$$

or

$$\left[\underline{\overline{\mathbf{C_q}}}\right]_{dep} \delta\overline{\mathbf{q}}_{dep} + \left[\underline{\overline{\mathbf{C_q}}}\right]_{in} \delta\overline{\mathbf{q}}_{in} = \overline{\mathbf{0}} \qquad (3.4.19)$$

where the vector $\overline{\mathbf{q}}_{dep}$ is selected such that the matrix $\left[\underline{\overline{\mathbf{C_q}}}\right]_{dep}$ is non-singular (Shabana, 1994:295). This is always possible if the constraint equations are linearly independent.

The coordinate partitioning is applied to make the numerical integration of the governing dynamic equation easier. Rismantab-Sany and Shabana (1989) discussed a numerical method that uses this coordinate partitioning technique. No algebraic manipulations are performed during the coordinate partitioning, it is only the positions of the elements that are changed.

Virtual Work and Generalised Force

It has been shown that the motion of any point (ρ) on a rigid body can be described by the translation of the centre of mass and a rotation about the centre of mass. If $\vec{\rho}$ is the position vector of a point in the rigid body, $\vec{r}$ the position vector of the centre of mass and $\vec{u}$ a vector from the centre of mass to the point then

$$\overline{\rho}^s = \overline{r}^s + \overline{u}^s, \tag{3.4.20}$$

and the velocity of this point is

$$\begin{aligned} \frac{d\overline{\rho}^s}{dt} &= \frac{d\overline{r}^s}{dt} + \underline{\widetilde{\omega}}^s_s \overline{u}^s \\ &= \frac{d\overline{r}^s}{dt} - \underline{\widetilde{\overline{u}}}^s_s \overline{\omega}^s \\ &= \frac{d\overline{r}^s}{dt} - \underline{\widetilde{\overline{u}}}^s_s \overline{G}^s \frac{d\overline{\theta}}{dt}. \end{aligned} \tag{3.4.21}$$

The incremental displacement that the point undergoes in a time interval dt can be obtained form equation (3.4.21) as

$$d\overline{\rho}^s = d\overline{r}^s - \underline{\widetilde{\overline{u}}}^s_s \overline{G}^s d\overline{\theta} \tag{3.4.22}$$

Virtual displacement of the point can then be obtained as:

$$\delta\overline{\rho}^{s} = \delta\overline{r}^{s} - \widetilde{\underline{\widetilde{u}}}_{s}^{s}\overline{G}^{s}\delta\overline{\theta} \tag{3.4.23}$$

If a force $\vec{F}$ is applied to point ρ on the rigid body, then the increment of work associated with the incremental displacement is

$$
\begin{aligned}
dW &= \underline{F}_{s}d\overline{\rho}^{s} \\
&= \underline{F}_{s}\left(d\overline{r}^{s} - \widetilde{\underline{\widetilde{u}}}_{s}^{s}\overline{G}^{s}d\overline{\theta}\right) \\
&= \underline{F}_{s}d\overline{r}^{s} + \left(\widetilde{\underline{\widetilde{u}}}_{s}^{s}\overline{F}^{s}\right)^{T}\overline{G}^{s}d\overline{\theta} \\
&= \underline{F}_{s}d\overline{r}^{s} + \underline{N}_{s}\overline{G}^{s}d\overline{\theta}
\end{aligned}
\tag{3.4.24}
$$

where $\vec{N}$ is the moment of the force about the body's centre of mass and $\overline{G}^{s}$ is a transformation matrix between the angular velocity vector and the first time derivative of the orientation coordinates.

Virtual work associated with this force is

$$\delta W = \underline{F}_{s}\delta\overline{r}^{s} + \underline{N}_{s}\overline{G}^{s}\delta\overline{\theta} \tag{3.4.25}$$

and can be written in terms of the generalised coordinates as

$$
\begin{aligned}
\delta W &= \underline{F}_{s}\left(\frac{\partial\overline{r}^{s}}{\partial\overline{q}}\delta\overline{q}\right) + \underline{N}_{s}\overline{G}^{s}\left(\frac{\partial\overline{\theta}}{\partial\overline{q}}\delta\overline{q}\right) \\
&= \left(\underline{F}_{s}\frac{\partial\overline{r}^{s}}{\partial\overline{q}} + \underline{N}_{s}\overline{G}^{s}\frac{\partial\overline{\theta}}{\partial\overline{q}}\right)\delta\overline{q} \\
&= \underline{Q}\,\delta\overline{q}
\end{aligned}
\tag{3.4.26}
$$

where $\underline{Q}$ is the generalised force vector.

Governing Dynamic Equation

The governing dynamics equations are obtained from the Newton-Euler equations. These equations must be transformed to the generalised coordinates if we want to apply them to the multibody system. We can write the Newton-Euler equations for the i'th body, subjected to a resultant applied force of $\underline{\mathbf{Fa}}_s^{(i)}$ and a resultant applied moment of $\underline{\mathbf{Na}}_s^{(i)}$ about its centre of mass (the contribution of the constraint forces will be included later), as

$$\underline{\mathbf{Fa}}_s^{(i)} = m_{(i)} \underline{\ddot{\mathbf{R}}}_s^{(i)} \tag{3.4.27}$$

$$\underline{\mathbf{Na}}_s^{(i)} = \underline{\dot{\omega}}_s^{(i)} \overline{\mathbf{J}_{(i)}}_s^s - \underline{\omega}_s^{(i)} \overline{\mathbf{J}_{(i)}}_s^s \underline{\widetilde{\omega_{(i)}}}_s^s \tag{3.4.28}$$

The relation between the angular velocity and the first time derivative of the orientation coordinates is given by the transformation

$$\overline{\omega}^s = \overline{\underline{\mathbf{G}}}^s \underline{\dot{\theta}} \tag{3.4.29}$$

The general equation for angular acceleration can be obtained by differentiating the above equation with respect to time.

$$\dot{\overline{\omega}}^s = \overline{\underline{\mathbf{G}}}^s \underline{\ddot{\theta}} + \dot{\overline{\underline{\mathbf{G}}}}^s \underline{\dot{\theta}} \tag{3.4.30}$$

By applying D'Alembert's principle and the angular acceleration transformation stated above, the Newton-Euler equations can be written in the form

$$\underline{\mathbf{Fa}}_s^{(i)} - m_{(i)} \underline{\ddot{\mathbf{r}}}_s^{(i)} = \underline{\mathbf{0}}_s \tag{3.4.31}$$

$$\underline{\mathbf{Na}}_s^{(i)} - \underline{\ddot{\theta}}^{(i)T} \overline{\mathbf{G}_{(i)}^T}_s \overline{\mathbf{J}_{(i)}}_s^s - \underline{\dot{\theta}}^{(i)T} \overline{\dot{\mathbf{G}_{(i)}^T}}_s \overline{\mathbf{J}_{(i)}}_s^s + \underline{\omega}_s^{(i)} \overline{\mathbf{J}_{(i)}}_s^s \underline{\widetilde{\omega_{(i)}}}_s^s = \underline{\mathbf{0}}_s \tag{3.4.32}$$

By applying the principle of virtual work to both the translation and rotation equations and adding them, it is possible to write the total virtual work for the *i'th* body as

$$\delta Wa_{(i)} + \delta Wi_{(i)} = 0 \tag{3.4.33}$$

where $\delta Wa_{(i)}$ is the virtual work of the applied force and moment system that can be written in terms of the generalised coordinates and generalised applied force ($\mathbf{Qa}^{(i)}$) as

$$
\begin{aligned}
\delta Wa_{(i)} &= \left(\underline{\mathbf{Fa}}_s^{(i)} \frac{\partial \overline{\mathbf{r}}_{(i)}^s}{\partial \overline{\mathbf{q}}} + \underline{\mathbf{Na}}_s^{(i)} \overline{\mathbf{G}_{(i)}}^s \frac{\partial \overline{\boldsymbol{\theta}}_{(i)}}{\partial \overline{\mathbf{q}}} \right) \delta \overline{\mathbf{q}} \\
&= \underline{\mathbf{Qa}}^{(i)} \delta \overline{\mathbf{q}},
\end{aligned}
\tag{3.4.34}
$$

and $\delta Wi_{(i)}$ is the virtual work of the inertial force and moment that can be written in terms of the generalised coordinates and generalised inertial force ($\underline{\mathbf{Qi}}^{(i)}$) as

$$
\begin{aligned}
\delta Wi_{(i)} &= \left(\underline{\mathbf{Fi}}_s^{(i)} \frac{\partial \overline{\mathbf{r}}_{(i)}^s}{\partial \overline{\mathbf{q}}} + \underline{\mathbf{Ni}}_s^{(i)} \overline{\mathbf{G}_{(i)}}^s \frac{\partial \overline{\boldsymbol{\theta}}_{(i)}}{\partial \overline{\mathbf{q}}} \right) \delta \overline{\mathbf{q}} \\
&= \underline{\mathbf{Qi}}^{(i)} \delta \overline{\mathbf{q}}.
\end{aligned}
\tag{3.4.35}
$$

The generalised inertial force is defined (using equations (3.4.31) and (3.4.32)) as

$$
\begin{aligned}
\underline{\mathbf{Qi}}^{(i)} &= -\left(m_{(i)} \underline{\ddot{\mathbf{r}}}_s^{(i)} \right) \frac{\partial \overline{\mathbf{r}}_{(i)}^s}{\partial \overline{\mathbf{q}}} - \left(\underline{\ddot{\boldsymbol{\theta}}}^{T\,(i)} \overline{\mathbf{G}_{(i)}^T}_s \overline{\mathbf{J}_{(i)}}_s^s + \underline{\dot{\boldsymbol{\theta}}}^{T\,(i)} \overline{\mathbf{G}_{(i)}^T}_s \overline{\dot{\mathbf{J}}_{(i)}}_s^s - \underline{\boldsymbol{\omega}}_s^{(i)} \overline{\mathbf{J}_{(i)}}_s^s \overline{\tilde{\boldsymbol{\omega}}_{(i)}}_s^s \right) \overline{\mathbf{G}_{(i)}}^s \frac{\partial \overline{\boldsymbol{\theta}}_{(i)}}{\partial \overline{\mathbf{q}}} \\
&= -\begin{bmatrix} \underline{\ddot{\mathbf{r}}}_s^{(i)} & \underline{\ddot{\boldsymbol{\theta}}}^{T\,(i)} \end{bmatrix} \begin{bmatrix} m_{(i)} \dfrac{\partial \overline{\mathbf{r}}_{(i)}^s}{\partial \overline{\mathbf{q}}} \\[2mm] \overline{\mathbf{G}_{(i)}^T}_s \overline{\mathbf{J}_{(i)}}_s^s \overline{\mathbf{G}_{(i)}}^s \dfrac{\partial \overline{\boldsymbol{\theta}}_{(i)}}{\partial \overline{\mathbf{q}}} \end{bmatrix} \\
&\quad - \left(\underline{\dot{\boldsymbol{\theta}}}^{T\,(i)} \overline{\mathbf{G}_{(i)}^T}_s \overline{\dot{\mathbf{J}}_{(i)}}_s^s - \underline{\boldsymbol{\omega}}_s^{(i)} \overline{\mathbf{J}_{(i)}}_s^s \overline{\tilde{\boldsymbol{\omega}}_{(i)}}_s^s \right) \overline{\mathbf{G}_{(i)}}^s \frac{\partial \overline{\boldsymbol{\theta}}_{(i)}}{\partial \overline{\mathbf{q}}} \\
&= -\underline{\ddot{\mathbf{q}}}^{T\,(i)} \overline{\mathbf{M}_{(i)}} - \underline{\mathbf{h}}^{(i)}
\end{aligned}
\tag{3.4.36}
$$

where

$$\overline{\mathbf{M}}_{(i)} = \begin{bmatrix} m_{(i)} \dfrac{\partial \overline{\mathbf{r}}_{(i)}^s}{\partial \overline{\mathbf{q}}} \\ \overline{\mathbf{G}_{(i)}^T \ {}_s\mathbf{J}_{(i)} \ {}_s\mathbf{G}_{(i)}}^s \dfrac{\partial \overline{\mathbf{\theta}}_{(i)}}{\partial \overline{\mathbf{q}}} \end{bmatrix} \quad \text{and}$$

$$\mathbf{h}^{(i)} = \left(\underline{\dot{\mathbf{\theta}}^{T\ (i)}} \ \overline{\mathbf{G}_{(i)}^T}_s \ \overline{\dot{\mathbf{J}}_{(i)}}_s^s - \underline{\mathbf{\omega}}_s^{(i)} \overline{\mathbf{J}_{(i)}}_s^s \ \overline{\widetilde{\mathbf{\omega}}_{(i)}}_s^s \right) \overline{\mathbf{G}_{(i)}}^s \dfrac{\partial \overline{\mathbf{\theta}}_{(i)}}{\partial \overline{\mathbf{q}}}$$

The system's generalised coordinate vector has been defined in equation (3.4.13) as the vector of generalised body coordinates or

$$\overline{\mathbf{q}} = \begin{bmatrix} \overline{\mathbf{q}}_{(1)} \\ \vdots \\ \overline{\mathbf{q}}_{(N)} \end{bmatrix}.$$

Similar to the vector of generalised coordinates, the system's vectors of generalised inertial forces and generalised applied forces are defined as the vectors of the generalised body forces.

$$\underline{\mathbf{Qi}} = \begin{bmatrix} \underline{\mathbf{Qi}}^{(1)} & \underline{\mathbf{Qi}}^{(2)} & \dots & \underline{\mathbf{Qi}}^{(N)} \end{bmatrix} \tag{3.4.37}$$

$$\underline{\mathbf{Qa}} = \begin{bmatrix} \underline{\mathbf{Qa}}^{(1)} & \underline{\mathbf{Qa}}^{(2)} & \dots & \underline{\mathbf{Qa}}^{(N)} \end{bmatrix} \tag{3.4.38}$$

By using equation (3.4.36) on each body's inertial force vector, the system's generalised inertial force vector can be written in the form

$$\underline{\mathbf{Qi}} = -\underline{\ddot{\mathbf{q}}}^T \begin{bmatrix} \overline{\mathbf{M}_{(1)}} \\ \overline{\mathbf{M}_{(2)}} \\ \overline{\mathbf{M}_{(3)}} \\ \vdots \\ \overline{\mathbf{M}_{(N)}} \end{bmatrix} - \begin{bmatrix} \underline{\mathbf{h}}^{(1)} & \underline{\mathbf{h}}^{(2)} & \underline{\mathbf{h}}^{(3)} & \ldots & \underline{\mathbf{h}}^{(N)} \end{bmatrix} \qquad (3.4.39)$$

This equation can be simplified into a single matrix equation

$$\underline{\mathbf{Qi}} = -\underline{\ddot{\mathbf{q}}}^T \, \overline{\mathbf{M}} - \underline{\mathbf{h}} \qquad (3.4.40)$$

By introducing the system's generalised applied and inertial forces in equations (3.4.34) and (3.4.35), the virtual work of the total system can then be obtained as

$$\delta Wa + \delta Wi = 0 \qquad (3.4.41)$$

We have seen previously that the generalised constraint forces, $\mathbf{Qc}$, do no work during virtual displacements.

$$\delta Wc = 0 \qquad (3.4.42)$$

If equation (3.4.42) is added to equation (3.4.41), one can write the virtual work of the system as

$$\delta Wa + \delta Wc + \delta Wi = 0 \qquad (3.4.43)$$

$$\Rightarrow \underline{\mathbf{Qa}} \, \delta\overline{\mathbf{q}} \ + \underline{\mathbf{Qc}} \, \delta\overline{\mathbf{q}} \ + \underline{\mathbf{Qi}} \, \delta\overline{\mathbf{q}} \ = 0 \qquad (3.4.44)$$

The vector of generalised constraint forces is stated by equation (3.4.11), which can be written in matrix form as

$$\underline{\mathbf{Qc}} = \underline{\lambda}^T \, \overline{\mathbf{C_q}} \qquad (3.4.45)$$

By introducing equation (3.4.45) in equation (3.4.44) we can write

$$\left(\mathbf{Qa} + \underline{\lambda}^T \, \overline{\mathbf{C_q}} + \mathbf{Qi}\right)\delta\overline{\mathbf{q}} = 0 \tag{3.4.46}$$

If some of the bodies are connected, the coefficients of the vector of virtual displacements $\delta\overline{\mathbf{q}}^s$, in equation (3.4.46), cannot be set equal to zero, because the coordinates are not independent (Shabana, 1994:295). If we apply the coordinate partitioning of equation (3.4.19), equation (3.4.46) can be written as

$$\left(\left[\underline{\mathbf{Qa}}^{dep} \quad \underline{\mathbf{Qa}}^{in}\right] + \underline{\lambda}^T\left[\left[\overline{\mathbf{C_q}}\right]_{dep} \quad \left[\overline{\mathbf{C_q}}\right]_{in}\right] + \left[\underline{\mathbf{Qi}}^{dep} \quad \underline{\mathbf{Qi}}^{in}\right]\right)\begin{bmatrix}\delta\overline{\mathbf{q}}_{dep} \\ \delta\overline{\mathbf{q}}_{in}\end{bmatrix} = 0$$

$$\left[\underline{\mathbf{Qa}}^{dep} + \underline{\lambda}^T\left[\overline{\mathbf{C_q}}\right]_{dep} + \underline{\mathbf{Qi}}^{dep}\right]\delta\overline{\mathbf{q}}_{dep} + \left[\underline{\mathbf{Qa}}^{in} + \underline{\lambda}^T\left[\overline{\mathbf{C_q}}\right]_{in} + \underline{\mathbf{Qi}}^{in}\right]\delta\overline{\mathbf{q}}_{in} = 0 \tag{3.4.47}$$

Since the elements of the vector $\delta\overline{\mathbf{q}}_{in}^s$ are independent, the following relation can be written from equation (3.4.49)

$$\underline{\mathbf{Qa}}^{in} + \underline{\lambda}^T\left[\overline{\mathbf{C_q}}\right]_{in} + \underline{\mathbf{Qi}}^{in} = \underline{0} \tag{3.4.48}$$

Equation (3.4.47) can now be written in two separate matrix equations

$$\left(\underline{\mathbf{Qa}}^{in} + \underline{\lambda}^T\left[\overline{\mathbf{C_q}}\right]_{in} + \underline{\mathbf{Qi}}^{in}\right)\delta\overline{\mathbf{q}}_{in} = 0 \tag{3.4.49}$$

$$\left(\underline{\mathbf{Qa}}^{dep} + \underline{\lambda}^T\left[\overline{\mathbf{C_q}}\right]_{dep} + \underline{\mathbf{Qi}}^{dep}\right)\delta\overline{\mathbf{q}}_{dep} = 0 \tag{3.4.50}$$

It was previously stated that the dependent coordinates could be selected such that the matrix $\left[\overline{\mathbf{C_q}}\right]_{dep}$ is square and non-singular. The vector of Lagrange multipliers can then be selected to be the unique solution of the expression

$$\underline{\lambda}^T \left[\overline{\underline{C_q}} \right]_{dep} = -\underline{Qa}^{dep} - \underline{Qi}^{dep} \tag{3.4.51}$$

This choice of Lagrange multipliers guarantees that the coefficients of the elements of the vector of dependent variables, $\delta \overline{\mathbf{q}}_{dep}^s$, in equation (3.4.50) are equal to zero.

By combining equation (3.4.49) and equation (3.4.51), one obtains

$$\left[\underline{Qi}^{dep} \quad \underline{Qi}^{in} \right] + \underline{\lambda}^T \left[\left[\overline{\underline{C_q}} \right]_{dep} \quad \left[\overline{\underline{C_q}} \right]_{in} \right] = -\left[\underline{Qa}^{dep} \quad \underline{Qa}^{in} \right] \tag{3.4.52}$$

that can be written in the general form

$$\underline{Qi} + \underline{\lambda}^T \, \overline{\underline{C_q}} = -\underline{Qa} \tag{3.4.53}$$

If equation (3.4.40) is introduced, one can write

$$\left[\underline{\ddot{q}}^T \quad -\underline{\lambda}^T \right] \left[\frac{\overline{\mathbf{M}}}{\underline{C_q}} \right] = \left[\underline{Qa} - \underline{h} \right] \tag{3.4.54}$$

The vector of generalised accelerations, $\overline{\ddot{\mathbf{q}}}$, and the vector of Lagrange multipliers, $\overline{\lambda}$, are the unknowns in equation (3.4.54). It can be seen that equation (3.4.54) contains n equations with $n + m$ unknowns. To solve this set of equations, m additional equations are needed. These equations are obtained from the auxiliary conditions given by equation (3.4.16). If one applies the chain rule of differentiation and differentiates equation (3.4.16) twice, with respect to time, one obtains a linear system of equations in the generalised acceleration vector, $\overline{\ddot{\mathbf{q}}}$, namely

$$\left(\frac{d}{dt} \overline{\underline{C_q}} \right) \dot{\overline{\mathbf{q}}} + \overline{\underline{C_q}} \, \ddot{\overline{\mathbf{q}}} + \frac{d}{dt} \left(\frac{\partial \overline{\mathbf{C}}}{\partial t} \right) = \overline{\mathbf{0}}$$

$$\Rightarrow \overline{\underline{C_q}} \, \ddot{\overline{\mathbf{q}}} = \overline{\mathbf{Qd}^T} \tag{3.4.55}$$

where $\mathbf{Qd}$ is the vector that represents the vector sum of the other terms. If the generalised coordinate and velocity vectors are known the coefficient matrix $\overline{\mathbf{C_q}}$ and the vector $\mathbf{Qd}$ can be evaluated. Equation (3.4.54) and equation (3.4.55) can be combined in one matrix equation as

$$\begin{bmatrix} \ddot{\underline{q}}^T & -\underline{\lambda}^T \end{bmatrix} \begin{bmatrix} \overline{\mathbf{M}} & \overline{\mathbf{C_q}^T} \\ \overline{\mathbf{C_q}} & \overline{\mathbf{0}} \end{bmatrix} = \begin{bmatrix} (\mathbf{Qa}-\underline{\mathbf{h}}) & \mathbf{Qd} \end{bmatrix} \qquad (3.4.56)$$

The above equation represents a system of loosely coupled equations. From this system of equations, the generalised accelerations, $\ddot{\overline{q}}$, and the vector of Lagrange multipliers, $\overline{\lambda}$, can be solved. For a given set of initial conditions, the vector of generalised accelerations can be integrated to determine the coordinates and velocities. The vector of Lagrange multipliers can be used to determine the generalised constraint forces that can be used to determine the actual reactions. When Euler Parameters is used to describe the orientation of the system's bodies, the set of constraints stated by equation (3.3.49) must be complied. This can either be achieved by introducing additional Lagrange multipliers and constraint equations in equation (3.4.56) or be incorporated in the numerical integration method. One numerical method with this property will be discussed in paragraph (3.6.3). It was found that the violations of these constraints are not very significant when a general numerical integration method is used and they are not included in equation (3.4.56); it is only necessary to normalise the parameters on a regular basis.

It is important to emphasise that, because of approximations occurring during the numerical integration process, the coordinates and velocities are not exact. The constraints of equation (3.4.16) will be violated to a degree depending on the accuracy of numerical integration method. The accuracy of the integration method depends on the order as well as the selected step size. In certain applications the violation of the constrains may be small and can be neglected, but in other applications it may be significant. Wehage (1980) proposed a method using the generalised coordinate partitioning of equation (3.4.19). This partitioning is applied to the vector of generalised accelerations. The independent accelerations are integrated forward in time to determine the independent coordinates and

velocities. An iterative Newton-Raphson algorithm can then be used to solve the nonlinear algebraic constraint equations for the dependent variables. Rismantab-Sany and Shabana (1989) compared the two methods of solving the equations of motion. They could not find a definite answer to which method yielded a better solution, except that the algorithm to integrate all the coordinates used less CPU time. Choi, *et al.* (1998a) experienced numerical difficulties with this method.

3.4.4 Relative Coordinate Method

Most multibody systems can be characterised as chains. If the multibody system has a tree structure, the motion of one body can be expressed relative to the preceding body. The motion of the first body in a chain, called the base-body, is expressed relative to the inertial system. If there are closed loops in a chain, it does not have a tree structure, but a spanning tree structure can be obtained by making cuts at a secondary joint in the closed loop. The connectivity conditions at this joint can be represented with constraint equations or a penalty function.

In the relative coordinate method, relative joint coordinates are used as a set of generalised coordinates and the equation of motion is formulated in terms of the joint degrees of freedom (Kim and Vanderploeg, 1986). This method uses Lagrange's form of d'Alembert's principle, also called Kane's equation, which provides the automatic elimination of the non-working internal constraint forces without introducing tedious differentiation or other calculations (Huston and Passerello, 1979). A minimum set of strongly coupled equations is obtained. The first time derivatives of the generalised coordinates are very important in the derivation of the equation of motion and are called the vector of generalised speeds.

It is easy to develop the governing dynamics equations for any general multibody system with a tree structure, because the geometry of the system is included in the vector of generalised coordinates. Choi, *et al.* (1998b) found that although this formulation leads to a minimum set of coordinates, the numerical algorithms are inefficient for chains that consist of a large number of bodies.

Describing the Geometry

An accounting procedure, describing the multibody system's configuration, is needed for the recursive description of the kinematic relations. Consider a system of bodies connected with joints that allow relative translation and rotations. The first step in describing the geometry is to number the bodies. One of the bodies is arbitrarily selected as the base-body and numbered as *Body* 1. The rest of the bodies is numbered in ascending progression away from the base-body, moving from branch to branch in the system until all the bodies are numbered. Each body, except the base-body, will have only one adjacent lower numbered body. This property will be used in the description of the geometry.
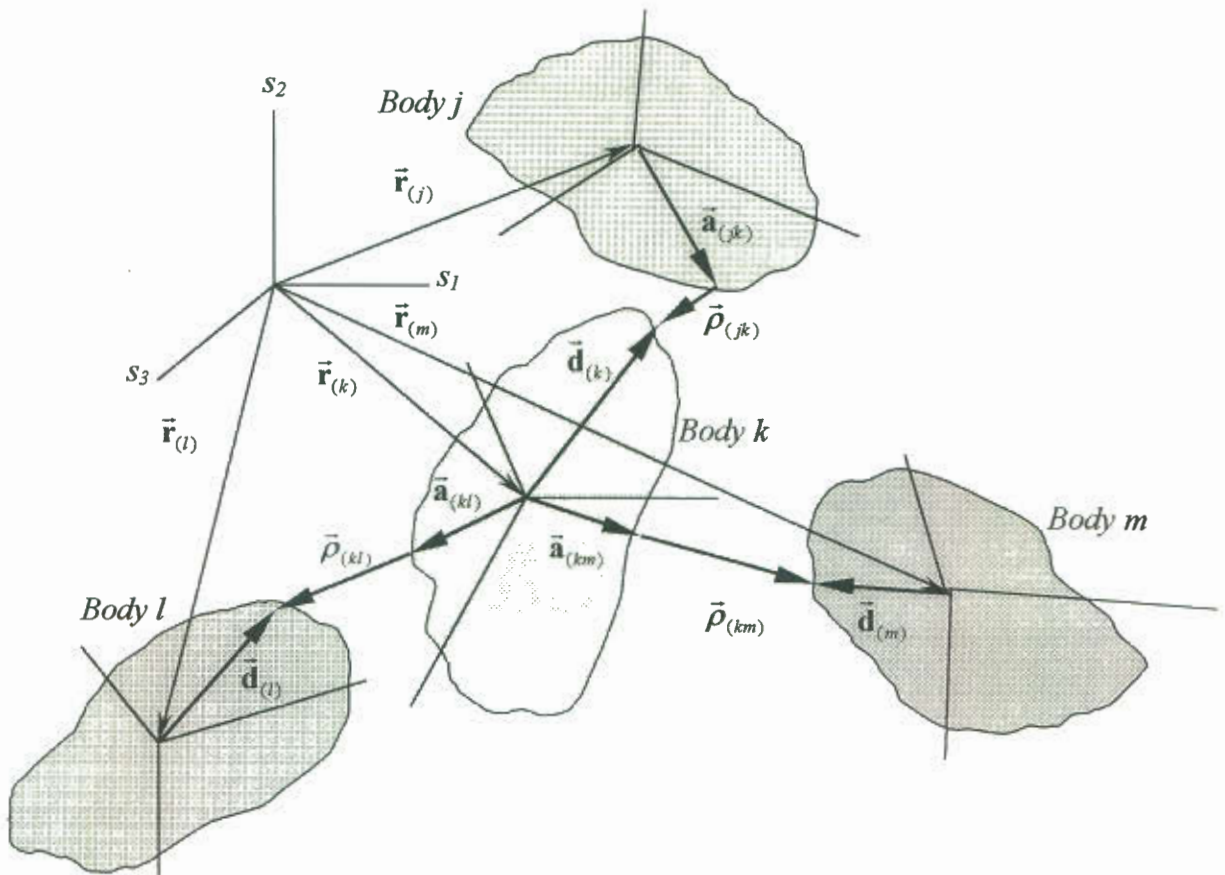
Figure 3.7   *Four bodies of a multibody system with the vectors that describe the geometry of the system and the position of the bodies.*

55

Figure (3.7) shows four bodies in the system; *Body j* is the predecessor of *Body k* and *Bodies l* and *m* are connected to *Body k*. Let the vector $\vec{r}$ describe the position of the centre of mass of the body relative to the inertial system. Let $\vec{a}$ be a vector, fixed in the body, that points from the centre of mass of the body to the position of an outboard joint. Let $\vec{d}$ be the vector, fixed in the body, that points from the centre of mass of the body to the position of the joint with the inboard body. It is clear that a body can have more that one $\vec{a}$ vector, but only one $\vec{d}$ vector because of the numbering procedure. The vector $\vec{\rho}$ defines the displacement in the joint.

A distinction is made among the $\vec{r}$ and $\vec{d}$ vectors of the different bodies by adding the body number as an index (written in brackets) to the vector. The $\vec{a}$ and $\vec{\rho}$ are named similarly to the method used for relative vectors discussed in the notation. An index is added that consist of the body number in which the vector is and the body number to which it points. This index is also written in brackets.

Recursive Description and Coordinate Transformation

We have stated that it is very easy to describe the kinematic relations for a system with a tree structure with recursive algorithms. All the kinematic relations of a body will be expressed relative to the predecessor or inboard body. In Figure (3.7) *Body j* is the predecessor of *Body k*. We assume that the following kinematic magnitudes of *Body j* are known:

(1) The absolute position of the body's centre of mass.
(2) The orientation of the body with respect to the inertial system.
(3) The absolute velocity of the body's centre of mass.
(4) The absolute angular velocity of the body.

If the multibody system's body-connecting configuration does not change during the time it is studied, the generalised coordinate transformation of equation (3.4.1) is not time dependent. The partial derivative of the body coordinates with respect to time is equal to zero and the relation of equation (3.4.2) simplifies to

$$\dot{\overline{\mathbf{x}}}_{(i)} = \frac{\partial \overline{\mathbf{x}}_{(i)}}{\partial \mathbf{q}} \dot{\overline{\mathbf{q}}} = \frac{\partial \dot{\overline{\mathbf{x}}}_{(i)}}{\partial \dot{\mathbf{q}}} \dot{\overline{\mathbf{q}}} \tag{3.4.57}$$

The vector of generalised speed is formed from the absolute velocity and angular velocity of the base-body and the relative velocity and angular velocity between connecting bodies.

$$\dot{\overline{\mathbf{q}}} = \overline{\mathbf{y}} = \left[\underline{\omega}_s^{(1)} \quad \cdots \quad \underline{\omega}_j^{(jk)} \quad \cdots \quad \underline{\omega}_{N-1}^{(\{N-1\}N)} \quad \dot{\underline{\mathbf{r}}}_s^{(1)} \quad \cdots \quad \dot{\underline{\rho}}_j^{(jk)} \quad \cdots \quad \dot{\underline{\rho}}_{N-1}^{(\{N-1\}N)} \right]^T \tag{3.4.58}$$

The absolute angular velocity of rigid *Body k* in a chain system is expressed in terms of the absolute angular velocity of the inboard body, *Body j*, and the relative angular velocity between the two bodies.

$$\vec{\omega}_{(k)} = \vec{\omega}_{(j)} + \vec{\omega}_{(jk)} \tag{3.4.59}$$

where $\vec{\omega}_{(jk)}$ is the relative angular velocity vector. We can state equation (3.4.59) in orthogonal base notation, with respect to base $\vec{\underline{\mathbf{E}}}_s$ as

$$\overline{\omega}_{(k)}^s = \overline{\omega}_{(j)}^s + \overline{\omega}_{(jk)}^s$$
$$= \overline{\omega}_{(j)}^s + \overline{\underline{\mathbf{E}}}_j^s \overline{\omega}_{(jk)}^j \tag{3.4.60}$$

In equation (3.4.57), it has been shown that the partial derivative of the body coordinates with respect to the vector of generalised speed is needed to express the derivatives of the body coordinates in terms of the generalised coordinates. The vector of generalised speed can express the angular velocity as

$$\overline{\omega}_{(i)}^s = \frac{\partial \overline{\omega}_{(i)}^s}{\partial \mathbf{y}} \overline{\mathbf{y}} \tag{3.4.61}$$

The matrix $\partial\overline{\omega}^s_{(i)}\big/\partial\overline{\mathbf{y}}$ is called the Jacobian matrix of the absolute angular velocity or the partial angular velocity array (Huston, 1990). It is obtained by taking the partial derivative of equation (3.4.60) with respect to the vector of generalised speed

$$
\begin{aligned}
\frac{\partial\overline{\omega}^s_{(k)}}{\partial\overline{\mathbf{y}}} &= \frac{\partial\overline{\omega}^s_{(j)}}{\partial\overline{\mathbf{y}}} + \frac{\partial}{\partial\overline{\mathbf{y}}}\left(\overline{\mathbf{E}}^s_j\,\overline{\omega}^j_{(jk)}\right) \\
&= \frac{\partial\overline{\omega}^s_{(j)}}{\partial\overline{\mathbf{y}}} + \overline{\mathbf{E}}^s_j\left(\frac{\partial\overline{\omega}^j_{(jk)}}{\partial\overline{\mathbf{y}}}\right)
\end{aligned}
\tag{3.4.62}
$$

The angular acceleration vector, $\dot{\overline{\omega}}^s_{(j)}$, can be obtained by taking the time derivative of equation (3.4.61) as

$$
\dot{\overline{\omega}}^s_{(j)} = \frac{\partial\overline{\omega}^s_{(j)}}{\partial\overline{\mathbf{y}}}\dot{\overline{\mathbf{y}}} + \frac{d}{dt}\left(\frac{\partial\overline{\omega}^s_{(j)}}{\partial\overline{\mathbf{y}}}\right)\overline{\mathbf{y}}
\tag{3.4.63}
$$

The time derivative of the angular velocity Jacobian matrix is obtained by differentiating equation (3.4.62) with respect to time.

$$
\begin{aligned}
\frac{d}{dt}\left(\frac{\partial\overline{\omega}^s_{(k)}}{\partial\overline{\mathbf{y}}}\right) &= \frac{d}{dt}\left(\frac{\partial\overline{\omega}^s_{(j)}}{\partial\overline{\mathbf{y}}}\right) + \frac{d}{dt}\left(\overline{\mathbf{E}}^s_j\,\frac{\partial\overline{\omega}^j_{(jk)}}{\partial\overline{\mathbf{y}}}\right) \\
&= \frac{d}{dt}\left(\frac{\partial\overline{\omega}^s_{(j)}}{\partial\overline{\mathbf{y}}}\right) + \widetilde{\underline{\omega^s_{(j)}}}_s\,\overline{\mathbf{E}}^s_j\,\frac{\partial\overline{\omega}^j_{(jk)}}{\partial\overline{\mathbf{y}}}
\end{aligned}
\tag{3.4.64}
$$

The position of the centre of mass of a body can be obtained from the position of the centre of mass of the inboard body (Figure 3.7).

$$
\vec{\mathbf{r}}_{(k)} = \vec{\mathbf{r}}_{(j)} + \vec{\mathbf{a}}_{(jk)} + \vec{\rho}_{(jk)} - \vec{\mathbf{d}}_{(k)}
\tag{3.4.65}
$$

which can be stated in orthogonal base notation, with respect to base $\vec{\underline{\mathbf{E}}}_s$, as

$$\overline{\mathbf{r}}_{(k)}^{s} = \overline{\mathbf{r}}_{(j)}^{s} + \overline{\mathbf{E}}_{j}^{s}\overline{\mathbf{a}}_{(jk)}^{j} + \overline{\mathbf{E}}_{j}^{s}\overline{\rho}_{(jk)}^{j} - \overline{\mathbf{E}}_{k}^{s}\overline{\mathbf{d}}_{(k)}^{k}.$$ (3.4.66)

Assuming that the absolute velocity vector can be expressed as a matrix product with the vector of generalised speeds, it is possible to write an equation similar to equation (3.4.57) for *Body j*

$$\dot{\overline{\mathbf{r}}}_{(j)}^{s} = \overline{\mathbf{V}_{(j)}}^{s}\overline{\mathbf{y}}$$ (3.4.67)

where $\overline{\mathbf{V}_{(j)}}^{s}$ is the velocity transformation matrix for *Body j*, also called the partial velocity array (Huston, 1990). Taking the time derivative of equation (3.4.66) and performing algebraic manipulations, the absolute velocity of body *k*'s centre of mass is

$$
\begin{aligned}
\dot{\overline{\mathbf{r}}}_{(k)}^{s} &= \dot{\overline{\mathbf{r}}}_{(j)}^{s} + \overline{\tilde{\boldsymbol{\omega}}_{(j)}}_{s}^{s}\overline{\mathbf{E}}_{j}^{s}\overline{\mathbf{a}}_{(jk)}^{j} + \overline{\tilde{\boldsymbol{\omega}}_{(j)}}_{s}^{s}\overline{\mathbf{E}}_{j}^{s}\overline{\rho}_{(jk)}^{j} + \overline{\mathbf{E}}_{j}^{s}\dot{\overline{\rho}}_{(jk)}^{j} - \overline{\tilde{\boldsymbol{\omega}}_{(k)}}_{s}^{s}\overline{\mathbf{E}}_{k}^{s}\overline{\mathbf{d}}_{(k)}^{k} \\
&= \overline{\mathbf{V}_{(j)}}^{s}\overline{\mathbf{y}} - \overline{\tilde{\mathbf{a}}_{(jk)}}_{s}^{s}\frac{\partial\overline{\boldsymbol{\omega}}_{(j)}^{s}}{\partial\overline{\mathbf{y}}}\overline{\mathbf{y}} - \overline{\tilde{\rho}_{(jk)}}_{s}^{s}\frac{\partial\overline{\boldsymbol{\omega}}_{(j)}^{s}}{\partial\overline{\mathbf{y}}}\overline{\mathbf{y}} + \overline{\tilde{\mathbf{d}}_{(k)}}_{s}^{s}\frac{\partial\overline{\boldsymbol{\omega}}_{(k)}^{s}}{\partial\overline{\mathbf{y}}}\overline{\mathbf{y}} + \overline{\mathbf{E}}_{j}^{s}\frac{\partial\dot{\overline{\rho}}_{(jk)}^{j}}{\partial\overline{\mathbf{y}}}\overline{\mathbf{y}} \\
&= \left[\overline{\mathbf{V}_{(j)}}^{s} - \left(\overline{\tilde{\mathbf{a}}_{(jk)}}_{s}^{s} + \overline{\tilde{\rho}_{(jk)}}_{s}^{s}\right)\frac{\partial\overline{\boldsymbol{\omega}}_{(j)}^{s}}{\partial\overline{\mathbf{y}}} + \overline{\tilde{\mathbf{d}}_{(k)}}_{s}^{s}\frac{\partial\overline{\boldsymbol{\omega}}_{(k)}^{s}}{\partial\overline{\mathbf{y}}} + \overline{\mathbf{E}}_{j}^{s}\frac{\partial\dot{\overline{\rho}}_{(jk)}^{j}}{\partial\overline{\mathbf{y}}}\right]\overline{\mathbf{y}} \\
&= \overline{\mathbf{V}_{(k)}}^{s}\overline{\mathbf{y}}
\end{aligned}
$$ (3.4.68)

where

$$\overline{\mathbf{V}_{(k)}}^{s} = \overline{\mathbf{V}_{(j)}}^{s} - \left(\overline{\tilde{\mathbf{a}}_{(jk)}}_{s}^{s} + \overline{\tilde{\rho}_{(jk)}}_{s}^{s}\right)\frac{\partial\overline{\boldsymbol{\omega}}_{(j)}^{s}}{\partial\overline{\mathbf{y}}} + \overline{\tilde{\mathbf{d}}_{(k)}}_{s}^{s}\frac{\partial\overline{\boldsymbol{\omega}}_{(k)}^{s}}{\partial\overline{\mathbf{y}}} + \overline{\mathbf{E}}_{j}^{s}\frac{\partial\dot{\overline{\rho}}_{(jk)}^{j}}{\partial\overline{\mathbf{y}}}$$ (3.4.69)

It can be seen that the assumption that has been made in equation (3.4.67) is correct if the partial velocity array of the inboard body is known. The acceleration of the centre of mass of a body is obtained by taking the time derivative of equation (3.4.68).

$$\ddot{\overline{\mathbf{r}}}_{(k)}^{s} = \overline{\mathbf{V}_{(k)}}^{s}\dot{\overline{\mathbf{y}}} + \left(\frac{d}{dt}\overline{\mathbf{V}_{(k)}}^{s}\right)\overline{\mathbf{y}}$$ (3.4.70)

We obtain the time derivative of the velocity transformation matrix by taking the time derivative of equation (3.4.69) as

$$
\frac{d}{dt}\overline{\mathbf{V}}_{(k)}^{s} = \frac{d}{dt}\overline{\mathbf{V}}_{(j)}^{s} - \left(\frac{d}{dt}\widetilde{\underline{\mathbf{a}}}_{(jk)_s}^{s} + \frac{d}{dt}\widetilde{\underline{\boldsymbol{\rho}}}_{(jk)_s}^{s}\right)\frac{\partial\overline{\boldsymbol{\omega}}_{(j)}^{s}}{\partial\mathbf{y}}
$$

$$
- \left(\widetilde{\underline{\mathbf{a}}}_{(jk)_s}^{s} + \widetilde{\underline{\boldsymbol{\rho}}}_{(jk)_s}^{s}\right)\left[\frac{d}{dt}\left(\frac{\partial\overline{\boldsymbol{\omega}}_{(j)}^{s}}{\partial\mathbf{y}}\right)\right] + \frac{d}{dt}\widetilde{\underline{\mathbf{d}}}_{(k)_s}^{s}\frac{\partial\overline{\boldsymbol{\omega}}_{(k)}^{s}}{\partial\mathbf{y}} \qquad (3.4.71)
$$

$$
+ \widetilde{\underline{\mathbf{d}}}_{(k)_s}^{s}\left[\frac{d}{dt}\left(\frac{\partial\overline{\boldsymbol{\omega}}_{(k)}^{s}}{\partial\mathbf{y}}\right)\right] + \widetilde{\underline{\boldsymbol{\omega}}}_{(j)_s}^{s}\overline{\mathbf{E}}_{j}^{s}\frac{\partial\dot{\overline{\boldsymbol{\rho}}}_{(jk)}^{j}}{\partial\mathbf{y}}
$$

with

$$
\frac{d}{dt}\widetilde{\underline{\mathbf{a}}}_{(jk)_s}^{s} = \overline{\widetilde{\underline{\boldsymbol{\omega}}}}_{(j)_s}^{s}\,\overline{\mathbf{a}}_{(jk)}^{s}\,,
$$

$$
\frac{d}{dt}\widetilde{\underline{\mathbf{d}}}_{(k)_s}^{s} = \overline{\widetilde{\underline{\boldsymbol{\omega}}}}_{(k)_s}^{s}\,\overline{\mathbf{d}}_{(k)}^{k}\quad\text{and}
$$

$$
\frac{d}{dt}\widetilde{\underline{\boldsymbol{\rho}}}_{(jk)_s}^{s} = \frac{d}{dt}\overline{\mathbf{E}}_{j}^{s}\overline{\boldsymbol{\rho}}_{(jk)}^{j} = \overline{\widetilde{\underline{\boldsymbol{\omega}}}}_{(j)_s}^{s}\overline{\boldsymbol{\rho}}_{(jk)}^{s} + \overline{\mathbf{E}}_{j}^{s}\dot{\overline{\boldsymbol{\rho}}}_{(jk)}^{j}
$$

In the derivation of the above equations, it has been assumed that the partial velocity and angular velocity arrays of the inboard body are known. If we want to describe the multibody system, the arrays for the base-body must be defined. From the coordinate relation of equation (3.4.57), one can write

$$
\overline{\boldsymbol{\omega}}_{(1)}^{s} = \frac{\partial\overline{\boldsymbol{\omega}}_{(1)}^{s}}{\partial\mathbf{y}}\overline{\mathbf{y}}
$$

where

$$\frac{\partial \overline{\omega}_{(1)}^{s}}{\partial \overline{\mathbf{y}}} = \begin{bmatrix} \dfrac{\partial \omega_{s1(1)}}{\partial \omega_{s1(1)}} & \dfrac{\partial \omega_{s1(1)}}{\partial \omega_{s2(1)}} & \dfrac{\partial \omega_{s1(1)}}{\partial \omega_{s3(1)}} & \dfrac{\partial \omega_{s1(1)}}{\partial \omega_{11(2)}} & \cdots & \dfrac{\partial \omega_{s1(1)}}{\partial \rho_{\{N-1\}3(N)}} \\ \dfrac{\partial \omega_{s2(1)}}{\partial \omega_{s1(1)}} & \dfrac{\partial \omega_{s2(1)}}{\partial \omega_{s2(1)}} & \dfrac{\partial \omega_{s2(1)}}{\partial \omega_{s3(1)}} & \dfrac{\partial \omega_{s2(1)}}{\partial \omega_{11(2)}} & \cdots & \dfrac{\partial \omega_{s2(1)}}{\partial \rho_{\{N-1\}3(N)}} \\ \dfrac{\partial \omega_{s3(1)}}{\partial \omega_{s1(1)}} & \dfrac{\partial \omega_{s3(1)}}{\partial \omega_{s2(1)}} & \dfrac{\partial \omega_{s3(1)}}{\partial \omega_{s3(1)}} & \dfrac{\partial \omega_{s3(1)}}{\partial \omega_{11(2)}} & \cdots & \dfrac{\partial \omega_{s3(1)}}{\partial \rho_{\{N-1\}3(N)}} \end{bmatrix}$$

$$= \begin{bmatrix} 1 & 0 & 0 & 0 & \cdots & 0 \\ 0 & 1 & 0 & 0 & \cdots & 0 \\ 0 & 0 & 1 & 0 & \cdots & 0 \end{bmatrix} \quad (3.4.72)$$

A similar relation can be written for the base-body, namely

$$\dot{\overline{\mathbf{r}}}_{(1)}^{s} = \frac{\partial \dot{\overline{\mathbf{r}}}_{(1)}^{s}}{\partial \overline{\mathbf{y}}} \overline{\mathbf{y}} = \overline{\mathbf{V}}_{(1)}^{s} \overline{\mathbf{y}}$$

where the partial velocity array, $\overline{\mathbf{V}}_{(1)}^{s}$, is the base-body's centre of mass velocity Jacobian matrix, which is

$$\frac{\partial \dot{\overline{\mathbf{r}}}_{(1)}^{s}}{\partial \overline{\mathbf{y}}} = \begin{bmatrix} \dfrac{\partial \dot{r}_{s1(1)}}{\partial \omega_{s1(1)}} & \cdots & \dfrac{\partial \dot{r}_{s1(1)}}{\partial \dot{r}_{s1(1)}} & \dfrac{\partial \dot{r}_{s1(1)}}{\partial \dot{r}_{s2(1)}} & \dfrac{\partial \dot{r}_{s1(1)}}{\partial \dot{r}_{s3(1)}} & \cdots & \dfrac{\partial \dot{r}_{s1(1)}}{\partial \rho_{\{N-1\}3(N)}} \\ \dfrac{\partial \dot{r}_{s2(1)}}{\partial \omega_{s1(1)}} & \cdots & \dfrac{\partial \dot{r}_{s2(1)}}{\partial \dot{r}_{s1(1)}} & \dfrac{\partial \dot{r}_{s2(1)}}{\partial \dot{r}_{s2(1)}} & \dfrac{\partial \dot{r}_{s2(1)}}{\partial \dot{r}_{s31}} & \cdots & \dfrac{\partial \dot{r}_{s2(1)}}{\partial \rho_{\{N-1\}3(N)}} \\ \dfrac{\partial \dot{r}_{s3(1)}}{\partial \omega_{s1(1)}} & \cdots & \dfrac{\partial \dot{r}_{s3(1)}}{\partial \dot{r}_{s1(1)}} & \dfrac{\partial \dot{r}_{s3(1)}}{\partial \dot{r}_{s2(1)}} & \dfrac{\partial \dot{r}_{s3(1)}}{\partial \dot{r}_{s31}} & \cdots & \dfrac{\partial \dot{r}_{s3(1)}}{\partial \rho_{\{N-1\}3(N)}} \end{bmatrix}$$

$$= \begin{bmatrix} 0 & \cdots & 1 & 0 & 0 & \cdots & 0 \\ 0 & \cdots & 0 & 1 & 0 & \cdots & 0 \\ 0 & \cdots & 0 & 0 & 1 & \cdots & 0 \end{bmatrix} \quad (3.4.73)$$

It can be seen that the time derivative of the base-body's partial velocity and partial angular velocity arrays, which are needed in equation (3.4.64) and equation (3.4.71), are zero matrixes. These zero matrixes have the same dimension as the partial velocity and partial angular velocity arrays.

61

Using equation (3.4.60), (3.4.62), (3.4.64), (3.4.65), (3.4.69) and (3.4.71), it is possible to describe the multibody system by starting with the base-body and moving along the chain to the last body in the tree structure.

Governing Dynamic Equations

By applying D'Alembert's principle, the Newton-Euler equation of motion can be written in the form

$$\underline{\mathbf{Fa}}_s^{(j)} + \underline{\mathbf{Fi}}_s^{(j)} = \underline{\mathbf{0}}_s \tag{3.4.74}$$

$$\underline{\mathbf{Na}}_s^{(j)} + \underline{\mathbf{Ni}}_s^{(j)} = \underline{\mathbf{0}}_s \tag{3.4.75}$$

where $\underline{\mathbf{Fa}}_s^{(j)}$ is the applied force and $\underline{\mathbf{Na}}_s^{(j)}$ is the applied moment. The inertial force, $\underline{\mathbf{Fi}}_s^{(j)}$, and the inertial moment, $\underline{\mathbf{Ni}}_s^{(j)}$, can be stated as

$$\underline{\mathbf{Fi}}_s^{(j)} = -m_{(j)} \underline{\ddot{\mathbf{R}}}_s^{(j)} \tag{3.4.76}$$

$$\underline{\mathbf{Ni}}_s^{(j)} = -\underline{\dot{\omega}}_s^{(j)} \overline{\mathbf{J}_{(j)}}_s^s + \underline{\omega}_s^{(j)} \overline{\mathbf{J}_{(j)}}_s^s \overline{\widetilde{\omega}_{(j)}}_s^s \tag{3.4.77}$$

If equation (3.4.74) is post-multiplied with the partial velocity array and equation (3.4.75) is post-multiplied with the partial angular velocity array, one obtains

$$\underline{\mathbf{Fa}}_s^{(j)} \overline{\mathbf{V}_{(j)}}^s + \underline{\mathbf{Fi}}_s^{(j)} \overline{\mathbf{V}_{(j)}}^s = \underline{\mathbf{0}} \tag{3.4.78}$$

$$\underline{\mathbf{Na}}_s^{(j)} \frac{\partial \overline{\omega}_{(j)}^s}{\partial \mathbf{y}} + \underline{\mathbf{Ni}}_s^{(j)} \frac{\partial \overline{\omega}_{(j)}^s}{\partial \mathbf{y}} = \underline{\mathbf{0}} \tag{3.4.79}$$

From the definition of the partial velocity and partial angular velocity arrays, it can be seen that it is possible to write equation (3.4.78) and equation (3.4.79) as a single matrix equation:

$$\underline{\mathbf{Qa}}^{(j)} + \underline{\mathbf{Qi}}^{(j)} = \underline{\mathbf{0}} \tag{3.4.80}$$

where

$$\underline{\mathbf{Qa}}^{(j)} = \underline{\mathbf{Fa}}_s^{(j)} \overline{\mathbf{V}_{(j)}}^s + \underline{\mathbf{Na}}_s^{(j)} \frac{\partial \overline{\omega}_{(j)}^s}{\partial \overline{\mathbf{y}}}, \tag{3.4.81}$$

is the generalised applied force and

$$\underline{\mathbf{Qi}}^{(j)} = \underline{\mathbf{Fi}}_s^{(j)} \overline{\mathbf{V}_{(j)}}^s + \underline{\mathbf{Ni}}_s^{(j)} \frac{\partial \overline{\omega}_{(j)}^s}{\partial \overline{\mathbf{y}}}, \tag{3.4.82}$$

is the generalised inertial force.

By introducing the coordinate transformations stated by equation (3.4.63) and equation (3.4.57), the inertial force and the inertial moment can be written in terms of the vector of generalised speeds

$$\underline{\mathbf{Fi}}_s^{(j)} = -m_{(j)} \left[\overline{\mathbf{V}_{(j)}}^s \dot{\overline{\mathbf{y}}} \right]^T - m_{(j)} \left[\frac{d}{dt} \left(\overline{\mathbf{V}_{(j)}}^s \right) \overline{\mathbf{y}} \right]^T \tag{3.4.83}$$

$$\underline{\mathbf{Ni}}_s^{(j)} = -\left[\frac{\partial \overline{\omega}_{(j)}^s}{\partial \overline{\mathbf{y}}} \dot{\overline{\mathbf{y}}} \right]^T \overline{\mathbf{J}_{(j)}}_s^s - \left[\frac{d}{dt} \left(\frac{\partial \overline{\omega}_{(j)}^s}{\partial \overline{\mathbf{y}}} \right) \overline{\mathbf{y}} \right]^T \overline{\mathbf{J}_{(j)}}_s^s + \left[\frac{\partial \overline{\omega}_{(j)}^s}{\partial \overline{\mathbf{y}}} \overline{\mathbf{y}} \right]^T \overline{\mathbf{J}_{(j)}}_s^s \widetilde{\overline{\omega}_{(j)}}_s^s$$

$$\tag{3.4.84}$$

The generalised inertial force is then given by

$$\underline{\mathbf{Qi}}^{(j)} = -\dot{\underline{\mathbf{y}}}^T \left[m_{(j)} \left[\overline{\mathbf{V}_{(j)}}^s \right]^T \overline{\mathbf{V}_{(j)}}^s + \left[\frac{\partial \overline{\omega}_{(j)}^s}{\partial \overline{\mathbf{y}}} \right]^T \overline{\mathbf{J}_{(j)}}_s^s \frac{\partial \overline{\omega}_{(j)}^s}{\partial \overline{\mathbf{y}}} \right]$$

$$- \underline{\mathbf{y}}^T \left[m_{(j)} \left[\frac{d}{dt} \left(\overline{\mathbf{V}_{(j)}}^s \right) \right]^T \overline{\mathbf{V}_{(j)}}^s + \left[\left[\frac{d}{dt} \left(\frac{\partial \overline{\omega}_{(j)}^s}{\partial \overline{\mathbf{y}}} \right) \right]^T \overline{\mathbf{J}_{(j)}}_s^s - \left[\frac{\partial \overline{\omega}_{(j)}^s}{\partial \overline{\mathbf{y}}} \right]^T \overline{\mathbf{J}_{(j)}}_s^s \widetilde{\overline{\omega}_{(j)}}_s^s \right] \frac{\partial \overline{\omega}_{(j)}^s}{\partial \overline{\mathbf{y}}} \right]$$

$$\tag{3.4.85}$$

By introducing the above equation into equation (3.4.80), we can write

$$\underline{\dot{\mathbf{y}}}^T \, \overline{\underline{\mathbf{M}}_{(j)}} = \underline{\mathbf{f}}^{(j)} \tag{3.4.86}$$

where

$$\overline{\underline{\mathbf{M}}_{(j)}} = m_{(j)} \left[\overline{\underline{\mathbf{V}}_{(j)}}^s \right]^T \overline{\underline{\mathbf{V}}_{(j)}}^s + \left[\frac{\partial \overline{\omega}_{(j)}^s}{\partial \overline{\mathbf{y}}} \right]^T \overline{\mathbf{J}}_{(j)}^s \frac{\partial \overline{\omega}_{(j)}^s}{\partial \overline{\mathbf{y}}} \tag{3.4.87}$$

and

$$\underline{\mathbf{f}}^{(j)} = \underline{\mathbf{Q}}\underline{\mathbf{a}}^{(j)} - \mathbf{y}^T \left[m_{(j)} \left[\frac{d}{dt}\left(\overline{\underline{\mathbf{V}}_{(j)}}^s \right) \right]^T \overline{\underline{\mathbf{V}}_{(j)}}^s + \left[\left[\frac{d}{dt}\left(\frac{\partial \overline{\omega}_{(j)}^s}{\partial \overline{\mathbf{y}}} \right) \right]^T \overline{\mathbf{J}}_{(j)}^s - \left[\frac{\partial \overline{\omega}_{(j)}^s}{\partial \overline{\mathbf{y}}} \right]^T \overline{\mathbf{J}}_{(j)}^s \tilde{\overline{\omega}}_{(j)}^s \right] \frac{\partial \overline{\omega}_{(j)}^s}{\partial \overline{\mathbf{y}}} \right] \tag{3.4.88}$$

Equation (3.4.80) represents the equations of motion of one body in the system. The governing dynamic equations of the system can be obtained by adding the contributions of all the bodies. We can write the equations of motion of the system as

$$\underline{\mathbf{Q}}\underline{\mathbf{a}} + \underline{\mathbf{Q}}\underline{\mathbf{i}} = \underline{\mathbf{0}} \tag{3.4.89}$$

from which we can obtain the governing dynamic equation of the system

$$\underline{\dot{\mathbf{y}}}^T \, \overline{\underline{\mathbf{M}}} = \underline{\mathbf{f}} \tag{3.4.90}$$

where

$$\overline{\underline{\mathbf{M}}} = \sum_{j=1}^{N} \overline{\underline{\mathbf{M}}_{(j)}} \tag{3.4.91}$$

64

$$\underline{\mathbf{f}} = \sum_{j=1}^{N} \underline{\mathbf{f}}^{(j)} \qquad\qquad (3.4.92)$$

If the generalised speeds are independent, the matrix $\overline{\mathbf{M}}$ in equation (3.4.91) is square and non-singular. The vector of generalised accelerations can be obtained by post-multiplying equation (3.4.90) with the inverse of $\overline{\mathbf{M}}$.

$$\underline{\dot{\mathbf{y}}}^{T} = \underline{\mathbf{f}} \left[\overline{\mathbf{M}} \right]^{-1} \qquad\qquad (3.4.93)$$

The above equation represents a system of strongly coupled differential equations that is linear in the generalised accelerations. Methods to solve these equations will be discussed later.

3.5 Coupling with Force Elements

3.5.1 General Description

We use force elements to introduce secondary joints, flexibility and contacts between bodies. The force elements do not restrict the freedom of motion of the particular bodies, but they generate forces that depend on the system's state. These forces are then introduced as applied forces in the governing equation. A force element is usually idealised as a single discrete force acting in a direction that is defined by the connection of the bodies. There are force elements for both translation and rotation.
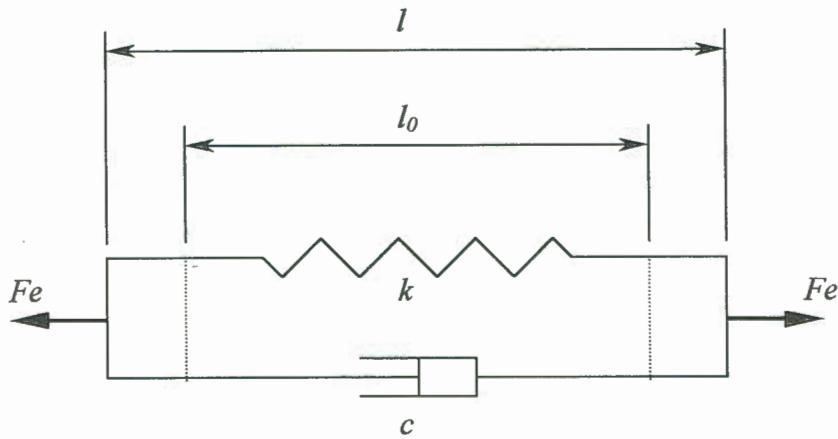
Figure 3.8   *A linear force element consisting of a spring and a damper.*

One of the simplest force elements used consists of a parallel combination of a linear spring and a linear damper as shown in Figure (3.8). The force exerted by this element is

$$Fe = k(l - l_0) + c\frac{d}{dt}(l) \tag{3.5.1}$$

where k is the spring constant, c the damping constant, l_0 the undeformed length of the element and l the current length. We use the convention that a positive force tries to elongate the length of the element. To obtain the contribution of the force element to the generalised applied force, consider two adjoining bodies (*Body j* and *Body m*) connected

with a force element as shown in Figure (3.9). The vector giving the relative displacement between the bodies is

$$\vec{\xi}_{(jm)} = \vec{\mathbf{R}}_{(m)} + \vec{\mathbf{a}}_{(mj)} - \vec{\mathbf{R}}_{(j)} - \vec{\mathbf{a}}_{(jm)} \tag{3.5.2}$$

It can be stated in orthogonal base notation, with respect to base $\vec{\underline{\mathbf{E}}}_s$ as

$$\overline{\xi}^{s}_{(jm)} = \overline{\mathbf{R}}^{s}_{(m)} + \overline{\underline{\mathbf{E}}}^{s}_{m}\overline{\mathbf{a}}^{m}_{(mj)} - \overline{\mathbf{R}}^{s}_{(j)} - \overline{\underline{\mathbf{E}}}^{s}_{j}\overline{\mathbf{a}}^{j}_{(jm)} \tag{3.5.3}$$
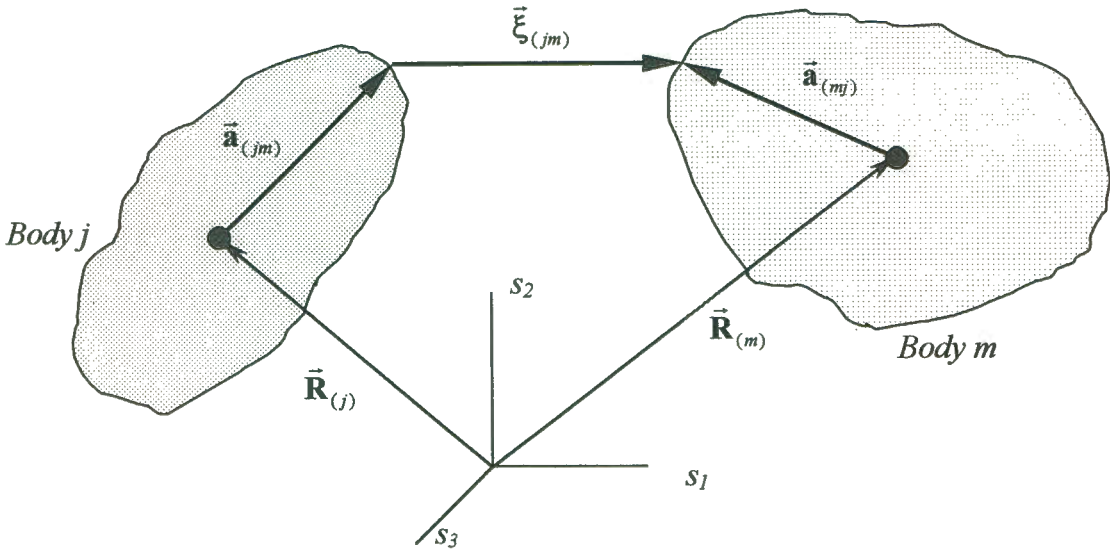
Figure 3.9   *Two bodies connected with a linear force element.*

The relative velocity between the two bodies is obtained by differentiating equation (3.5.3) with respect to time.

$$\dot{\overline{\xi}}^{s}_{(jm)} = \dot{\overline{\mathbf{R}}}^{s}_{(m)} + \widetilde{\underline{\omega(m)}}^{s}_{s}\,\overline{\underline{\mathbf{E}}}^{s}_{m}\overline{\mathbf{a}}^{m}_{(mj)} - \dot{\overline{\mathbf{R}}}^{s}_{(j)} - \widetilde{\underline{\omega(j)}}^{s}_{s}\,\overline{\underline{\mathbf{E}}}^{s}_{j}\overline{\mathbf{a}}^{j}_{(jm)} \tag{3.5.4}$$

The length of the force element is the length of the relative displacement vector.

$$l = \left| \overline{\xi}^{s}_{(jm)} \right| \tag{3.5.5}$$

The rate of change of the force element's length is given by

$$\begin{aligned}
\frac{d}{dt}(l) &= \frac{d}{dt}\sqrt{\overline{\xi}^{s}_{(jm)} \bullet \overline{\xi}^{s}_{(jm)}} \\
&= \frac{1}{2}\left(\overline{\xi}^{s}_{(jm)} \bullet \overline{\xi}^{s}_{(jm)}\right)^{-0.5}\left(\dot{\overline{\xi}}^{s}_{(jm)} \bullet \overline{\xi}^{s}_{(jm)} + \overline{\xi}^{s}_{(jm)} \bullet \dot{\overline{\xi}}^{s}_{(jm)}\right) \\
&= \left(\overline{\xi}^{s}_{(jm)} \bullet \overline{\xi}^{s}_{(jm)}\right)^{-0.5}\left(\dot{\overline{\xi}}^{s}_{(jm)} \bullet \overline{\xi}^{s}_{(jm)}\right) \\
&= \dot{\overline{\xi}}^{s}_{(jm)} \bullet \left(\overline{\xi}^{s}_{(jm)}\bigg/\sqrt{\overline{\xi}^{s}_{(jm)} \bullet \overline{\xi}^{s}_{(jm)}}\right) \\
&= \dot{\overline{\xi}}^{s}_{(jm)} \bullet \overline{\mathbf{n}}\xi^{s}_{(jm)}
\end{aligned} \tag{3.5.6}$$

where $\overline{\mathbf{n}}\xi^{s}_{(jm)}$ is the unit vector along the relative displacement.

The force exerted by the force element on *Body j* is in the direction of the relative displacement

$$\overline{\mathbf{Fe}}^{s}_{(j)} = Fe \cdot \overline{\mathbf{n}}\xi^{s}_{(jm)} \tag{3.5.7}$$

and the force on *Body m* is in the opposite direction

$$\overline{\mathbf{Fe}}^{s}_{(m)} = Fe \cdot \overline{\mathbf{n}}\xi^{s}_{(mj)} = -Fe \cdot \overline{\mathbf{n}}\xi^{s}_{(jm)} \tag{3.5.8}$$

The line of action of this force is generally not through the body's centre of mass and it causes a moment about the centre of mass. The moment that the force element cause about the centre of mass of *Body j* is

$$\overline{\mathbf{Ne}}^{s}_{(j)} = \overline{\mathbf{a}}^{s}_{(jm)} \times \overline{\mathbf{Fe}}^{s}_{(j)} \tag{3.5.9}$$

Similarly, the moment about the centre of mass *Body m* is

$$\overline{\mathbf{Ne}}^{s}_{(m)} = \overline{\mathbf{a}}^{s}_{(mj)} \times \overline{\mathbf{Fe}}^{s}_{(m)} \qquad (3.5.10)$$

3.5.2 Collisions and Contacts between Bodies

Two bodies collide when the relative distance between their outer surfaces vanishes and they will stay in contact as long as the normal force on the contacting surfaces is compressive (Pheiffer and Glocker, 1996). During the collision, the bodies deform. This deformation is composed of a compressive and expansion phase. In general, it will be somewhere between the extremes of perfectly inelastic and perfectly elastic. The force governing the deformation depends on the kinematics and dynamics of the system and the material properties of the bodies. Kinetic energy is dissipated during the impact by plastic deformations, visco-elasticity of the material and elastic waves excited by the impact (Schäfer *et al*, 1996). The elasticity of the impact is described by the coefficient of restitution *e*

$$e = \frac{v_{n_f}}{v_{n_i}} \text{ and } 0 \leq e \leq 1 \qquad (3.5.11)$$

where v_{n_i} and v_{n_f} are the magnitude of the normal relative velocity before and after the collision respectively. The coefficient of restitution can also be viewed as a velocity constraint parameter (Brach, 1989). This view of *e* implicitly introduces energy loss into the impact equations without the direct use of energy terms.

An ambiguity becomes apparent when the collision between rigid bodies is studied: The contact forces of the non-deforming bodies are governed by their deformations. Thus, the inflexibility of the rigid bodies is violated in the collision region. This violation of the rigidity of the bodies can be resolved by realising that the rigidity is an approximate description of real bodies that are suitably stiff (Chatterjee and Ruina, 1998) and whose mass moment of inertial and rotational energy is not insignificant (Brach, 1989). Assuming

69

that the contact area is small compared to the overall dimension of the bodies and that the relative distance between pairs of points that are not in the contact deformation region can be accurately calculated by treating the bodies as rigid, the notion of rigidity of the bodies can still be retained.

Modelling the contact force during a collision requires repulsive and dissipative interaction between the bodies. The simplest force with the desired properties is a force element consisting of a linear spring dashpot that exerts a force of

$$F_n = \min(0, -k\xi - c\dot{\xi}) \tag{3.5.12}$$

where k is the spring constant and c is the damping constant. The form of the contact surfaces and the material properties of the bodies determine the spring constant. The damping constant can be obtained from the coefficient of restitution (equation 3.5.11). It is assumed that the bodies do not stick together during the collision and therefore the contact force can only be compressive.

A more refined contact force can be obtained from the Hertz theory of elastic contact. Using the description of the Hertz contact force given by Boresi, *et al.* (1978), it is possible to predict the repulsive force between two bodies with curved surfaces of two different radii that are pressed against each other as

$$F_n = -\Psi \, \xi^{3/2} \leq 0 \tag{3.5.13}$$

where Ψ is a constant that depends on the shape of the surfaces near the contact point before the deformation and the material properties of the contact bodies. The Hertz contact theory is discussed in Appendix B.

3.5.3 Friction

When two bodies in contact are moving relative to each other there exists a tangential force or shear force opposing the relative tangential motion. The classical law of friction, also known as Coulomb friction, states that the friction force is directly proportional to the normal force, but independent of the contact area and magnitude of relative velocity (Greenwood, 1988:114), namely

$$F_s \leq \mu_s F_n \text{ for static friction} \tag{3.5.14}$$
$$F_s = \mu_d F_n \text{ for dynamic friction} \tag{3.5.15}$$

where F_n is the normal force and μ_s and μ_d are the coefficients of static and dynamic friction. The inequality used in the case of static friction is used to maintain a zero relative tangential velocity ($v_s = 0$) when an external force is applied. If the external force is larger than $\mu_s F_n$, there is a relative tangential velocity, and dynamic friction occurs. The force required to initiate sliding for a static situation is normally larger than needed to sustain sliding, thus

$$\mu_s > \mu_d \tag{3.5.16}$$

The simplest friction model applies only the Coulomb law of dynamic friction

$$\vec{F}_s = -\mu_d \cdot F_n \cdot \text{sign}(v_s) \cdot \vec{n}_{v_s} \tag{3.5.17}$$

This force is discontinuous at $v_s = 0$ and cannot provide for the reversal of the relative tangential velocity; it can only decrease the velocity to zero. When $v_s \rightarrow 0$, the sign of the dynamic friction force (F_s) changes and the state of static friction is never reach.

Another friction model uses viscose friction where the friction force is a linear function of the initial velocity.

$$\vec{F}_s = -\gamma \cdot \vec{v}_s \qquad\qquad (3.5.18)$$

where γ is a shear-damping constant without physical meaning. Again static friction is never reach.

The discontinuity of the Coulomb friction force can be avoided by introducing viscose friction in the region where the relative velocity is low.

$$\vec{F}_s = -\min(\mu_d \cdot F_n, \gamma \cdot v_s) \cdot \text{sign}(v_s) \cdot \vec{n}_{vs} \qquad\qquad (3.5.19)$$

The value of γ should be chosen so that the collisional properties do not differ substantially from the pure Coulomb friction force.

3.5.4 Contact between a Rope and a Pulley

The interaction between a rope and a pulley can be described as a special contact problem. A finite segment approach is used to model the rope. In this model the rope is considered as a series of rigid bodies connected with spherical or universal joints (Huston and Kamman, 1982, Winget and Huston, 1976).

Assuming that the rope diameter is negligible compared to the pulley radius, a rope segment is defined to be in contact with the pulley whenever the relative distance between the rope segment's centre of mass and the centre of the pulley is smaller than or equal to the pulley radius. The pulley constrains the motion of the section of the rope that is in contact with it to stay in a plane perpendicular to the pulley's axis that runs through the pulley's centre. This plane is defined as the pulley plane.

In the multibody dynamics model two sets of force elements are used to model the interaction between a pulley and a rope. The one set acts in the pulley plain between the pulley's centre and the rope segment's centre of mass to prevent the rope segments from

penetrating the pulley. The second set of force elements works in a direction normal to the plane of the pulley. They are active only when a rope segment is in contact with the pulley.

Consider the interaction between a pulley and one rope segment as shown in Figure (3.10). The relative displacement vector between the centre of mass position of a rope segment and the centre of the pulley is

$$\vec{r}_{(pj)} = \vec{r}_{(j)} - \vec{r}_{(p)} \tag{3.5.20}$$

It can be stated in orthogonal base notation with respect to base $\underline{\vec{E}}_s$ as

$$\overline{r}^s_{(pj)} = \overline{r}^s_{(j)} - \overline{r}^s_{(p)} \tag{3.5.21}$$
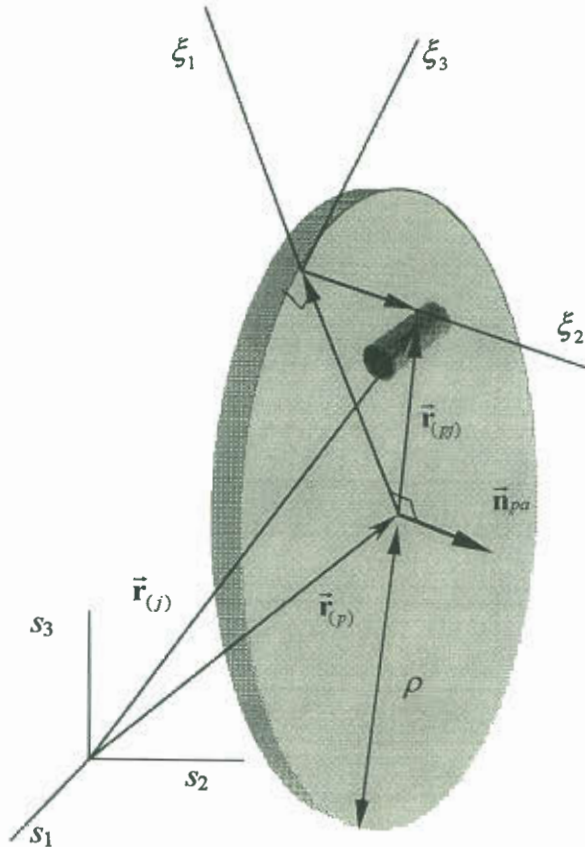
Figure 3.10   *A pulley with radius ρ and a rope segment.*

The relative velocity between the centre of mass of the rope segment and the centre of the pulley is

$$\dot{\overline{\mathbf{r}}}_{(pj)}^{s} = \dot{\overline{\mathbf{r}}}_{(j)}^{s} - \dot{\overline{\mathbf{r}}}_{(p)}^{s} \tag{3.5.22}$$

To calculate the contact force, the relative displacement is decomposed into two components: (1) A displacement in the plane of the pulley and (2) a displacement parallel to the pulley axis.

We define a triad ξ (as shown in Figure (3.10)) at the contact point on the pulley with the base vectors defined as follow:

The first direction is defined in the direction of the displacement in the plane of the pulley. The displacement vector in this direction is

$$
\begin{aligned}
\overline{\mathbf{r}}_{(pj)_1}^{s} &= \overline{\mathbf{r}}_{(pj)}^{s} - (\underline{\mathbf{r}}_{s}^{(pj)} \, \overline{\mathbf{n}}_{pa}^{s}) \, \overline{\mathbf{n}}_{pa}^{s} \\
&= \overline{\mathbf{r}}_{(pj)}^{s} (\underline{\mathbf{n}}_{pa}{}_{s} \, \overline{\mathbf{n}}_{pa}^{s}) - (\underline{\mathbf{r}}_{s}^{(pj)} \, \overline{\mathbf{n}}_{pa}^{s}) \, \overline{\mathbf{n}}_{pa}^{s} \\
&= - \, \overline{\mathbf{n}}_{pa}^{s} \times (\, \overline{\mathbf{n}}_{pa}^{s} \times \overline{\mathbf{r}}_{(pj)}^{s})
\end{aligned}
\tag{3.5.23}
$$

The base vector in this direction is

$$\overline{\mathbf{e}}_{\xi 1}^{s} = - \frac{\overline{\mathbf{n}}_{pa}^{s} \times (\, \overline{\mathbf{n}}_{pa}^{s} \times \overline{\mathbf{r}}_{(pj)}^{s})}{\left| \, \overline{\mathbf{n}}_{pa}^{s} \times (\, \overline{\mathbf{n}}_{pa}^{s} \times \overline{\mathbf{r}}_{(pj)}^{s}) \, \right|} \tag{3.5.24}$$

The second direction is parallel to the axis of the pulley. The base vector in this direction is

$$\overline{\mathbf{e}}_{\xi 2}^{s} = \overline{\mathbf{n}}_{pa}^{s} \tag{3.5.25}$$

74

The third base vector is defined to complete the triad. It is perpendicular to the other two base vectors and is defined as:

$$\overline{\mathbf{e}}_{\xi 3}^{s} = \frac{\overline{\mathbf{e}}_{\xi 1}^{s} \times \overline{\mathbf{e}}_{\xi 2}^{s}}{\left| \overline{\mathbf{e}}_{\xi 1}^{s} \times \overline{\mathbf{e}}_{\xi 2}^{s} \right|} \qquad (3.5.26)$$

It can be seen that the first two base vectors are in the same direction as the contact force elements, and the friction direction corresponds with the third base vector.

The transformation matrix between the inertial system s and the triad ξ is then defined by

$$\overline{\underline{\mathbf{E}}}_{\xi}^{s} = \begin{bmatrix} \overline{\mathbf{e}}_{\xi 1}^{s} & \overline{\mathbf{e}}_{\xi 2}^{s} & \overline{\mathbf{e}}_{\xi 3}^{s} \end{bmatrix} \qquad (3.5.27)$$

The relative displacement vector with respect to base $\vec{\underline{\mathbf{E}}}_{\xi}$ is given by:

$$\overline{\mathbf{r}}_{(pj)}^{\xi} = \overline{\underline{\mathbf{E}}}_{s}^{\xi} \overline{\mathbf{r}}_{(pj)}^{s} = \begin{bmatrix} \mathbf{r}_{(pj)\xi 1} \\ \mathbf{r}_{(pj)\xi 2} \\ 0 \end{bmatrix} \qquad (3.5.28)$$

The components of the contact force on a rope segment in the ξ_1 and ξ_2 directions with respect to the base $\vec{\underline{\mathbf{E}}}_{\xi}$ are the force of the respective force elements. If linear spring dashpot force elements are used, the force that these elements exert can be calculated by using equation (3.5.12).

The force exerted by the force element in the plane of the pulley is:

$$F_{(jp)\xi 1} = -k_{\xi 1}(\mathbf{r}_{(pj)\xi 1} - \rho) - c_{\xi 1}(\dot{\underline{\mathbf{r}}}_{s}^{(pj)}\overline{\mathbf{e}}_{\xi 1}^{s}) \geq 0 \qquad (3.5.29)$$

where $k_{\xi 1}$ is the spring constant and $c_{\xi 1}$ is the damping constant in the ξ_1 direction.

The force element that works in the direction of the pulley axis is only active when the force element in the pulley plane is active (Figure (3.10)). The force exerted by this force element is

$$F_{(jp)_{\xi 2}} = -k_{\xi 2}(r_{(pj)_{\xi 2}}) - c_{\xi 2}(\dot{\underline{\mathbf{r}}}_s^{(pj)}\overline{\mathbf{e}}_{\xi 2}^s), \text{ if } F_{(jp)_{\xi 1}} \geq 0 \qquad (3.5.30)$$

where $k_{\xi 2}$ is the spring constant and $c_{\xi 2}$ is the damping constant in the ξ_2 direction.

The Hertz contact force (equation 3.5.13) can be used instead of the linear spring force.

The third component of the contact force is the friction force between the contact surfaces of the rope and the pulley. It can be calculated with equations (3.5.17), (3.5.18) or (3.5.19). The relative tangential velocity between the contact surfaces is needed in all of the above equations.

The relative velocity between the contact surfaces on the rope and the pulley is

$$\begin{aligned}
\overline{\mathbf{v}}_r^s &= \dot{\overline{\mathbf{r}}}_{(j)}^s - \dot{\overline{\mathbf{r}}}_{(p)}^s - \overline{\boldsymbol{\omega}}_{(p)}^s \times (r_{(pj)_{\xi 1}}\overline{\mathbf{e}}_{\xi 1}^s) \\
&= \dot{\overline{\mathbf{r}}}_{(pj)}^s - \overline{\boldsymbol{\omega}}_{(p)}^s \times (r_{(pj)_{\xi 1}}\overline{\mathbf{e}}_{\xi 1}^s)
\end{aligned} \qquad (3.5.31)$$

The relative tangential velocity between the contact surfaces can be obtained from scalar product

$$v_\tau = \underline{\mathbf{v}}_{r_s}\overline{\mathbf{e}}_{\xi 3}^s \qquad (3.5.32)$$

If equation (3.5.19) is used, the friction force or contact force on the rope segment in the ξ_3 direction is

$$F_{(jp)_{\xi 3}} = -\min(\mu_d F_{\xi 1}, \gamma v_\tau) \cdot \text{sign}(v_\tau) \qquad (3.5.33)$$

76

where μ_d is the coefficient of dynamic friction and γ is a shear-damping constant that does not have a physical meaning, but whose value should be chosen such that the friction force do not differ substantially from the pure Coulomb friction force.

The total contact force on the rope segment can now be given by

$$\underline{\mathbf{F}}_\xi^{(jp)} = \begin{bmatrix} F_{(jp)_{\xi 1}} & F_{(jp)_{\xi 2}} & F_{(jp)_{\xi 3}} \end{bmatrix} ,$$
(3.5.34)

and with respect to base $\underline{\vec{\mathbf{E}}}_s$

$$\underline{\mathbf{F}}_s^{(jp)} = \underline{\mathbf{F}}_\xi^{(jp)} \overline{\underline{\mathbf{E}}}_s^\xi$$
(3.5.35)

The contact force on the pulley is

$$\underline{\mathbf{F}}_s^{(pj)} = -\underline{\mathbf{F}}_s^{(jp)}$$
(3.5.36)

This contact force causes a moment about the centre of the pulley that can be obtained as

$$\underline{\mathbf{N}}_s^{(pj)} = \left((\mathbf{r}_{(pj)_{\xi 1}} \overline{\mathbf{e}}_{\xi 1}^s) \times \overline{\mathbf{F}}_{(pj)}^s \right)^T$$
(3.5.37)

The contact forces and moment are introduced as applied forces in the governing differential equation.

This method can be identified as a penalty function method, because whenever a rope segment penetrates the pulley, a force is applied to eliminate the interference.

3.6 Solving Dynamic Equations

The governing dynamic equations that have been developed in the previous sections are either a set of differential algebraic equations (equation 3.4.56) or a set of nonlinear ordinary differential equations (equation 3.4.93). If the position, orientation, velocity and angular velocity of all the bodies are known, then an initial value problem can be composed with either equation (3.4.56) or (3.4.93).

The governing equations stated by equation (3.4.93) represent a system of second order nonlinear differential equations in the generalised coordinates. In general, no closed form solution exists for these differential equations and they must be solved with a numeric method. The form of these equations is not suitable for the numeric integration methods used in structural dynamics and a numeric method for general ordinary differential equations must be used. Many of the existing accurate numeric integration algorithms are developed for first-order differential equations. To apply these methods, the governing equations must be written in state space form. The system of second-order equations is then reduced to a system of first-order equations. The state vector is defined as the combination of the vector of generalised coordinates and the vector of generalised speeds

$$\underline{z} = [\underline{q} \quad \underline{y}] \qquad (3.6.1)$$

If Euler parameters (equation 3.3.48) are used as orientation coordinates, a multibody system that consists of N free rigid bodies will have $13N$ first order differential equations in the state space description of the governing equations.

Frequently the governing differential equations of large mechanical and structural systems are stiff. Special numerical integration methods are needed to solve the stiff systems of equations as describe by Brown, *et al.* (1989), Shampine and Gear (1979), Shampine and Reichelt (1997) and Steihaug and Wolfbrandt (1979). These methods are mostly implicit, but the form of equation (3.4.93) is more suitable for explicit methods. The implicit methods need the Jacobian matrix of the state variables. It is not available as an analytic expression if equation (3.4.93) is used and must be calculated using a finite difference

method. This is a very inefficient process, because the computation and evaluation of the state equations are the major cost factors in the simulation of large systems. Yen and Chou (1993) developed a method to obtain an approximate Jacobian matrix using an analytic method, if the governing equations are stated by a set of differential algebraic equations.

The most popular numeric method used is a fourth order Runge-Kutta method. Various authors have found this method to be efficient and reliable (Huston, 1990, McPhee and Dubey, 1991). Krinke and Huston (1980) found that it is easier and more convenient to use a method with an automatic step size adjustment to control the accuracy of the solution. Pheiffer and Glocker (1996:164) stated that a Runge-Kutta method of order 2/3 is reliable and efficient.

3.6.1 Discussion of Numeric Methods

All the methods that are considered solve the system of equations $d\overline{\mathbf{z}}/dt = \overline{\mathbf{f}}(t, \overline{\mathbf{z}})$ on an interval $t = [a, b]$ with initial value $\overline{\mathbf{z}}(a) = \overline{\mathbf{A}}$ by generating approximations $\overline{\mathbf{z}}_0$ to $\overline{\mathbf{z}}_N$ on a mesh $a = t_0 < t_1 < \ldots < t_N = b$. The object is to take steps $h_{n+1} = t_{n+1} - t_n$ as large as possible while still meeting some specified error criterion.

Euler Method

The Euler method is the simplest numerical integration method and is obtained by using the first two terms of a Taylor series expansion. The Euler method is a single step method with an order of integration equal to one. This method is a first-order method, because the accumulated truncation error tends to zero as $h \to 0$ (Gear, 1971:25).

The algorithm for the Euler method is

$$\overline{\mathbf{z}}_{n+1} = \overline{\mathbf{z}}_n + h\,\overline{\mathbf{f}}(t_n, \overline{\mathbf{y}}_n) \tag{3.6.2}$$

where $t_n = nh$.

Runge-Kutta Methods

The explicit Runge-Kutta methods use the value of $\bar{\mathbf{f}}(t,\bar{\mathbf{z}})$ at a variety of points in a time step to obtain a higher order of integration. The general form of an R-stage Runge-Kutta method is

$$
\begin{aligned}
\bar{\mathbf{z}}_{n+1} &= \bar{\mathbf{z}}_n + \sum_{r=1}^{R} w_r \bar{\mathbf{k}}_r \\
\bar{\mathbf{k}}_1 &= h_{n+1}\bar{\mathbf{f}}(t_n, \bar{\mathbf{z}}_n) \\
\bar{\mathbf{k}}_r &= h_{n+1}\bar{\mathbf{f}}(t + \alpha_r h_{n+1}, \bar{\mathbf{z}}_n + \sum_{s=1}^{r-1} \beta_{rs}\bar{\mathbf{k}}_s), \qquad r = 2,\,3,\dots,R
\end{aligned}
\tag{3.6.3}
$$

where the constants w_r, α_r, and β_r are characteristics of the method (Shampine *et al*, 1976). Given an initial value at t_0, one can step along manipulating h to pass some error test and obtain an approximate solution over the desired time interval. The function $\bar{\mathbf{f}}(t,\bar{\mathbf{z}})$ must be evaluated R times for an R stage method during a time step.

The second order Runge-Kutta method is given by

$$
\begin{aligned}
\bar{\mathbf{z}}_{n+1} &= \bar{\mathbf{z}}_n + \alpha\,\bar{\mathbf{k}}_1 + \beta\,\bar{\mathbf{k}}_2 \\
\bar{\mathbf{k}}_1 &= h\,\bar{\mathbf{f}}(t_n, \bar{\mathbf{z}}_n) \\
\bar{\mathbf{k}}_2 &= h\,\bar{\mathbf{f}}(t_n + \alpha h, \bar{\mathbf{z}}_n + \beta\,\bar{\mathbf{k}}_1)
\end{aligned}
\tag{3.6.4}
$$

where $\beta = 1 - \gamma$, $\alpha = 1/(2\gamma)$ and γ is a free parameter that can be chosen to optimise any desired feature of the process (Gear, 1971:30). This method has an accuracy of $O(h^2)$.

The classical Runge-Kutta method is a four-stage, fourth order method.

$$
\begin{aligned}
\bar{\mathbf{z}}_{n+1} &= \bar{\mathbf{z}}_n + \tfrac{1}{6}\left(\bar{\mathbf{k}}_1 + 2\bar{\mathbf{k}}_2 + 2\bar{\mathbf{k}}_3 + \bar{\mathbf{k}}_4\right) \\
\bar{\mathbf{k}}_1 &= h\,\bar{\mathbf{f}}(t_n, \bar{\mathbf{z}}_n) \\
\bar{\mathbf{k}}_2 &= h\,\bar{\mathbf{f}}(t_n + \tfrac{1}{2}h, \bar{\mathbf{z}}_n + \tfrac{1}{2}\bar{\mathbf{k}}_1) \\
\bar{\mathbf{k}}_3 &= h\,\bar{\mathbf{f}}(t_n + \tfrac{1}{2}h, \bar{\mathbf{z}}_n + \tfrac{1}{2}\bar{\mathbf{k}}_2) \\
\bar{\mathbf{k}}_4 &= h\,\bar{\mathbf{f}}(t_n + h, \bar{\mathbf{z}}_n + \bar{\mathbf{k}}_3)
\end{aligned}
\tag{3.6.5}
$$

This method has a accuracy of $O(h^4)$.

3.6.2 Choice of Step Size.

The objective of the numerical integration is to obtain a result close to the desired goal with a minimum of effort. One of the important parameters that must be chosen is the size of the time step h. The ideal situation is to use the optimal step size for the given problem with a specified accuracy during the integration. The error made in a time step is estimated and this estimation is used to determine if the result can be accepted and to calculate the size of the next step.

Choice of Step Size for Runge-Kutta Methods

Two methods are used to determine if the results are sufficiently accurate. The first method is to recompute the value at the end of each interval with the step size halved (Gerald and Wheatly, 1994:405). The result is only accepted if the difference between the values at the end of the interval is small, otherwise the step size is halved again. This is a very expensive method. The second approach uses two Runge-Kutta methods of different order and the results are compared after each time step to obtain the local error. This method is very economical if the same values of $\overline{\mathbf{k}}$ are used with different w values. An example is the Runge-Kutta-Fehlberg method that is a six-stage fourth-order method.

$$
\begin{aligned}
\overline{\mathbf{k}}_1 &= h\overline{\mathbf{f}}(t_n, \overline{\mathbf{z}}_n) \\
\overline{\mathbf{k}}_2 &= h\overline{\mathbf{f}}(t_n + \tfrac{1}{4}h, \overline{\mathbf{z}}_n + \tfrac{1}{4}\overline{\mathbf{k}}_1) \\
\overline{\mathbf{k}}_3 &= h\overline{\mathbf{f}}(t_n + \tfrac{3}{8}h, \overline{\mathbf{z}}_n + \tfrac{3}{32}\overline{\mathbf{k}}_1 + \tfrac{9}{32}\overline{\mathbf{k}}_2) \\
\overline{\mathbf{k}}_4 &= h\overline{\mathbf{f}}(t_n + \tfrac{12}{13}h, \overline{\mathbf{z}}_n + \tfrac{1932}{2197}\overline{\mathbf{k}}_1 - \tfrac{7200}{2197}\overline{\mathbf{k}}_2 + \tfrac{7296}{2197}\overline{\mathbf{k}}_3) \\
\overline{\mathbf{k}}_5 &= h\overline{\mathbf{f}}(t_n + h, \overline{\mathbf{z}}_n + \tfrac{439}{216}\overline{\mathbf{k}}_1 - 8\overline{\mathbf{k}}_2 + \tfrac{3680}{513}\overline{\mathbf{k}}_3 - \tfrac{845}{4104}\overline{\mathbf{k}}_4) \\
\overline{\mathbf{k}}_6 &= h\overline{\mathbf{f}}(t_n + \tfrac{1}{2}h, \overline{\mathbf{z}}_n - \tfrac{8}{27}\overline{\mathbf{k}}_1 + 2\overline{\mathbf{k}}_2 - \tfrac{3544}{2565}\overline{\mathbf{k}}_3 + \tfrac{1859}{4104}\overline{\mathbf{k}}_4 - \tfrac{11}{40}\overline{\mathbf{k}}_5) \\
\overline{\mathbf{z}}_{n+1}^* &= \overline{\mathbf{z}}_n + \left(\tfrac{25}{216}\overline{\mathbf{k}}_1 + \tfrac{1408}{2565}\overline{\mathbf{k}}_3 + \tfrac{2197}{4104}\overline{\mathbf{k}}_4 - \tfrac{1}{5}\overline{\mathbf{k}}_5\right), \text{ with global error } O(h^4) \\
\overline{\mathbf{z}}_{n+1} &= \overline{\mathbf{z}}_n + \left(\tfrac{16}{135}\overline{\mathbf{k}}_1 + \tfrac{6656}{12825}\overline{\mathbf{k}}_3 + \tfrac{28561}{56430}\overline{\mathbf{k}}_4 - \tfrac{9}{50}\overline{\mathbf{k}}_5 + \tfrac{2}{55}\overline{\mathbf{k}}_6\right), \text{ with global}
\end{aligned}
$$
$$\text{error } O(h^5)$$

(3.6.6)

The difference between $\overline{z}_{n+1}^{*}$ and $\overline{z}_{n+1}$ is used to estimate the error in the current integration step. If the estimated error is large, the current step is rejected and the calculation is repeated using a smaller time step. Otherwise, the estimated error is used to predict an approximate choice of the step size for the next integration step.

It is very easy to change the step size during the integration in all the single step methods.

A discussion of the stability of the methods is given in Appendix C.

3.6.3 Integration of Euler Parameters

Wertz, *et al.* (1978) discussed a useful integration process for the Euler parameters. The relation between the Euler parameters and their time derivatives was stated in equation (3.3.62) as

$$\dot{\overline{\varepsilon}} = \tfrac{1}{2}\,\overline{\underline{\Omega}}\;\overline{\varepsilon} \quad \text{with} \quad \overline{\underline{\Omega}}_s^s = \begin{bmatrix} 0 & \omega_{s3} & -\omega_{s2} & \omega_{s1} \\ -\omega_{s3} & 0 & \omega_{s1} & \omega_{s2} \\ \omega_{s2} & -\omega_{s1} & 0 & \omega_{s3} \\ -\omega_{s1} & -\omega_{s2} & -\omega_{s3} & 0 \end{bmatrix} \tag{3.6.7}$$

The matrix $\overline{\underline{\Omega}}$ has the property that

$$\begin{aligned} \left[\overline{\underline{\Omega}}\right]^T \overline{\underline{\Omega}} &= -\overline{\underline{\Omega}}\,\overline{\underline{\Omega}} = -\left[\overline{\underline{\Omega}}\right]^2 \\ &= -(\omega_{s1}^2 + \omega_{s2}^2 + \omega_{s3}^2)\,\overline{\underline{I}} = -\omega^2\,\overline{\underline{I}} \end{aligned} \tag{3.6.8}$$

and for all $k > 0$

$$\left[\overline{\underline{\Omega}}\right]^{2k} = (-1)^k\,\omega^{2k}\,\overline{\underline{I}} \tag{3.6.9}$$

$$\left[\overline{\underline{\Omega}}\right]^{2k+1} = (-1)^k\,\omega^{2k}\,\overline{\underline{\Omega}} \tag{3.6.10}$$

Consider the Taylor series expansion of an updated set for Euler Parameters

$$\bar{\varepsilon}(t + \Delta t) = \bar{\varepsilon}(t) + \Delta t \dot{\bar{\varepsilon}}(t) + \tfrac{1}{2}(\Delta t^2)\ddot{\bar{\varepsilon}}(t) + O(\Delta t^3) \qquad (3.6.11)$$

If we introduce equation (3.6.7) and perform algebraic manipulations, we get

$$\begin{aligned}
\bar{\varepsilon}(t + \Delta t) &= \left[\underline{\mathbf{I}} + \tfrac{1}{2}\Delta t \underline{\overline{\Omega}} + \frac{\left(\tfrac{1}{2}\Delta t \underline{\overline{\Omega}}\right)^2}{2!} + \frac{\left(\tfrac{\Delta t}{2}\underline{\overline{\Omega}}\right)^3}{3!} + \dots \right]\bar{\varepsilon}(t) \\
&+ \left[\tfrac{1}{4}\dot{\underline{\overline{\Omega}}} + \tfrac{1}{12}\Delta t \ddot{\underline{\overline{\Omega}}} + \dots \right]\Delta t^2 \bar{\varepsilon}(t) \qquad (3.6.12)\\
&+ \left[\tfrac{1}{12}\dot{\underline{\overline{\Omega}}}\,\underline{\overline{\Omega}} + \tfrac{1}{24}\dot{\underline{\overline{\Omega}}}\,\underline{\overline{\Omega}} + \dots \right]\Delta t^3 \bar{\varepsilon}(t) + \dots
\end{aligned}$$

That can be written as

$$\bar{\varepsilon}(t + \Delta t) = e^{\frac{1}{2}\Delta t \underline{\overline{\Omega}}}\,\bar{\varepsilon}(t) + O(\Delta t^2) \qquad (3.6.13)$$

A better approximation can be achieved if we take the average angular velocity over the time increment Δt. The average angular velocity matrix is defined as

$$\underline{\overline{\Omega_{av}}} = \frac{1}{\Delta t}\int_{t}^{t+\Delta t}\underline{\overline{\Omega(\tau)}}\;d\tau \qquad (3.6.14)$$

By integrating the Taylor series expansion of the integrand of the above equation, the average angular velocity matrix can be written as

$$\underline{\overline{\Omega_{av}}} = \underline{\overline{\Omega}} + \tfrac{1}{2}\Delta t \dot{\underline{\overline{\Omega}}} + \tfrac{1}{6}\Delta t^3 \ddot{\underline{\overline{\Omega}}} + \dots \qquad (3.6.15)$$

then

$$e^{\frac{\Delta t}{2}\overline{\underline{\Omega}_{av}}} = \left[I + \tfrac{1}{2}\Delta t\overline{\underline{\Omega}_t} + \frac{\left(\tfrac{1}{2}\Delta t\overline{\underline{\Omega}_t}\right)^2}{2!} + \frac{\left(\tfrac{\Delta t}{2}\overline{\underline{\Omega}_t}\right)^3}{3!} + \ldots \right]$$
$$+ \left[\tfrac{1}{4}\dot{\underline{\Omega}_t} + \tfrac{1}{12}\Delta t\ddot{\underline{\Omega}_t} + \ldots \right] \Delta t^2 \tag{3.6.16}$$
$$+ \left[\tfrac{1}{12}\ddot{\underline{\Omega}_t}\underline{\Omega}_t + \dot{\underline{\Omega}_t}\dot{\underline{\Omega}_t} + \ldots \right] \Delta t^3 + \ldots$$

and

$$\bar{\varepsilon}(t+\Delta t) = e^{\frac{1}{2}\Delta t\overline{\underline{\Omega}_{av}}}\,\bar{\varepsilon}(t) + O(\Delta t^3) \tag{3.6.17}$$

By writing the Maclaurin series of the natural exponent and introducing equation (3.6.9) and equation (3.6.10), it is possible to write

$$e^{\frac{1}{2}\Delta t\overline{\underline{\Omega}_{av}}} = \sum_{k=0}^{\infty} \frac{\tfrac{1}{2}\Delta t\overline{\underline{\Omega}_{av}}}{k!}$$
$$= \bar{\underline{I}}\sum_{k=0}^{\infty} \frac{(-1)^k \left(\tfrac{1}{2}\Delta t\omega_{av}\right)^{2k}}{(2k)!} + \frac{1}{\omega_{av}}\overline{\underline{\Omega}_{av}}\sum_{k=0}^{\infty} \frac{(-1)^k \left(\tfrac{1}{2}\Delta t\omega_{av}\right)^{2k+1}}{(2k+1)!}$$
$$= \bar{\underline{I}}\cos\!\left(\tfrac{1}{2}\Delta t\omega_{av}\right) + \frac{1}{\omega_{av}}\overline{\underline{\Omega}_{av}}\sin\!\left(\tfrac{1}{2}\Delta t\omega_{av}\right) \tag{3.6.18}$$

where ω_{av} is the magnitude of the average angular velocity over the time increment Δt. The above equation is finite for all values of ω_{av} because

$$\lim_{\omega_{av}\to 0} \frac{1}{\omega_{av}}\sin\!\left(\tfrac{1}{2}\Delta t\omega_{av}\right) = \frac{1}{2}\Delta t \tag{3.6.19}$$

Thus, the updated vector of Euler parameters of equation (3.6.17) can be written as

$$\bar{\varepsilon}(t+\Delta t) = \left[\bar{\underline{I}}\cos\!\left(\tfrac{1}{2}\Delta t\omega_{av}\right) + \frac{1}{\omega_{av}}\overline{\underline{\Omega}_{av}}\sin\!\left(\tfrac{1}{2}\Delta t\omega_{av}\right) \right]\bar{\varepsilon}(t) + O(\Delta t^2) \tag{3.6.20}$$

That can be written as a single matrix equation

$$\bar{\varepsilon}(t + \Delta t) = \begin{bmatrix} c & n_{s3}s & -n_{s2}s & n_{s1}s \\ -n_{s3}s & c & n_{s1}s & n_{s2}s \\ n_{s2}s & -n_{s1}s & c & n_{s3}s \\ -n_{s1}s & -n_{s2}s & -n_{s3}s & c \end{bmatrix} \bar{\varepsilon}(t) + O(\Delta t^2) \qquad (3.6.21)$$

with

$c = \cos\left(\frac{1}{2}\Delta t \omega_{av}\right)$, $s = \dfrac{1}{\omega_{av}}\sin\left(\frac{1}{2}\Delta t \omega_{av}\right)$ and where $\overline{\mathbf{n}}^s$ is the unit vector that define the

rotation axis.

Closed Form Solution

If $\underline{\overline{\Omega}}$ is constant (when the angular velocity is constant), equation (3.6.7) can be integrated

to obtain

$$\bar{\varepsilon}(t) = \exp\left(\tfrac{1}{2}t\underline{\overline{\Omega}}\right)\bar{\varepsilon}(t_0) \qquad (3.6.22)$$

that we can write in the form

$$\bar{\varepsilon}(t) = \underline{\overline{\mathbf{I}}}\cos\left(\tfrac{1}{2}t\omega\right) + \frac{\sin\left(\tfrac{1}{2}t\omega\right)}{\omega}\underline{\overline{\Omega}} \qquad (3.6.23)$$

using equation (3.6.18).

In the case of a constant rotation axis, the integration can still be carried out to yield

$$\bar{\varepsilon}(t) = \exp\left(\tfrac{1}{2}\int_{t_0}^{t}\underline{\overline{\Omega(t')}}\,dt'\right)\bar{\varepsilon}(t_0) \qquad (3.6.24)$$

Taking the angular velocity as constant over a small time increment Δt, the closed form solution is

$$\bar{\varepsilon}(t + \Delta t) = e^{\frac{1}{2}\Delta t \bar{\bar{\Omega}}} \, \bar{\varepsilon}(t) \qquad\qquad (3.6.25)$$

It can be seen that the updated Euler parameters obtained with equations (3.6.20) and (3.6.25) do not violate the constraint equation (3.3.49) and therefore it is not necessary to normalise them at regular intervals.

3.7 Joint Constraints

Joint constraints define the connectivity between the bodies in the system.

3.7.1 Absolute Coordinate Method

In the case of using absolute coordinates in the analysis of mechanical systems, the formulation of the kinematic constraints that describe a joint between arbitrary bodies can be made independent of the system's topological structure since similar sets of coordinates are used to describe the motion of the bodies. Small sub-matrices representing the different joint constraint Jacobian matrices can be combined to obtain the system's joint constraint Jacobian matrix.

Spherical Joint

A spherical joint eliminates the freedom of relative translation between two connected bodies. It allows only the three degrees of freedom of the relative rotations.
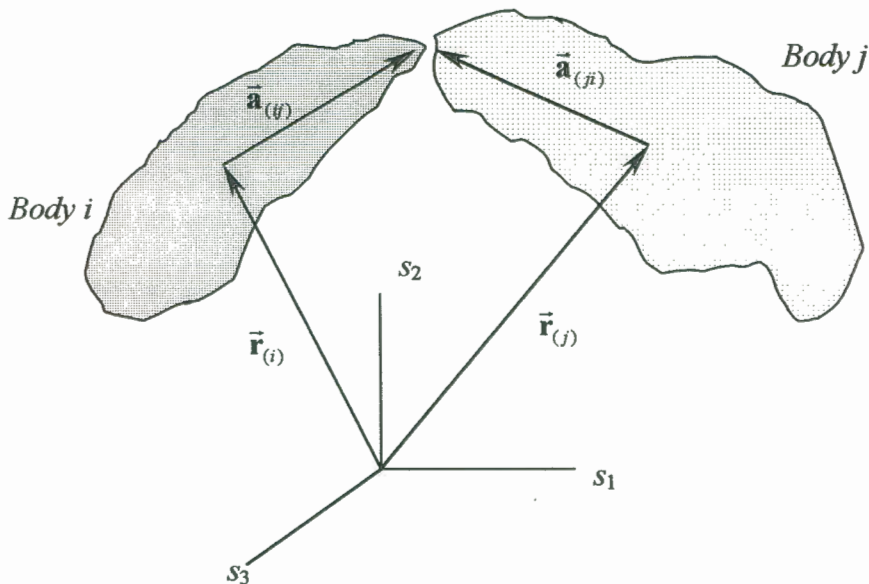

Figure 3.11   *Two bodies connected with a spherical joint.*

Consider two bodies (*Body i* and *Body j*) connected with a spherical joint as shown in Figure (3.11). Let $\vec{\mathbf{a}}_{(ij)}$ be the vector pointing from the centre of mass of *Body i* to the joint with *Body j* and $\vec{\mathbf{a}}_{(ji)}$ be the vector pointing from the centre of mass of *Body j* to the joint with *Body i*.[2] The kinematic constraint of a spherical joint requires that the connection points on each body coincide throughout the motion.

$$\vec{\mathbf{r}}_{(i)} + \vec{\mathbf{a}}_{(ij)} = \vec{\mathbf{r}}_{(j)} + \vec{\mathbf{a}}_{(ji)} \tag{3.7.1}$$

The constraint equation can be written with respect to the inertial system as

$$\overline{\mathbf{r}}_{(i)}^{s} + \overline{\mathbf{a}}_{(ij)}^{s} - \overline{\mathbf{r}}_{(j)}^{s} - \overline{\mathbf{a}}_{(ji)}^{s} = \overline{\mathbf{0}}^{s} \tag{3.7.2}$$

A virtual change in the kinematic constraint can be written in terms of the generalised coordinates using equations (3.4.14) and (3.4.15) as

$$\frac{\partial \overline{\mathbf{r}}_{(i)}^{s}}{\partial \overline{\mathbf{q}}} \delta \overline{\mathbf{q}} - \underline{\widetilde{\overline{\mathbf{a}}}}_{(ij)_{s}}^{s} \overline{\mathbf{G}}_{(i)}^{s} \frac{\partial \overline{\mathbf{\theta}}_{(i)}}{\partial \overline{\mathbf{q}}} \delta \overline{\mathbf{q}} - \frac{\partial \overline{\mathbf{r}}_{(j)}^{s}}{\partial \overline{\mathbf{q}}} \delta \overline{\mathbf{q}} + \underline{\widetilde{\overline{\mathbf{a}}}}_{(ji)_{s}}^{s} \overline{\mathbf{G}}_{(j)}^{s} \frac{\partial \overline{\mathbf{\theta}}_{(j)}}{\partial \overline{\mathbf{q}}} \delta \overline{\mathbf{q}} = \overline{\mathbf{0}}^{s}$$

$$\left[\frac{\partial \overline{\mathbf{r}}_{(i)}^{s}}{\partial \overline{\mathbf{q}}} - \underline{\widetilde{\overline{\mathbf{a}}}}_{(ij)_{s}}^{s} \overline{\mathbf{G}}_{(i)}^{s} \frac{\partial \overline{\mathbf{\theta}}_{(i)}}{\partial \overline{\mathbf{q}}} - \frac{\partial \overline{\mathbf{r}}_{(j)}^{s}}{\partial \overline{\mathbf{q}}} + \underline{\widetilde{\overline{\mathbf{a}}}}_{(ji)_{s}}^{s} \overline{\mathbf{G}}_{(j)}^{s} \frac{\partial \overline{\mathbf{\theta}}_{(j)}}{\partial \overline{\mathbf{q}}} \right] \delta \overline{\mathbf{q}} = \overline{\mathbf{0}}^{s} \tag{3.7.3}$$

That can be written in the form

$$\overline{\underline{\mathbf{C}}}_{\mathbf{q}}^{s} \, \delta \overline{\mathbf{q}} = \overline{\mathbf{0}}^{s} \tag{3.7.4}$$

where $\overline{\underline{\mathbf{C}}}_{\mathbf{q}}^{s}$ is the Jacobian matrix of the spherical joint constraint and can be written as

---

[2] $\vec{\mathbf{a}}_{(ij)}$ and $\vec{\mathbf{a}}_{(ji)}$ are two unrelated vectors and therefore $\vec{\mathbf{a}}_{(ij)} \neq -\vec{\mathbf{a}}_{(ji)}$.

$$\overline{\mathbf{C}}_{\mathbf{q}}^{s} = \left[\ \overline{\underline{\mathbf{H}_{(i)}}}^{s} + \overline{\underline{\mathbf{H}_{(j)}}}^{s} \ \right] \tag{3.7.5}$$

where

$$\overline{\underline{\mathbf{H}_{(i)}}}^{s} = \left[\frac{\partial \overline{\mathbf{r}}_{(i)}^{s}}{\partial \overline{\mathbf{q}}} - \underline{\widetilde{\mathbf{a}}_{(ij)}}_{s}^{s} \ \overline{\underline{\mathbf{G}_{(i)}}}^{s} \ \frac{\partial \overline{\boldsymbol{\theta}}_{(i)}}{\partial \overline{\mathbf{q}}} \right] \tag{3.7.6}$$

$$\overline{\underline{\mathbf{H}_{(j)}}}^{s} = \left[-\frac{\partial \overline{\mathbf{r}}_{(j)}^{s}}{\partial \overline{\mathbf{q}}} + \underline{\widetilde{\mathbf{a}}_{(ji)}}_{s}^{s} \ \overline{\underline{\mathbf{G}_{(j)}}}^{s} \ \frac{\partial \overline{\boldsymbol{\theta}}_{(j)}}{\partial \overline{\mathbf{q}}} \right] \tag{3.7.7}$$

Equation (3.7.5) consists of three linear independent constraint equations.

Revolute Joint

A revolute joint has one rotational degree of freedom and can be considered as a special case of a spherical joint in which the relative rotation between the two connected bodies is only allowed along the joint axis. The kinematic constraints of a revolute joint requires that a points on each body at the connection of the two bodies coincides and that two vectors along the joint axis on each body remain parallel to each other during the motion.

A revolute joint needs five constraint equations because it has only one degree of freedom. Three of the constraint equations represent the relative translation constraints and are the same as the constraints for a spherical joint. The other two kinematic constraint equations are obtained with the condition that two vectors (one on each body) stay parallel to each other. Figure (3.12) shows two bodies connected with a revolute joint. $\vec{\mathbf{p}}_{(i)}$ and $\vec{\mathbf{p}}_{(j)}$ are two vectors on *Bodies i* and *j*, respectively, defining the joint axis. These two vectors must be parallel, therefore

$$\overline{\mathbf{p}}_{(i)}^{s} \times \overline{\mathbf{p}}_{(j)}^{s} = \overline{\mathbf{0}}^{s} \tag{3.7.8}$$

The above equation represents two independent constraint equations. It is possible to obtain the two constraint equations as separate equations by defining two vectors, $\vec{\mathbf{p}}_{(i)_{\xi 2}}$ and $\vec{\mathbf{p}}_{(i)_{\xi 3}}$, that are fixed to *Body i* and are orthogonal to $\vec{\mathbf{p}}_{(j)}$. It is then possible to write two scalar products that represent the constraint equation (3.7.8), namely

$$\underline{\mathbf{p}}_s^{(j)} \overline{\mathbf{p}}_{(i)_{\xi 2}}^s = 0 \text{, and } \underline{\mathbf{p}}_s^{(j)} \overline{\mathbf{p}}_{(i)_{\xi 3}}^s = 0 \qquad (3.7.9)$$
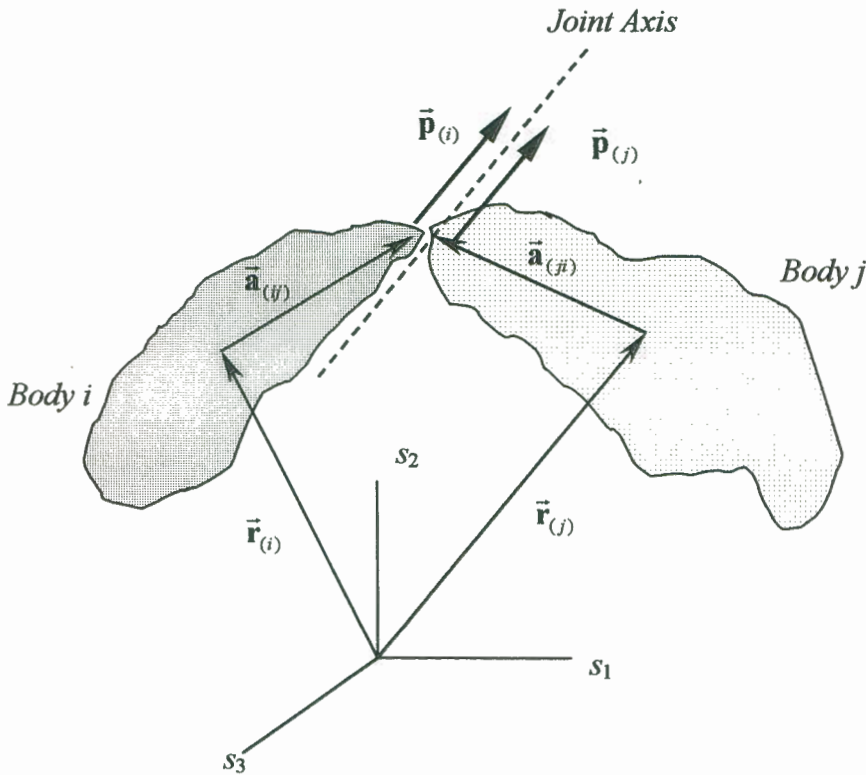

Figure 3.12 *Two bodies connected with a revolute joint.*

A virtual change in the first kinematic constraint of equation (3.7.9) can be obtained using equation (3.4.23) as

$$-\underline{\mathbf{p}}_s^{(j)}\left(\overline{\widetilde{\mathbf{p}(i)}_{\xi2}}^s\,{}_s\overline{\mathbf{G}(i)}^s\delta\overline{\theta}_{(i)}\right)-\left(\overline{\widetilde{\mathbf{p}(j)}}^s\,{}_s\overline{\mathbf{G}(j)}^s\delta\overline{\theta}_{(j)}\right)^T\,\overline{\mathbf{P}}_{(i)_{\xi2}}^s=0$$

$$\underline{\mathbf{p}}_s^{(j)}\left(\overline{\widetilde{\mathbf{p}(i)}_{\xi2}}^s\,{}_s\overline{\mathbf{G}(i)}^s\delta\overline{\theta}_{(i)}\right)+\underline{\mathbf{p}}_s^{(i)^{\xi2}}\left(\overline{\widetilde{\mathbf{p}(j)}}^s\,{}_s\overline{\mathbf{G}(j)}^s\delta\overline{\theta}_{(j)}\right)=0 \qquad (3.7.10)$$

The above equation can be written with respect to the generalised coordinates using equation (3.4.15)

$$\left[\underline{\mathbf{p}}_s^{(j)}\left(\overline{\widetilde{\mathbf{p}(i)}_{\xi2}}^s\,{}_s\overline{\mathbf{G}(i)}^s\,\frac{\partial\overline{\theta}_{(i)}}{\partial\overline{\mathbf{q}}}\right)+\underline{\mathbf{p}}_s^{(i)^{\xi2}}\left(\overline{\widetilde{\mathbf{p}(j)}}^s\,{}_s\overline{\mathbf{G}(j)}^s\,\frac{\partial\overline{\theta}_{(j)}}{\partial\overline{\mathbf{q}}}\right)\right]\delta\overline{\mathbf{q}}=0 \qquad (3.7.11)$$

A similar constraint equation can be obtained for a virtual change in the second kinematic constraint of equation (3.7.9), namely

$$\left[\underline{\mathbf{p}}_s^{(j)}\left(\overline{\widetilde{\mathbf{p}(i)}_{\xi3}}^s\,{}_s\overline{\mathbf{G}(i)}^s\,\frac{\partial\overline{\theta}_{(i)}}{\partial\overline{\mathbf{q}}}\right)+\underline{\mathbf{p}}_s^{(i)^{\xi3}}\left(\overline{\widetilde{\mathbf{p}(j)}}^s\,{}_s\overline{\mathbf{G}(j)}^s\,\frac{\partial\overline{\theta}_{(j)}}{\partial\overline{\mathbf{q}}}\right)\right]\delta\overline{\mathbf{q}}=0 \qquad (3.7.12)$$

The five kinematic constraints of a revolute joint are stated by equations (3.7.5), (3.7.11) and (3.7.12). It can be combined in a single matrix equation

$$\overline{\underline{\mathbf{C}}}_q\,\delta\overline{\mathbf{q}}=\overline{\mathbf{0}} \qquad (3.7.13)$$

where

$$\overline{\underline{\mathbf{C}}}_{\mathbf{q}} = \left[\begin{array}{c} \overline{\mathbf{H}_{(i)}}^s + \overline{\mathbf{H}_{(j)}}^s \\[2ex] \underline{\mathbf{p}}_s^{(j)}\left(\overline{\underline{\tilde{\mathbf{p}}^{(i)}}_{\xi 2}}^s {}_s\overline{\mathbf{G}_{(i)}}^s \frac{\partial\overline{\boldsymbol{\theta}}_{(i)}}{\partial\overline{\mathbf{q}}}\right) + \underline{\mathbf{p}}_s^{(i)^{\xi 2}}\left(\overline{\underline{\tilde{\mathbf{p}}_{(j)}}}^s {}_s\overline{\mathbf{G}_{(j)}}^s \frac{\partial\overline{\boldsymbol{\theta}}_{(j)}}{\partial\overline{\mathbf{q}}}\right) \\[3ex] \underline{\mathbf{p}}_s^{(j)}\left(\overline{\underline{\tilde{\mathbf{p}}^{(i)}}_{\xi 3}}^s {}_s\overline{\mathbf{G}_{(i)}}^s \frac{\partial\overline{\boldsymbol{\theta}}_{(i)}}{\partial\overline{\mathbf{q}}}\right) + \underline{\mathbf{p}}_s^{(i)^{\xi 3}}\left(\overline{\underline{\tilde{\mathbf{p}}_{(j)}}}^s {}_s\overline{\mathbf{G}_{(j)}}^s \frac{\partial\overline{\boldsymbol{\theta}}_{(j)}}{\partial\overline{\mathbf{q}}}\right) \end{array}\right] \qquad (3.7.14)$$

Shabana (1994:403), Chung and Haug (1993) and Nikravesh and Ambrosio (1991) give the definition and constraint equations of various other types of mechanical joints.

3.7.2 Relative Coordinate Method

Equation (3.4.93) is valid for any general system having six degrees of freedom at each mechanical joint. If there are geometric or kinematic constraints at some of the joints, the system will have fewer than six degrees of freedom at those joints. Choosing the orientation of the body coordinate systems to coincide with the direction of the joint constraints will reduce the number of unknown generalised speeds in the governing equation (3.4.93). The governing differential equation that needs to be solved can be obtained by subtracting the known generalised speeds from the original governing equations and by omitting the equations that correspond to the known generalised speeds (Huston, 1990:271). After the unknown generalised speeds have been obtained, they can be used to calculate the generalised constraint forces and moments (Huston, 1990:275).

3.8 Summary of Multibody Method

In the previous sections the algorithms were developed to give a numeric description of a general system of connected rigid bodies with the properties needed to develop a dynamic model of a dragline. The multibody system is permitted to have closed loops, and collisions and contacts between the bodies are permitted.

The first step in the modelling of a system of rigid bodies is to specify the number of bodies. A coordinate system must be assigned to each body. The origin of this coordinate system must be located at each body's centre of mass. The inertial properties and geometry (position of joints) must be defined with respect to this coordinate system. The next step is to define the topology of the system (which bodies are connected and the type of joint).

A set of generalised coordinates must be defined and the initial state of the system must be defined in this set of coordinates.

It is possible to calculate the dynamic behaviour of the system if the forgoing properties are defined. Figure (3.13) shows the flowchart of the modelling procedure when the relative coordinate method is used. The modelling procedure that is applicable to both the absolute and relative coordinate method can be summed as follow:

- Calculate inertial and geometric properties of each body with respect to the inertial system.
- Calculate the force applied to each body and the inertial force of each body. Apply the generalised coordinate transformation to these forces.
- Calculate the Jacobian matrix of the constraint equations if needed.
- Determine the governing differential equations.
- Identify and integrate the equations for the unknown generalised coordinates.

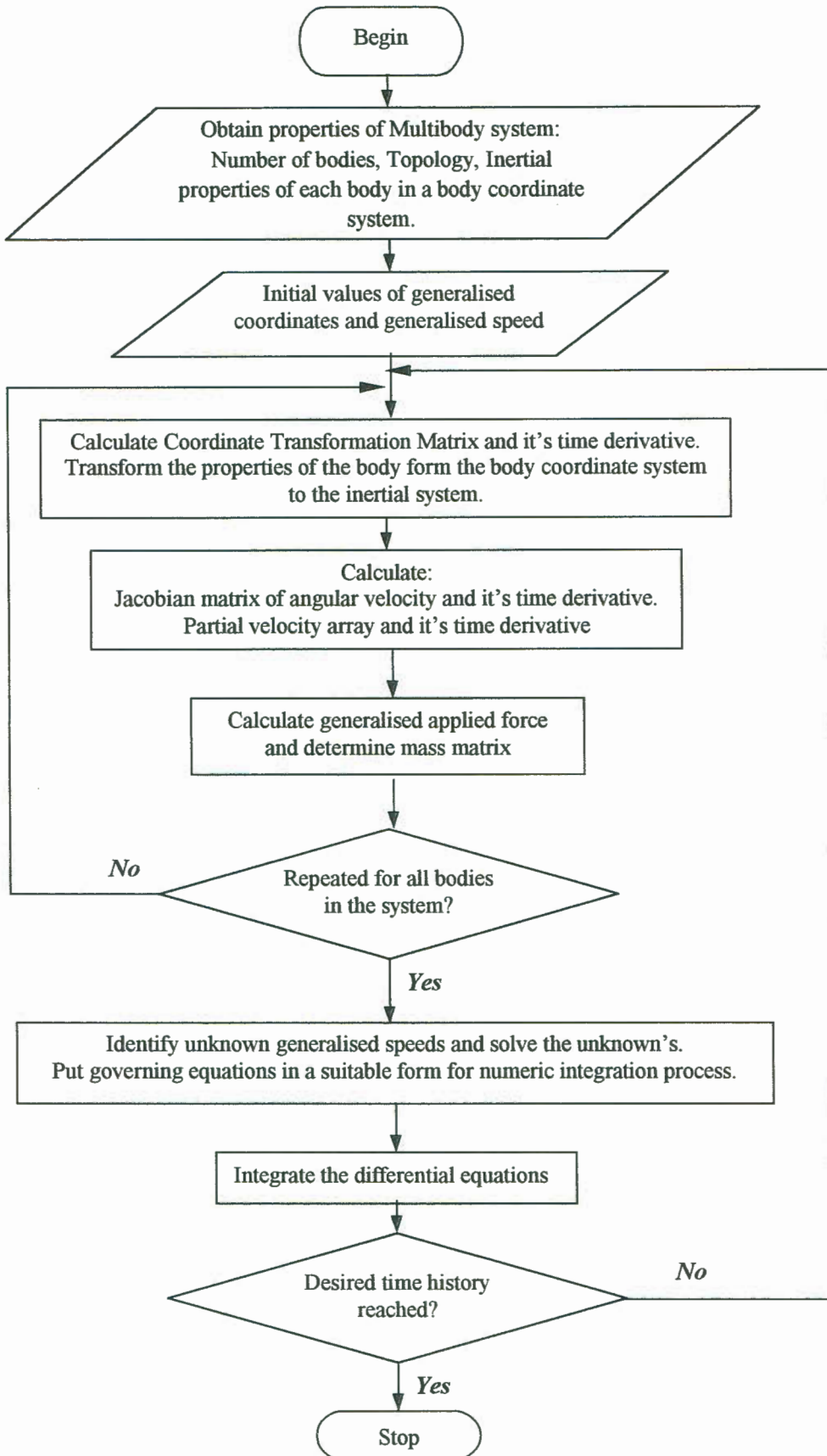This process must be repeated until the desired time history is obtained.

```
                          ┌─────────────┐
                          │    Begin    │
                          └─────────────┘
                                 │
                                 ▼
        ╱─────────────────────────────────────────────╲
       ╱   Obtain properties of Multibody system:       ╲
      ╱    Number of bodies, Topology, Inertial          ╲
      ╲    properties of each body in a body coordinate   ╱
       ╲                   system.                       ╱
        ╲─────────────────────────────────────────────╱
                                 │
                                 ▼
            ╱───────────────────────────────────╲
           ╱   Initial values of generalised       ╲
           ╲   coordinates and generalised speed   ╱
            ╲───────────────────────────────────╱
                                 │
                                 ▼
       ┌───────────────────────────────────────────────┐
       │ Calculate Coordinate Transformation Matrix and  │
       │ it's time derivative. Transform the properties  │
       │ of the body form the body coordinate system     │
       │ to the inertial system.                         │
       └───────────────────────────────────────────────┘
                                 │
                                 ▼
          ┌────────────────────────────────────────┐
          │ Calculate:                               │
          │ Jacobian matrix of angular velocity and  │
          │ it's time derivative.                    │
          │ Partial velocity array and it's time     │
          │ derivative                               │
          └────────────────────────────────────────┘
                                 │
                                 ▼
            ┌──────────────────────────────────┐
            │ Calculate generalised applied     │
            │ force and determine mass matrix    │
            └──────────────────────────────────┘
                                 │
                                 ▼
   No                    ◇───────────────◇
  ◄───────────────────── ◇ Repeated for all ◇
                         ◇ bodies in the     ◇
                          ◇   system?        ◇
                           ◇───────────────◇
                                 │ Yes
                                 ▼
       ┌───────────────────────────────────────────────┐
       │ Identify unknown generalised speeds and solve   │
       │ the unknown's.                                  │
       │ Put governing equations in a suitable form for  │
       │ numeric integration process.                    │
       └───────────────────────────────────────────────┘
                                 │
                                 ▼
            ┌──────────────────────────────────┐
            │ Integrate the differential         │
            │ equations                          │
            └──────────────────────────────────┘
                                 │
                                 ▼
                    ◇───────────────◇      No
                    ◇ Desired time    ◇ ─────────►
                    ◇ history reached? ◇
                     ◇───────────────◇
                           │ Yes
                           ▼
                    ┌─────────────┐
                    │    Stop     │
                    └─────────────┘
```

Figure 3.13   *Flowchart for the multibody method using relative coordinates.*

94

It may look as if the method that has been developed can be used to predict the motion of a system of rigid bodies for an unlimited time into the future, given the forces on the bodies and their initial positions and velocities. Quite often the motion of very simple dynamic systems cannot always be predicted accurately far into the future. Such motions are labeled as chaotic (Moon, 1987) and can be characterize as systems whose time history is very sensitive to initial conditions. If the motions of two identical chaotic systems are started with nearly identical initial conditions, the motions of the two systems will diverge from each other exponentially. If the initial conditions were precisely the same, the motion will be identical for all time. Since there is always some uncertainty in the starting condition of physical systems, the divergence of the resulting motion cannot be avoided. With this in mind one may well ask if there is any sense in obtaining the time history of such a system with the numerical integration of the governing dynamic equation, since the numeric solution is an approximation at each time step. Numerical solutions obtained with different time steps or different numeric methods would also diverge, but these different trajectories represent uncorrelated versions of the same chaos pattern (Thomson and Stewart, 1986).

The multibody method was verified for various problems using analytic and experimental techniques. The problems and a comparison of the analytic verification are given in Appendix D. The experimental verification is describe in the next chapter.

CHAPTER 4

MULTIBODY EXPERIMENT

The interaction between a rope and a pulley is very complex, especially when the pulley is not fixed in space and if the system is subjected to impulsive forces. Analytic solutions can be obtained easily for simple problems as describe in Appendix D. For complex problems, like the interaction between a rope and a pulley, it is easier to verify the multibody method using experimental techniques.

It is difficult to measure the trajectory of a point on a rope that is moving. In order to verify the description of the rope and pulley interaction, the motion of a component of the system that is exited by the motion of the rope will be measured and used for the verification. The system that is used for the verification is shown in Figure (4.1).
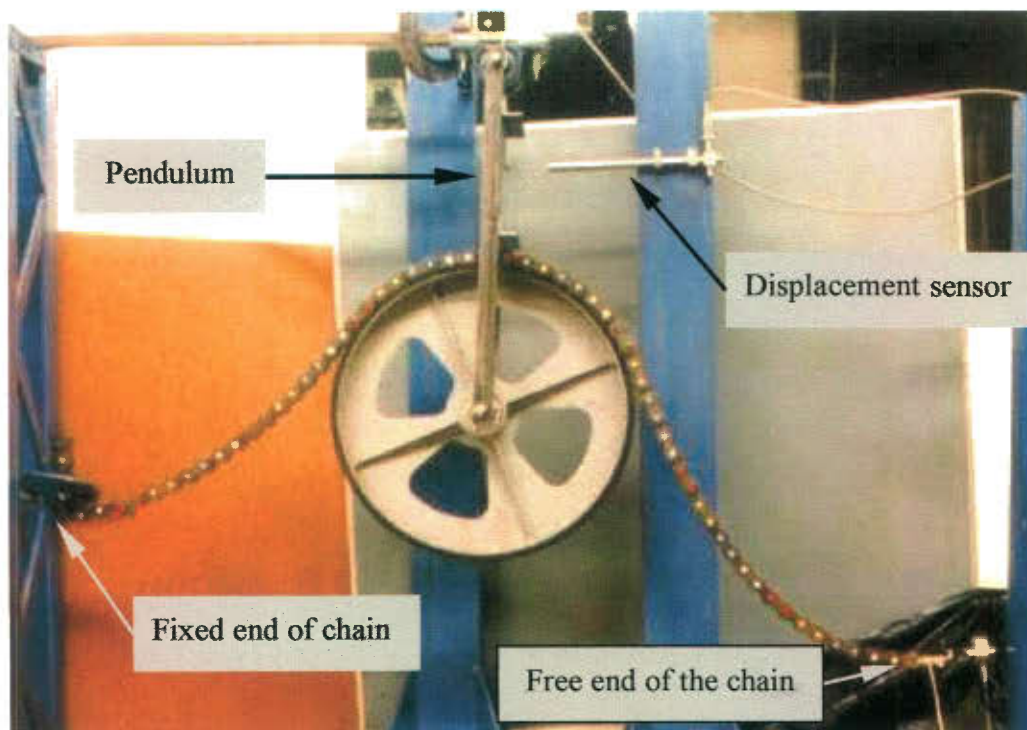
Figure 4.1   *The system that is used for the verification.*

Figure (4.2) shows the layout and the initial conditions. It is composed of a pulley that is connected to a pendulum. The one end of the rope is fixed in space. A chain is used in the experiment to represent the rope because it corresponds to the rigid segment description of the rope in the multibody model. The angular displacement of the pendulum is measured during the motion of the system using a sample frequency of 1000 Hz.
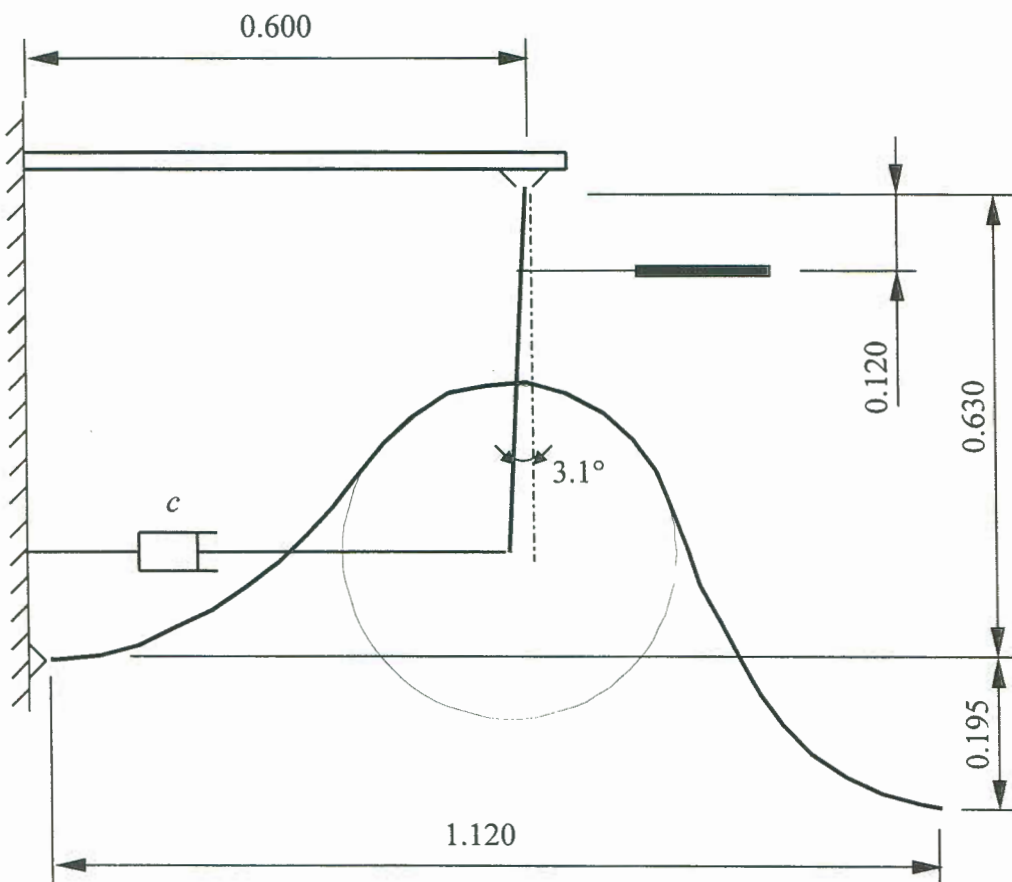
Figure 4.2   *A diagram showing the initial condition and layout of the experiment and multibody model. (All dimensions are in metre.)*

4.1 Description of the Components in the Model

Pulley

The pulley that is used has a radius of 0.2 m and a mass of 4.24 kg. The principle moments of inertial are calculated to be:

$$J_{xx} = J_{yy} = 4.15 \times 10^{-2} \text{ kg m}^2 \text{ and}$$

$$J_{zz} = 8.3 \times 10^{-2} \text{ kg m}^2$$

about the principle axis (as show in Figure (4.3)).
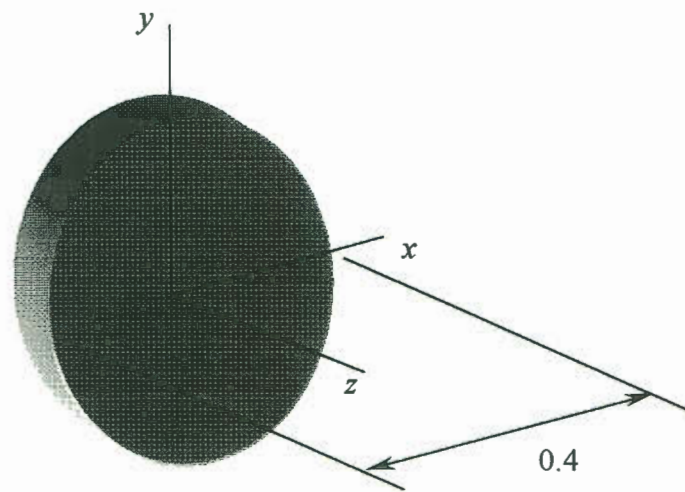
Figure 4.3   *The principle axis and the diameter of the pulley.*

Pendulum

The pendulum that supports the pulley has a length of 0.46 m and a mass of 1.48 kg. The positions of the centre of mass and the reference axis of the pulley are shown in Figure (4.4). The moments of inertia about the centre of mass are:

$$J_{xx} = 0 \text{ kg m}^2 \text{ and}$$

$$J_{yy} = J_{zz} = 3.183 \times 10^{-2} \text{ kg m}^2.$$
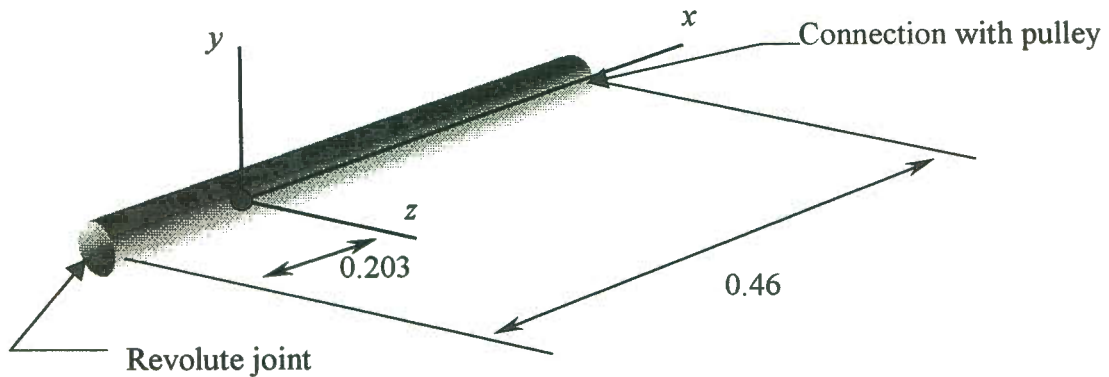
Figure 4.4   *The position of the centre of mass of the pendulum and the body reference axis.*

The rope

An ANSI No. 80 simplex transmission chain represents the rope in the experiment. This chain has a mass of 2.695 kg/m. A 1.475 m length of chain is used in the experiment. In the multibody simulation two links are modelled as a single rigid body to decrease the size of the model and decrease the simulation time. The mass of each rigid body is 0.1348 kg. The moments of inertial are:

$$J_{xx} = 1.2638 \times 10^{-2} \text{ kg m}^2$$
$$J_{yy} = 6.6277 \times 10^{-2} \text{ kg m}^2$$
$$J_{zz} = 3.0602 \times 10^{-2} \text{ kg m}^2$$

Figure (4.5) shows the dimension of the rigid body and the coordinate system of the body that has its origin at the body's centre of mass
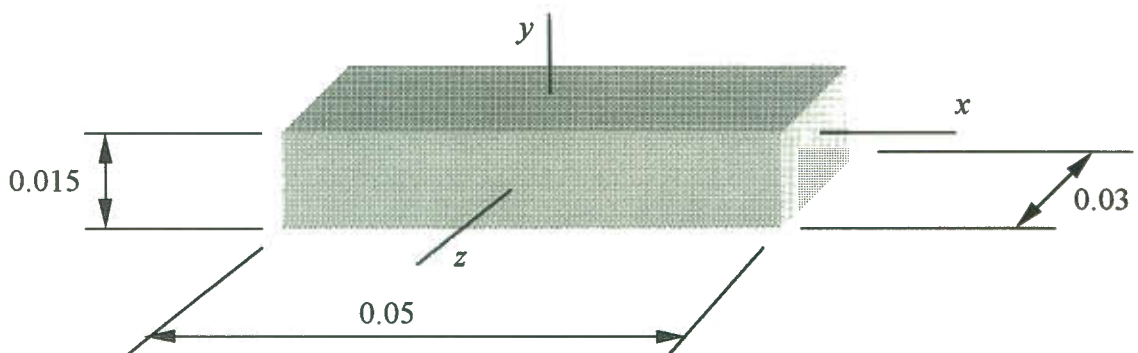
Figure 4.5   *The rigid body used in the multibody model that represents two links of the chain.*

4.2 Experiment and Simulation

The system was set in the position as shown in Figure (4.2) by constraining the position of the free end of the chain. The system was allowed to reach a static equilibrium condition before the motion was initiated by removing the position constraint from the free end of the rope. The chain falls down onto the pulley and causes the pulley-pendulum assembly to swing. This swinging motion of the pulley was measured with a linear variable differential transformer.
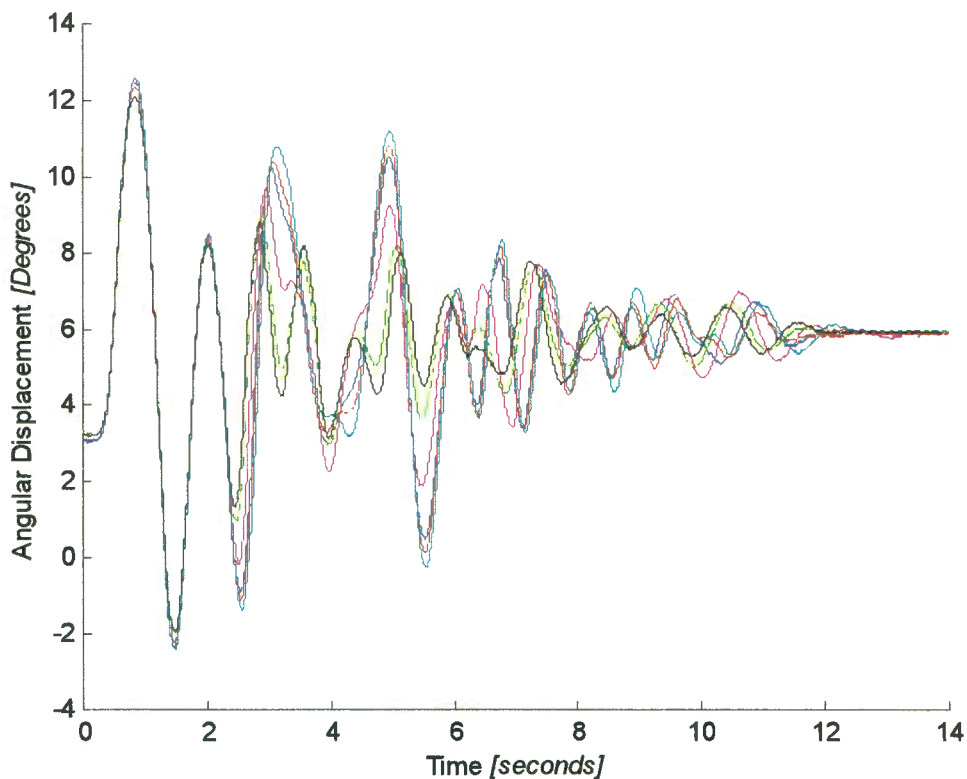
Figure 4.6   *The angular displacement of the pendulum measured during different experiments.*

The experiment was repeated a number of times. The angular displacement of the pendulum during the motion is shown in Figure (4.6). It can be seen clearly that chaotic motion occurred in the experiments. It is therefore clear that it would be impossible to obtain an exact solution for one of the experiments with the multibody method. It can also be seen that there is an amount of energy dissipation in the system because a static

100

equilibrium condition is reached after 14 seconds. Friction in the bearing that supports the pendulum and friction between the links of the chain contribute to this energy dissipation. A viscous damper is included in the multibody model to introduce energy dissipation in the numeric model.

Figure (4.7) shows solutions obtained with the numeric multibody method. These results were obtained using a fourth order Runge-Kutta method with a time step of 0.001 seconds. The pulley was modelled with an effective radius of 0.21 m. The contact elements between the pulley and chain segments had a stiffness of 5000 N/m and a damping constant of 500 $Nm^{-1}s$. The motion was simulated for different values of the damping constant of the force element that represents the friction effects of the displacement sensor.
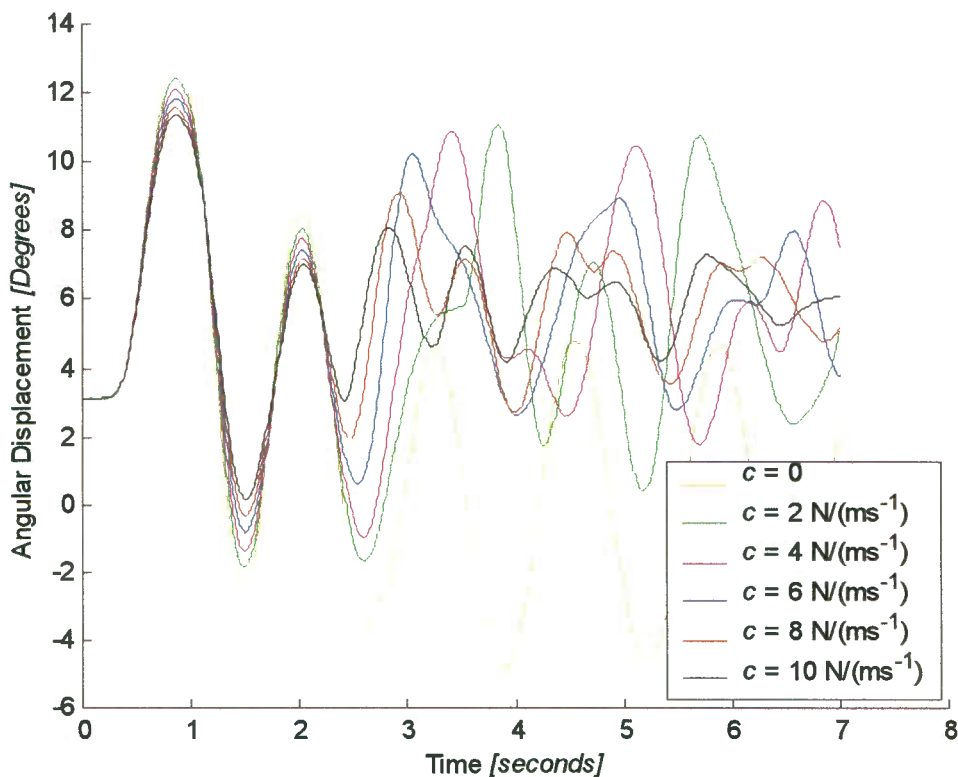
Figure 4.7   *The angular displacement calculated with the multibody method.*

In Figure (4.8) the angular displacement of the pendulum measured during the experiment and the result obtained with the multibody method are compared.

101
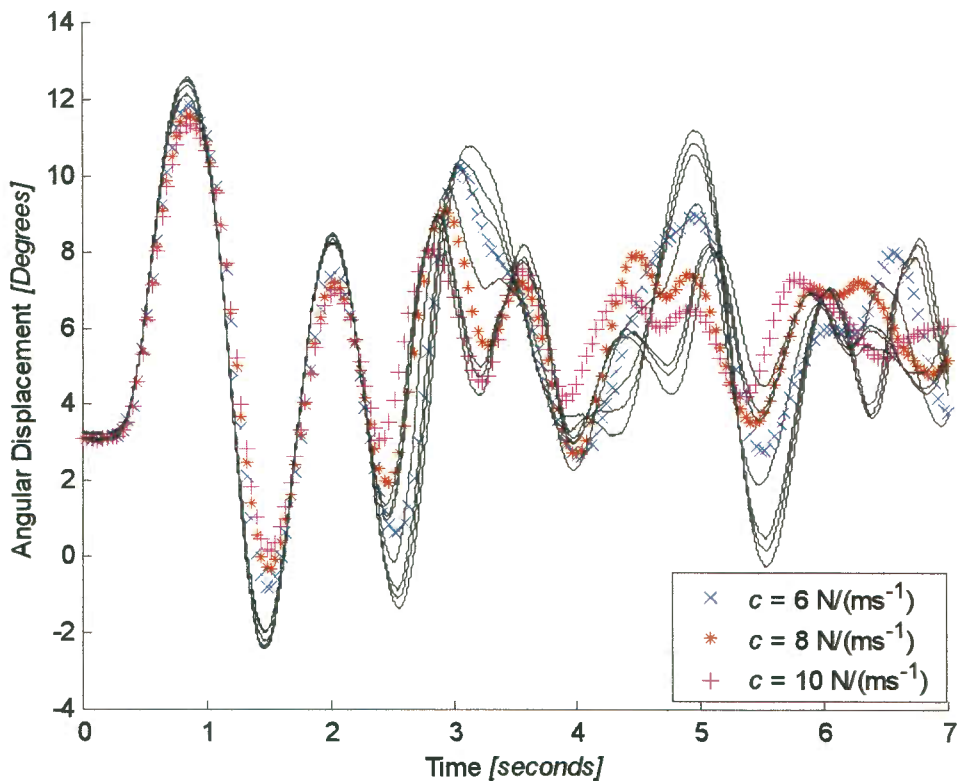
Figure 4.8   A *comparison of experimental and numeric results.*

Conclusion

It can be seen that there is a very good correspondence between the measured and calculated values of the angular displacement. The differences that occur are the result of the chaotic behaviour of the system where approximations in both the initial state and during the numeric integration of the governing dynamic equations have a significant effect on the time history obtained with the multibody method. A better prediction of the motion can be made if all the segments of the chain is modelled as separate bodies.

The position of the system at various instances in time obtained with the multibody method is shown in Figure (4.9).

t = 0 seconds

t = 0.29 seconds

t = 0.59 seconds

t = 0.89 seconds

t = 1.19 seconds

t = 1.49 seconds

t = 1.79 seconds

t = 2.09 seconds

t = 2.39 seconds

t = 2.69 seconds

t = 2.99 seconds

t = 3.29 seconds
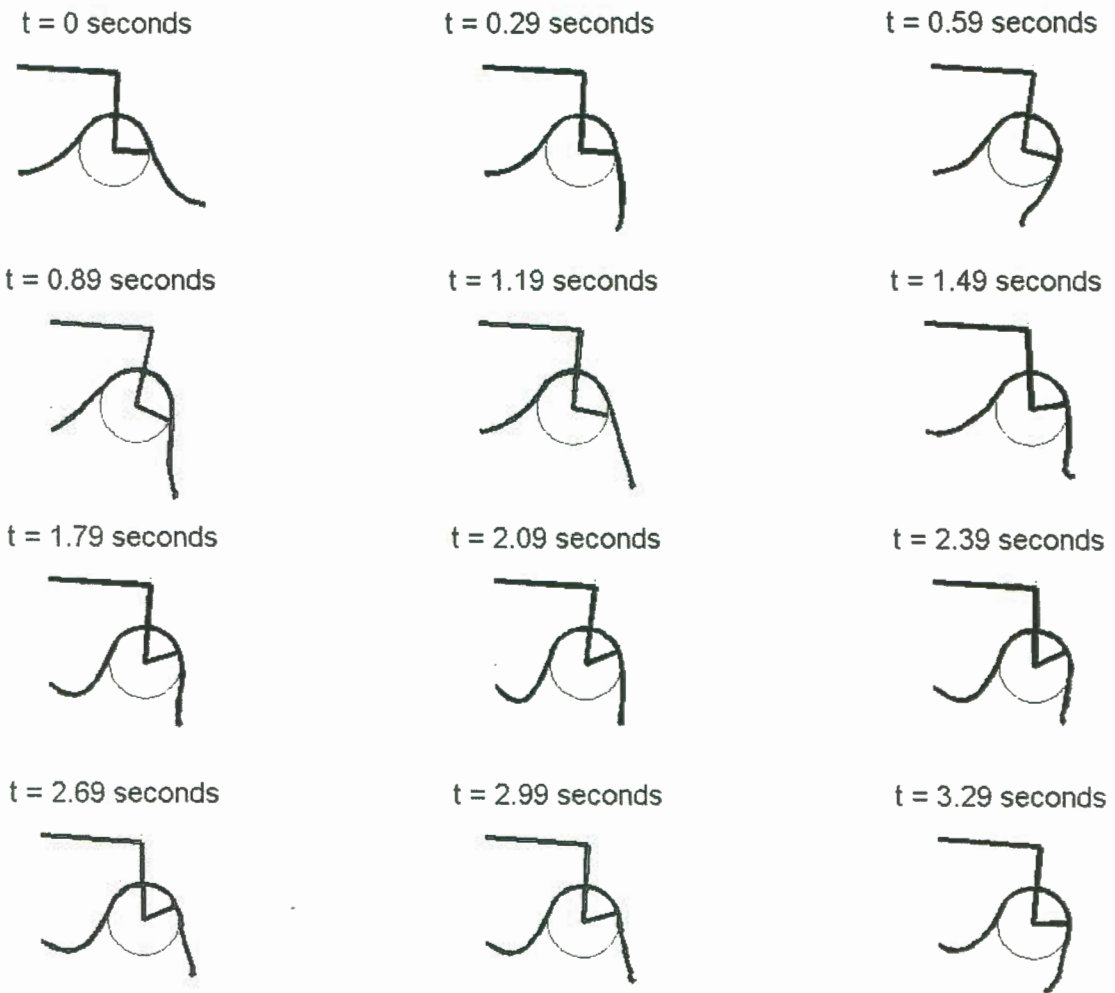
Figure 4.9   *The position of the system at different instances in time calculated with the multibody program.*

CHAPTER 5

MODELLING A DRAGLINE

A method to describe the motion of connected rigid bodies has been developed in Chapter 3. In this chapter it is implemented to describe the motion of a dragline bucket during an operational cycle. This model is composed of sets of connected rigid bodies and force elements.
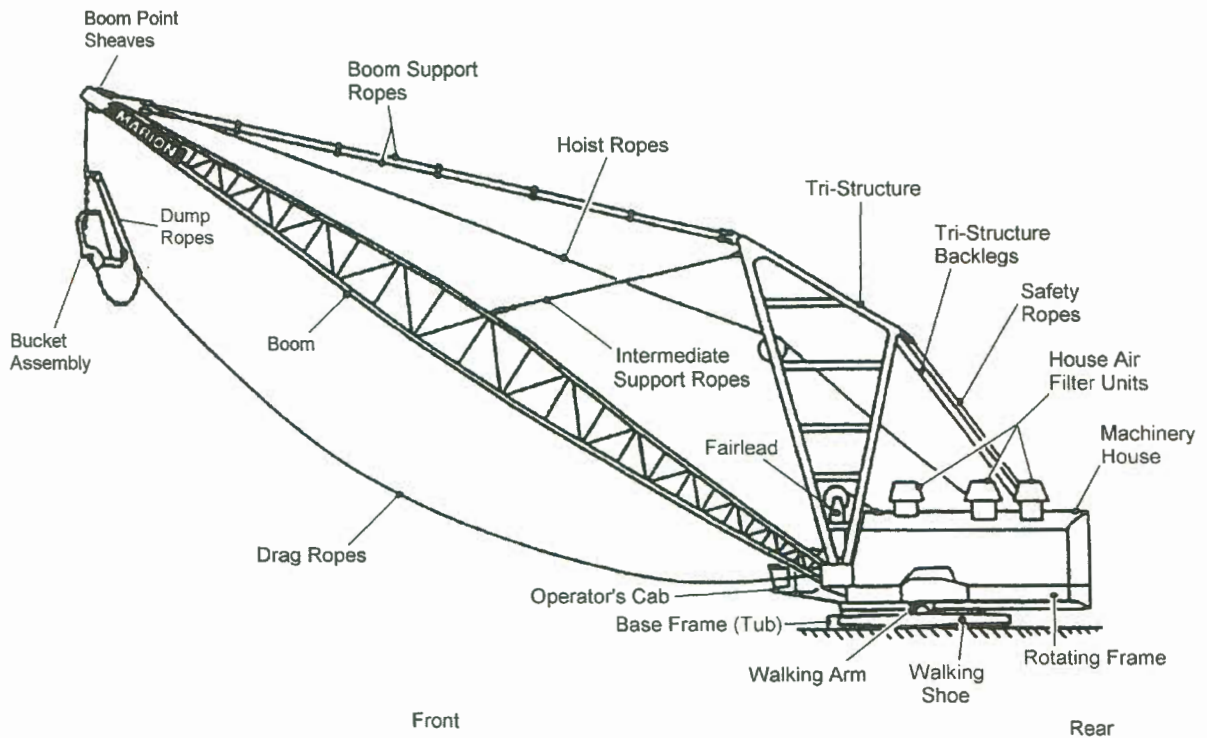
Figure 5.1 *The components of a dragline.*

The configuration of the dragline is slightly changed in the numerical model in order to increase the speed of calculating a simulation of an operational cycle. These changes do not have a significant effect on the predicted motion of a bucket, but it reduce the size (number of bodies) and complexity of the rigid body model. A major change in the

configuration is the position of the hoist and drag winches that are located in the machine house. In the numerical model the drag winch is positioned at the fairlead and the hoist winch is positioned at the boom point. A further simplification is that the winches wind the rope onto the drum in a single plane; it does not introduce a lateral displacement of the rope as it is wound onto the drum.[3] The deformation of the components when they are subjected to loads is also ignored.

The various components of the dragline (Figure 5.1) that have an effect on the motion of the bucket are modelled as follow:

- *Hoist, Drag and Dump Ropes*

  A finite segment approach is used to model these components. In the physical system these components have axial and torsional stiffness. In the rigid body model they are modelled as totally axially stiff (no deformation) and with either total torsional stiffness by using universal joints between the bodies or with no torsional stiffness using spherical joints. Some of the torsional stiffness characteristics can be introduced by using spherical joints that have torsional springs between the bodies.

- *Hoist Chains*

  The weight of the bucket keeps the hoist chains under tension during the swing cycle. This causes adjacent shackles always to be in close contact with each other. The contact surfaces between the two shackles allow relative rotations along two perpendicular axes in a plane perpendicular to the reference line of the chain. This connection can be modelled as a universal joint and the shackles as rigid bodies. Dampers can be included in the joints to model friction effects. These dampers can be linear or non-linear. The lower hoist chains are connected with revolute joints (permit relative rotation along a given vector) to the bucket. The lower hoist chains and the upper hoist chains can be modelled as single rigid bodies during the time in which they are subjected to tensile forces.

---

[3] It is not a very big simplification, because both the boom point sheaves and the fairlead guide the hoist and drag ropes to stay in the vertical plane underneath the boom.

- *Drag Chain*

  The drag chains do not always experience tension. The tension is relieved to allow dumping. During this process, adjacent shackles can have relative translations to each other. It is suspected that this effect would not have a significant influence on the global behaviour of the system and the shackles are modelled as if they are always in close contact with no relative translations. The chains are modelled as rigid bodies connected with universal joints.

- *Bars*

  The spreader bar and equalisation bars are modelled as rigid bodies connected with revolute joints to the rest of the model.

- *Bucket*

  The empty bucket is modelled as a rigid body with a constant mass, a fixed centre of mass (in a local body reference system) and constant moments of inertia (in a local body reference system).

- *Payload (Overburden inside the bucket)*

  The total mass, the position of the centre of mass and the moments of inertia of the payload change when the bucket disengages from the ground and during the swing and dumping cycles. These changes are caused by the behaviour of the overburden inside the bucket when the bucket is subjected to changes in the attitude and acceleration. The loss of overburden causes the changes the mass and the moment of inertia of the payload to change. The movement of the overburden inside the bucket causes the changes in the position of the centre of gravity and the moments of inertia.

  The observation of a dragline in operation has lead to the conclusion that the overburden inside the bucket stays fairly stationary (relative to the bucket) during the largest part of the swing cycle. As a first approximation of the motion, to identify trends of the carry angle during rigging design, the payload can be

considered as a solid body. To create a better approximation and to model the bucket ground interaction, the disengagement and the dumping phase, a granular description of the payload must be included in the dynamic model of the dragline.

The inertial properties of a body (with respect to the body reference system) are not allowed to change during the simulation. Newton's laws that form the foundation of the multibody method cannot be applied if the inertial properties change. To model the system for the case where material is lost from the bucket, the material that is suspected to fall from the bucket must be modelled as separate bodies. These bodies can then be coupled with bonding force elements (permitting compressive force and breakage if a specified tensile force is reached) to the body that represents the payload.

The payload can also be modelled using the multibody description that McPhee and Dubey (1991) developed that can be used for variable mass systems. This description is based on the Reynolds transport theorem.

- *Dump block*

  The dump block is modelled as a pulley. The interaction between the dump block and dump rope is modelled using the penalty function method described in paragraph (3.5.4).

- *Winches*

  The hoist and drag winches are modelled as pulleys to which the first rope segment is connected with a revolute joint. The interaction between the rope and pulley is also modelled with the method described in paragraph (3.5.4).

By specifying the swing motion of the machine and the rotational speed of or the moment applied to the winches, an operational cycle can be simulated. The time value of these variables can be obtained from measurements taken during an operational cycle of a dragline.

After numerous numerical experiments on different test systems, it has been decided to use the relative coordinate description method instead of the absolute coordinate formulation because it has been found that violations of the constraint equations during integration of the absolute coordinate method have a significant influence on the result. The relative coordinate formulation has the advantage that the non-working constraint forces are eliminated from the equations of motion. Disadvantages of this method are that it is computationally less efficient than the absolute coordinate formulation (Huston, *et al.* 1994) and that the simulations take longer.

The system is modelled as two separate sub-systems and the interaction between the two systems is enforced with force elements. The machine base, the drag winch and rope, the hoist winch and rope and the upper hoist assembly (including the dump block) of the rigging form the first sub-system. The bucket, the payload, the dump rope and the drag chains form the second sub-system. The machine base and the bucket are taken as the base bodies of each sub-system. The machine base is constrained in such a way that it has only one rotational degree of freedom (permitting rotation about the machine's rotation axis). The bucket is not subjected to any constraints and it has six degrees of freedom. The lower hoist chains, the drag chains and the dump rope are connected with revolute joints to the bucket. Closed loops that occur in both systems are cut at secondary joints to obtain a tree structure and the connectivity conditions are enforced with force elements.

With this description it is possible to simulate the dynamic behaviour of the dragline. It was unfortunately not possible to perform this simulation because of the absence of a super-computer to perform the large volume of complex numeric calculations that have to be performed. Simpler methods can be developed to give an approximation of the dynamic behaviour of the bucket during an operation cycle. The motion of the bucket during the filling and dumping cycles are very complex and any method simpler that the method described will give highly inaccurate results during these cycles. An accurate calculation of the dynamic behaviour of the bucket during these cycles is crucial for the optimisation of the bucket and the rigging.

CHAPTER 6

CONCLUSION AND RECOMMENDATIONS

A numeric method was formulated to describe the dynamic behaviour of a dragline bucket during an operational cycle. Among the results that can be obtained with this model are the attitude of the bucket and the forces on the components. These results are very important in the optimisation of the bucket's rigging and the design of high performance buckets. The numeric multibody dynamic method can be used to calculate the dynamic behaviour of any system that can be idealised by one or more rigid component.

The method to describe the contact (with friction) between a rope and a pulley was used in the dragline model to describe the interaction between the dump block and dump rope, as well as the interaction between the hoist and drag ropes and the winches. This method can be applied to model the interaction, including friction effects, between any thin rigid body and circular disc.

The value of the damping constant used in the model to describe the rope and pulley interaction cause of numerical problems. It was found that when the damping constant was calculated, using the coefficient of restitution that describes the energy loss when a rope segment collides with the pulley, numerical instabilities occurred. It was found that the damping constant must be chosen such that the mass spring damper system of a rope-segment and pulley is overdamped. The solution is then more stable and accurate.

Future Work

Many of the computational problems that arose in some of the areas of the multibody dynamic formulation present opportunities for future research.

The absolute coordinate formulation needs to be considered in more detail, especially for large systems. This method is very efficient because it eliminates a lot of computations that must be made in the relative coordinate formulation. Most of the elements of the Jacobian matrixes of the position and orientation coordinates are zero and all the non-zero elements are equal to one. A transformation of any body property to the generalised coordinates by multiplying it with a Jacobian matrix does not change the values of the property's elements; it only defines the position of the elements in the system's generalised property. The coefficient matrix of the vector of second coordinate derivatives and Lagrange multipliers in equation (3.4.56) is sparse. This should be exploited to economise on the space needed to store the matrix in the computer's memory and the running time of the simulation. It is possible to create a banded coefficient matrix by numbering the bodies in a correct sequence. The disadvantage of this method is that violations of the constraint equations that occur during the solution process cause numeric instabilities in the solution. This problem can be partially eliminated by using a numerical procedure that can solve and integrate a system of differential algebraic equations.

For future work an in-depth study of the processes to obtain a numeric solution of a set of stiff initial value ordinary differential equations and the solution of a set of differential algebraic equations are very important. During the testing and the verifying of the numerical procedure, many numerical problems were experienced with the numerical integration processes.

The complexity and the amount of numeric calculations that needs to be performed make it a necessity to have access to a supercomputer. As an alternative parallel processing can be utilised to decrease the time that is needed to perform the multibody analysis.

APPENDIX A

NOTATION AND VECTOR OPERATIONS

In multibody dynamics the motion of a system of connected bodies is studied. The behaviour of both the individual bodies and the system is important. A mathematical notation that can distinguish between the different bodies in the system is needed. A combination of the matrix tensor notation proposed by Hassenpflug (1993, 1995) and index notation is used. The properties of the bodies are described in matrix tensor notation and the index notation is used to distinguish between the various bodies in the system. The indices for the bodies are written in brackets to distinguish them from the indices of the elements of the vectors and tensors written in matrix tensor notation. The vectors that are written in matrix tensor notation are mostly in 3-dimensional Euclidean space (R^3) and the vectors written in index notation are mostly in a multidimensional space. The number of bodies in the system determines the dimension of the multidimensional space. The vectors related to the generalised coordinates are in general not orthogonal.

Vector

A column vector is indicated by a bar over the symbol used to name the vector.

$$\overline{\mathbf{v}} \equiv \begin{bmatrix} v_1 \\ v_2 \\ v_3 \end{bmatrix} \tag{A.1}$$

A row vector is indicated by a bar beneath the symbol.

$$\underline{\mathbf{v}} \equiv \begin{bmatrix} v_1 & v_2 & v_3 \end{bmatrix} \tag{A.2}$$

111

The transpose changes the row column character of a vector and therefore the transpose vector has a transposed vector bar symbol.

$$\left[\overline{\mathbf{v}}\right]^T = \underline{\mathbf{v}^T} \tag{A.3}$$

$$\left[\underline{\mathbf{v}}\right]^T = \overline{\mathbf{v}^T} \tag{A.4}$$

Matrix

Matrices have a dual row/column character and are indicated by an underbar as well as an overbar.

$$\overline{\underline{\mathbf{M}}} \equiv \begin{bmatrix} m_{11} & m_{12} & m_{13} \\ m_{21} & m_{22} & m_{23} \\ m_{31} & m_{32} & m_{33} \end{bmatrix} \tag{A.5}$$

Multiplication Rules

The vector bars cancel diagonally across the multiplication sign. The remaining vector bar symbols on both sides of a matrix equation must be equal after the cancellation.

$$\overline{\underline{\mathbf{A}}} \cdot \overset{+}{\mathbf{v}} = \overline{\overline{\mathbf{r}}} \tag{A.6}$$

Scalar product

The scalar product of two vector $\overline{\mathbf{a}}$ and $\overline{\mathbf{c}}$ is a scalar.

$$\overline{\mathbf{a}} \bullet \overline{\mathbf{c}} \equiv \underline{\mathbf{a}}\,\overline{\mathbf{c}} \equiv |\overline{\mathbf{a}}||\overline{\mathbf{c}}|\cos\theta \tag{A.7}$$

$$\overline{\mathbf{a}} \bullet \overline{\mathbf{c}} \equiv \underline{\mathbf{a}}\,\overline{\mathbf{c}} \equiv a_1 c_1 + a_2 c_2 + a_3 c_3 \tag{A.8}$$

From equation (A.7) it can be seen that the scalar product of two column vectors may be obtained by multiplying the one vector with the transpose of the other vector or by multiplying a row vector with a column vector.

Norm

The norm of a vector is the magnitude or length of the vector. The Euclidean norm of a vector is:

$$|\vec{v}| \equiv v \equiv \sqrt{\vec{v} \bullet \vec{v}} = \sqrt{\underline{v}\,\underline{v}} = \sqrt{v_1^2 + v_2^2 + v_3^2} \tag{A.9}$$

Physical Vectors

Physical vectors are indicated by an arrow above the vector name: $\vec{v}$
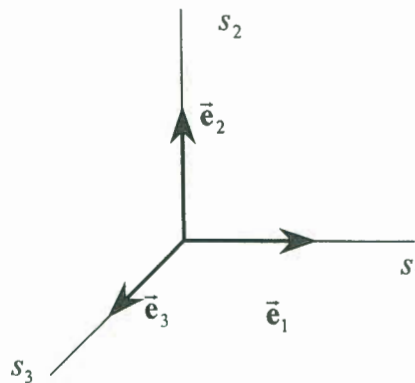
Figure A.1   *Coordinate axis and base vectors*

Figure (A.1) shows three orthogonal coordinate axes s_1, s_2, s_3 and three orthogonal unit vectors $\vec{e}_1$, $\vec{e}_2$ and $\vec{e}_3$. Any physical vector in 3D Euclidean space can be described as:

$$\vec{v} \equiv \vec{e}_1 v_1 + \vec{e}_2 v_2 + \vec{e}_3 v_3 \tag{A.10}$$

The unit vectors have the physical dimension of direction only and a numeric size of 1. These vectors form a base of R^3

Base

The base vectors have a very important physical meaning and are defined as a single quantity. The row vector of the orthogonal base vectors is defined as:

$$\underline{\vec{E}} \equiv \begin{bmatrix} \vec{e}_1 & \vec{e}_2 & \vec{e}_3 \end{bmatrix} \qquad (A.11)$$

With this relation one can write Equation (A.10) as:

$$\vec{v} = \underline{\vec{E}} \cdot \overline{v} \qquad (A.12)$$

We distinguish a base of a coordinate system by adding the name to the underbar of the base. We define the base of coordinate system s as: $\underline{\vec{E}}_s = \begin{bmatrix} \vec{e}_{s1} & \vec{e}_{s2} & \vec{e}_{s3} \end{bmatrix}$. The components of a vector measured in a base are subscripted similarly to the direction vectors. The base name is added to the vector bar.

$$\overline{v}^s = \begin{bmatrix} v_{s1} \\ v_{s2} \\ v_{s3} \end{bmatrix} \qquad (A.13)$$

Using this relation, one can describe a physical vector in base $\underline{\vec{E}}_s$ with the equation:

$$\begin{aligned}
\vec{v} &= \vec{e}_{s1} v_{s1} + \vec{e}_{s2} v_{s2} + \vec{e}_{s3} v_{s3} \\
&= \begin{bmatrix} \vec{e}_{s1} & \vec{e}_{s2} & \vec{e}_{s3} \end{bmatrix} \cdot \begin{bmatrix} v_{s1} \\ v_{s2} \\ v_{s3} \end{bmatrix} \\
&= \underline{\vec{E}}_s \cdot \overline{v}^s
\end{aligned} \qquad (A.14)$$

The base is an orthogonal matrix, because its columns $\vec{e}_1$, $\vec{e}_2$ and $\vec{e}_3$ form an orthogonal set. The inverse of the base is equal to its transpose.

The direction vectors of base *r* can be described in base *s* by applying equation (A.14) to each of the physical base vectors of base *r*.

$$
\begin{aligned}
\left[\bar{e}_{r1}^{s} \quad \bar{e}_{r2}^{s} \quad \bar{e}_{r3}^{s} \right] &= \left[\underline{\bar{E}}^{s} \cdot \vec{e}_{r1} \quad \underline{\bar{E}}^{s} \cdot \vec{e}_{r2} \quad \underline{\bar{E}}^{s} \cdot \vec{e}_{r3} \right] \\
&= \underline{\bar{E}}^{s} \cdot \left[\vec{e}_{r1} \quad \vec{e}_{r2} \quad \vec{e}_{r3} \right] \\
&= \underline{\bar{E}}^{s} \cdot \vec{\underline{E}}_{r} \\
&\equiv \underline{\bar{E}}_{r}^{s}
\end{aligned}
$$

The quantity $\underline{\bar{E}}_{r}^{s}$ is called the transformation matrix between the two sets of coordinate axis *s* and *r* and it is defined as:

$$
\underline{\bar{E}}_{r}^{s} \equiv \left[\bar{e}_{r1}^{s} \quad \bar{e}_{r2}^{s} \quad \bar{e}_{r3}^{s} \right] \tag{A.17}
$$

This is also an orthogonal matrix and the following relations can be stated:

$$
\begin{aligned}
\underline{\bar{E}}_{r}^{s} &= \left[\underline{\bar{E}}_{s}^{r} \right]^{T} \\
&= \left[\underline{\bar{E}}_{s}^{r} \right]^{-1}
\end{aligned} \tag{A.18}
$$

The physical vector $\vec{v}$ can be described with respect to both bases as:

$$
\begin{aligned}
\vec{v} &= \vec{\underline{E}}_{s} \bar{v}^{s} = \vec{\underline{E}}_{r} \bar{v}^{r} \\
\bar{v}^{s} &= \left[\vec{\underline{E}}_{s} \right]^{T} \vec{\underline{E}}_{r} \bar{v}^{r} = \underline{\bar{E}}_{r}^{s} \bar{v}^{r} \text{ or } \bar{v}^{r} = \left[\vec{\underline{E}}_{r} \right]^{T} \vec{\underline{E}}_{s} \bar{v}^{s} = \underline{\bar{E}}_{s}^{r} \bar{v}^{s}
\end{aligned} \tag{A.19}
$$

The transformation matrix is also called the direction cosine matrix.

Using the row form of a physical vector, it is possible to write

$$
\begin{aligned}
\underline{v} \cdot \vec{\underline{E}}_{s} &= \underline{v}_{s} \\
&= \left[v_{s1} \quad v_{s2} \quad v_{s3} \right]
\end{aligned}
$$

Therefore, $\underline{\mathbf{v}}_s$ means the row vector of the same components as $\overline{\mathbf{v}}^s$. This implies that for an orthonormal base the following relations hold:

$$\left[\overline{\mathbf{v}}^s\right]^T \equiv \underline{\mathbf{v}}_s^T = \underline{\mathbf{v}}_s \text{ and } \left[\underline{\mathbf{v}}_s\right]^T \equiv \overline{\mathbf{v}^T}^s = \overline{\mathbf{v}}^s \qquad (A.20)$$
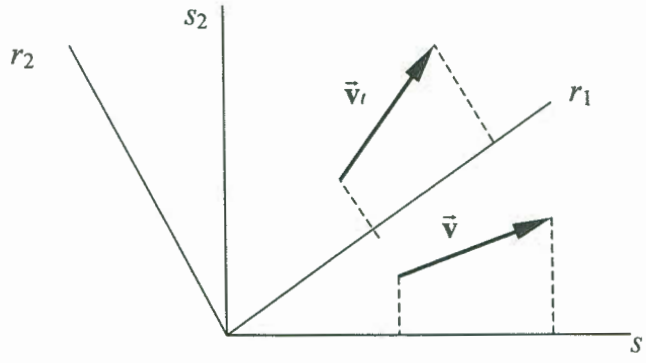
Rotations

Figure A.3   *The rotation of a vector.*

Consider the case of a vector that is fixed in a rotating base $\underline{\vec{\mathbf{E}}}_r$ with its initial position $\vec{\mathbf{v}}$ and final position $\vec{\mathbf{v}}_{\prime}$ shown in Figure (A.3). The initial orientation of $\underline{\vec{\mathbf{E}}}_r$ corresponds with $\underline{\vec{\mathbf{E}}}_s$. We can write the transformation for the vector $\vec{\mathbf{v}}_{\prime}$

$$\overline{\mathbf{v}}_{\prime}{}^s = \underline{\overline{\mathbf{E}}}_r^s \overline{\mathbf{v}}_{\prime}{}^r \qquad (A.21)$$

but the vector is fixed in the base $\underline{\vec{\mathbf{E}}}_r$ and $\overline{\mathbf{v}}^s = \overline{\mathbf{v}}_{\prime}{}^r$, therefore

$$\overline{\mathbf{v}}_{\prime}{}^s = \underline{\overline{\mathbf{E}}}_r^s \overline{\mathbf{v}}^s \qquad (A.22)$$

We define a new entity $\overline{\underline{\mathbf{R}}}$, the rotation tensor, to make a distinction between the rotation of a vector in a base and a transformation between two bases.

$$\overline{v}_i^s = \overline{\overline{R}}_s^s \overline{v}^s \quad \text{with} \quad \overline{\overline{R}}_s^s = \overline{\overline{E}}_r^s \tag{A.23}$$

Vector or cross product

The cross product of two vectors $\vec{a}$ and $\vec{c}$ is a vector perpendicular to both $\vec{a}$ and $\vec{c}$. The computational rule for the cross product is usually given in the form:

$$\vec{a} \times \vec{c} = \begin{vmatrix} \vec{e}_1 & \vec{e}_2 & \vec{e}_3 \\ a_1 & a_2 & a_3 \\ c_1 & c_2 & c_3 \end{vmatrix}$$
$$= (a_2 c_3 - a_3 c_2)\vec{e}_1 + (a_3 c_1 - a_1 c_3)\vec{e}_2 + (a_1 c_2 - a_2 c_1)\vec{e}_3 \tag{A.24}$$

or in orthogonal base notation

$$\overline{a} \times \overline{c} = \begin{vmatrix} \overline{e}_1 & \overline{e}_2 & \overline{e}_3 \\ a_1 & a_2 & a_3 \\ c_1 & c_2 & c_3 \end{vmatrix} = \begin{bmatrix} \overline{e}_1 & \overline{e}_2 & \overline{e}_3 \end{bmatrix} \cdot \begin{bmatrix} a_2 c_3 - a_3 c_2 \\ a_3 c_1 - a_1 c_3 \\ a_1 c_2 - a_2 c_1 \end{bmatrix} \tag{A.25}$$

One can write this equation in matrix form as:

$$\overline{a} \times \overline{c} = \overline{\tilde{\tilde{a}}} \cdot \overline{c} \tag{A.26}$$

where $\tilde{\tilde{a}}$ is the skew symmetric tensor of the components of the column vector $\overline{a}$. It is also called the cross product tensor and is defined as:

$$\overline{\tilde{\tilde{a}}} \equiv \begin{bmatrix} 0 & -a_3 & a_2 \\ a_3 & 0 & -a_1 \\ -a_2 & a_1 & 0 \end{bmatrix} \tag{A.27}$$

This tensor has the property that its transpose is equal to the negative of the tensor.

$$\overline{\tilde{\tilde{a}}}^T = -\overline{\tilde{\tilde{a}}} \tag{A.28}$$

118

Using equation (A.25) one can find:

$$\overline{\mathbf{a}} \times \overline{\mathbf{c}} = -\overline{\mathbf{c}} \times \overline{\mathbf{a}} \tag{A.29}$$

That can be written in matrix form as:

$$\widetilde{\underline{\mathbf{a}}} \cdot \overline{\mathbf{c}} = -\widetilde{\underline{\mathbf{c}}} \cdot \overline{\mathbf{a}} = \widetilde{\underline{\mathbf{c}}}^T \cdot \overline{\mathbf{a}} \tag{A.30}$$

Rotating Base

Let $\vec{\underline{\mathbf{E}}}_r$ be a rotating base. The time derivative of a rotating base is given by

$$\frac{d}{dt}\vec{\underline{\mathbf{E}}}_r \equiv \dot{\vec{\underline{\mathbf{E}}}}_r = \vec{\omega} \times \vec{\underline{\mathbf{E}}}_r$$
$$= \widetilde{\underline{\omega}} \cdot \vec{\underline{\mathbf{E}}}_r \tag{A.31}$$

where $\widetilde{\underline{\omega}}$ is defined as the cross product tensor of the angular velocity vector $\vec{\omega}$. If equation (A.30) is transformed to a fixed base $\vec{\underline{\mathbf{E}}}_s$, one obtains

$$\dot{\vec{\underline{\mathbf{E}}}}_r^s = \widetilde{\underline{\omega}}_s^s \vec{\underline{\mathbf{E}}}_r^s \tag{A.32}$$

Combined notation

The kinematic and inertial properties of a body are stated in matrix tensor notation. The index notation is used to distinguish between the properties of the different bodies in the system. The properties of the various bodies are grouped into vectors.

A vector for a particular body is indicated by the normal symbol for a vector in matrix tensor notation to which an index is added. This index is written in brackets and corresponds to the body number. The components of the vector are distinguished by adding

119

the body index to the normal element index. A column vector in base $\underline{\bar{\mathbf{E}}}_s$ for *Body j* is defined as

$$\overline{\mathbf{v}}_{(j)}^s \equiv \begin{bmatrix} \mathbf{v}_{s1(j)} \\ \mathbf{v}_{s2(j)} \\ \mathbf{v}_{s3(j)} \end{bmatrix} \tag{A.33}$$

The transpose of this column vector, a row vector[4], is defined as

$$\left[\overline{\mathbf{v}}_{(j)}^s\right]^T = \underline{\mathbf{v}}_s^{(j)} \tag{A.34}$$

We define the difference vector between body i and body j as

$$\overline{\mathbf{v}}_{(ij)}^s = \overline{\mathbf{v}}_{(j)}^s - \overline{\mathbf{v}}_{(i)}^s \tag{A.35}$$

where the double index in brackets is used to show that it is the vector quantity pointing from body i to body j.

A matrix quantity for a specific body is indicated by

$$\overline{\overline{\mathbf{M}}}_{(j)} \tag{A.36}$$

---

[4] The vector is stated relative to the orthonormal base s, therefore the components of the column and row vectors are the same.

APPENDIX B

HERTZ CONTACT FORCE

In the multibody dynamic description of a system of bodies, a penalty function method is used to describe the contacts between bodies. It is necessary to calculate the force that exists between two bodies when there is an interference of their non-deformed outer surfaces. To describe the system as accurately as possible a force scheme that corresponds with the physical system is needed. An expression for this contact force can be obtained from the description of the Hertz contact stress as described by Boresi, et al. (1978:604). The force that is obtained using this method gives only an approximate result since the elastic strains in the bodies away from the contact region are neglected.

When two semicircular elastic bodies are pressed together, the surface of the solids deform elastically over a region surrounding the initial point of contact. The bodies are then in contact over a small area in the neighbourhood of the initial point of contact.

Consider two semicircular disks, as shown in Figure (B.1), that are pressed together by a force (F_n) normal to the contact surface such that the total deformation of the bodies at the contact point is ξ. Let R_1, R_1', R_2 and R_2' be the principal values of the radii of the respective contact surfaces, where the plane sections in which R_1 and R_1' (similarly R_2 and R_2') lie are perpendicular to each other. If the contact surface of a body is convex, the sign of the radius is positive and if it is concave, the sign of the radius is negative. Let α be the angle that the planes of curvature of the bodies make at the contact point. If E_1 and E_2 are the tensile moduli of elasticity and υ_1 and υ_2 the Poisson ratios of the respective bodies then the relation between the deformation (ξ) and the contact force (F_n) can be obtained from Boresi, et al. (1978) as
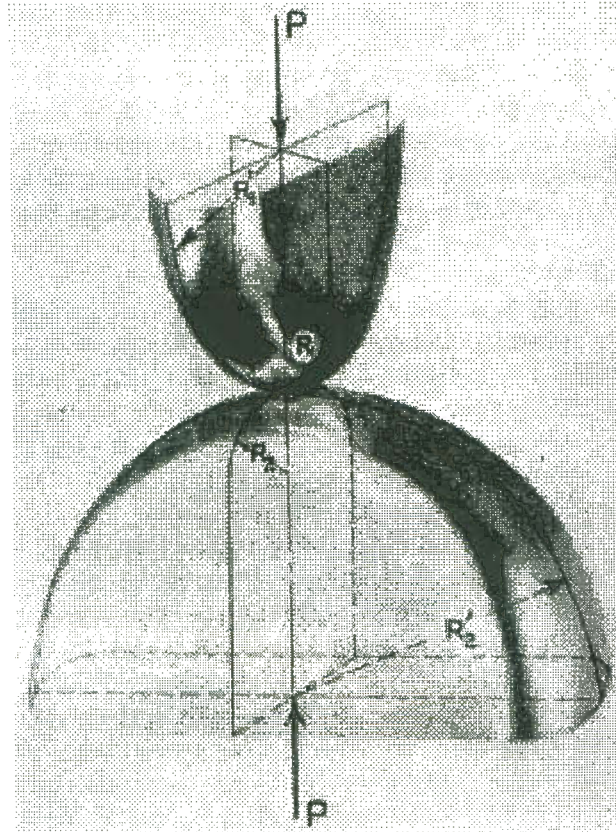
Figure B.1   *Two semicircular disks in contact.*

$$F_n = \frac{1}{\Delta} \sqrt{\left(\frac{2\pi}{3kK(k')(A+B)}\right)^3 \left(\frac{3kE(k')}{2\pi}\right)} \xi^{3/2}$$

$$= \Psi \xi^{3/2} \tag{B.1}$$

where

$$A = \frac{1}{4}\left(\frac{1}{R_1} + \frac{1}{R_1'} + \frac{1}{R_2} + \frac{1}{R_2'}\right)$$
$$- \frac{1}{4}\sqrt{\left[\left(\frac{1}{R_1} - \frac{1}{R_1'}\right) + \left(\frac{1}{R_2} - \frac{1}{R_2'}\right)\right]^2 - 4\left(\frac{1}{R_1} - \frac{1}{R_1'}\right)\left(\frac{1}{R_2} - \frac{1}{R_2'}\right)\sin^2\alpha}$$

$$B = \frac{1}{4}\left(\frac{1}{R_1} + \frac{1}{R_1'} + \frac{1}{R_2} + \frac{1}{R_2'}\right)$$

$$+ \frac{1}{4}\sqrt{\left[\left(\frac{1}{R_1} - \frac{1}{R_1'}\right) + \left(\frac{1}{R_2} - \frac{1}{R_2'}\right)\right]^2 - 4\left(\frac{1}{R_1} - \frac{1}{R_1'}\right)\left(\frac{1}{R_2} - \frac{1}{R_2'}\right)\sin^2\alpha}$$

$$\Delta = \frac{1}{A+B}\left(\frac{1-\upsilon_1^2}{E_1} + \frac{1-\upsilon_2^2}{E_2}\right)$$

$$K(k') = \int_0^{0.5\pi} \frac{d\theta}{\sqrt{1 - k'^2 \sin^2\theta}}$$

$$E(k') = \int_0^{0.5\pi} \sqrt{1 - k'^2 \sin^2\theta}\, d\theta$$

$$k' = \sqrt{1 - k^2}$$

and k is obtained from the relation

$$\frac{B}{A} = \frac{(1/k^2)E(k') - K(k')}{K(k') - E(k')} \tag{B.2}$$

By integrating the elliptic integrals $K(k')$ and $E(k')$ numerically using Simpson's rule for various k values and by evaluating equation (B.2), it is possible to find the following empirical relation:

$$k = 0.97268(B/A)^{-0.64127} \tag{B.3}$$

A comparison between the empirical relation of equation (B.3) and the numeric solution of equation (B.2) is shown in Figure (B.2).

APPENDIX C

NUMERICAL INTEGRATION

C.1   Introduction

The initial value problem, which we wish to solve numerically, is

$$\frac{dy}{dt} = f(t, y), \qquad t \in [a, b] \tag{C.1}$$

with the initial value $y(a) = y_0$

The following class of general k – step numeric methods solves the system of equations over the specified interval by generating the sequence y_n $(n = 0, 1, \ldots, N)$ that is an approximation to $y(t_n)$ where $t_n = a + nh$ and $Nh = b - a$:

$$\sum_{j=0}^{k} \alpha_j y_{n+1} = h\phi_f(t_n; y_{n+k}, y_{n+k-1}, \ldots, y_n; h) \tag{C.2}$$

The object is to take steps $h_{n+1} = t_{n+1} - t_n$ as large as possible while still meeting some specified error criterion.

It is convenient to define the (first) characteristic polynomial of (C.2) by (Hall and Watt, 1976)

$$\rho(r) = \sum_{j=0}^{k} \alpha_j r^j \tag{C.3}$$

125

C.2   Convergence

The global discretization error at t_n, when the numeric method (stated by equation (C.2)) is applied to the initial value problem (stated by equation (C.1)), is defined to be $y_n - y(t_n)$, $0 \le n \le N$. If this error tends to zero as h tends to zero, the method is said to be convergent (Hall and Watt, 1976). Convergence can also be defined as follows:

A numeric integration method is convergent if $y_n \to y(t)$ as $h \to 0$ (where $n = (t - a)/h$) when it is applied to any initial value problem.

The starting values and all subsequent values must converge for the method to be convergent.

The local discretization error $T_n(h)$ at t_n of the numeric method is defined as

$$\sum_{j=0}^{k} \alpha_j y(t_{n+j}) = h\phi_f(t_n; y(t_{n+k}), \dots y(t_n); h) + T_n(h) \tag{C.4}$$

where $y(t)$ is the solution of the initial value problem.

C.3   Stability

We need to know that small changes in the initial values produce bounded changes in the numeric approximation provided by the method. The stability of the approximations is related to the method as well as to the initial value problem.

C.3.1   Stability of the Initial value problem

Let $(\delta(t), \delta)$ and $(\delta^*(t), \delta^*)$ be any two perturbations and let $z(t)$ and $z^*(t)$ be the resulting perturbed solutions. The initial value problem is defined to be totally stable if there exists a positive constant S such that for all $t \in [a, b]$,

126

$\left| z(t) - z^*(t) \right| \le S\varepsilon$ whenever $\left| \delta(t) - \delta^*(t) \right| \le \varepsilon$ and $\left| \delta - \delta^* \right| \le \varepsilon$.

If an initial value problem is not totally stable, then there is no chance of obtaining an acceptable numeric solution by any discretization method (Hall and Watt, 1976).

C.3.2 Stability of the Numeric Method

The numeric method must also satisfy a similar stability property:

Let δ_n and δ_n^* be any two perturbations and let z_n and z_n^* be the resulting perturbed solutions for $n = 0, 1, \ldots, N$. If there exist constants h_0 and S that for all $h \in (0, h_0)$,

$$\left| z_n - z_n^* \right| \le S\varepsilon \text{ whenever } \left| \delta_n - \delta_n^* \right| \le \varepsilon, \quad (n = 0, 1, \ldots, N),$$

then the integration method is defined to be zero-stable (Hall and Watt, 1976).

For a method to be zero-stable all the roots of the characteristic polynomial $\rho(r)$ must lie within a unit circle in the complex plain and those on the unit circle must be simple (Hall and Watt, 1976). If the method is consistent, then $\rho(r)$ has a root at $r = 1$.

C.4 Region of absolute stability

The concepts of zero-stability and convergence of a numeric method are concerned with the limiting process as $h \to 0$. In practice, we must compute with a finite number of steps. We are concerned with the size of errors for such a non-zero h. The stability of a numeric method is very dependent on the specific initial value problem. To study the absolute stability properties of a numeric integration scheme, the following initial value problem is used:

$$\frac{dy}{dt} = \lambda y \tag{C.5}$$

where λ is a complex constant.

We make the assumption that for the test equation, ϕ_f of equation (C.2) is a linear function in y_{n+1} and

$$\phi_{f=\lambda y} = \lambda \sum_{j=0}^{k} \gamma_j (h\lambda) y_{n+j} \qquad (C.6)$$

The local discretization error is then

$$\sum_{j=0}^{k} \alpha_j y(t_{n+j}) = h\lambda \sum_{j=0}^{k} \gamma_j (h\lambda) y(t_{n+j}) + hT_{n+k}(h), \qquad n \le 0 . \qquad (C.7)$$

The numeric values y_n produced by the numeric method stated by equation (C.2) satisfy

$$\sum_{j=0}^{k} \alpha_j y_{n+j} = h\lambda \sum_{j=0}^{k} \gamma_j (h\lambda) y_{n+j} + \vartheta_{n+k}, \qquad n \le 0 \qquad (C.8)$$

where ϑ_n represents the local rounding error.

On subtracting equation (C.7) from equation (C.8) the global error $\varepsilon_n = y_n - y(t_n)$ satisfies

$$\sum_{j=0}^{k} \left[\alpha_j - h\lambda\gamma_j (h\lambda) \right] \varepsilon_{n+j} = \vartheta_{n+k} - hT_{n+k}(h), \qquad n \le 0 \qquad (C.9)$$

The stability polynomial is defined as

$$\pi(r, h\lambda) = \sum_{j=0}^{k} \left[\alpha_j - h\lambda\gamma_j (h\lambda) \right] r^j \qquad (C.10)$$

with roots r_v, $v = 0, 1, \ldots, k$, (Hall and Watt, 1976).

The global error will propagate in a stable manner as $n \rightarrow 0$ for a finite h, if the roots of the stability polynomial satisfy

$$|r_v| < 1, \qquad v = 1, 2, \ldots \tag{C.11}$$

Hall and Watt (1976) states that a method is absolutely stable for a given $h\lambda$ if all the roots of the stability polynomial lie within the unit circle.

The step size must be such that $h\lambda$ is within the stability region and h must be small enough so that the local discretization error is small.

C.4.1 Stability of Runge-Kutta methods

Gear (1971) states that the region of absolute stability is the area in which

$$\left| \sum_{n=0}^{R} \frac{(h\lambda)^n}{n!} \right| < 1 \tag{C.12}$$

where R is the order of the method. The stability region for the test equation of the first four orders is shown in Figure (C.1).

For $\lambda < 0$ we may be interested either in accuracy or in absolute stability. If $\lambda > 0$ the solution of the initial value problem (C.1) is growing and h must be chosen small enough so that the error in the integration is acceptable. The value of $h\lambda$ will not lie in the region of absolute stability, but it is not important because the solution is growing; h must be chosen so that the error does not grow faster than the solution.
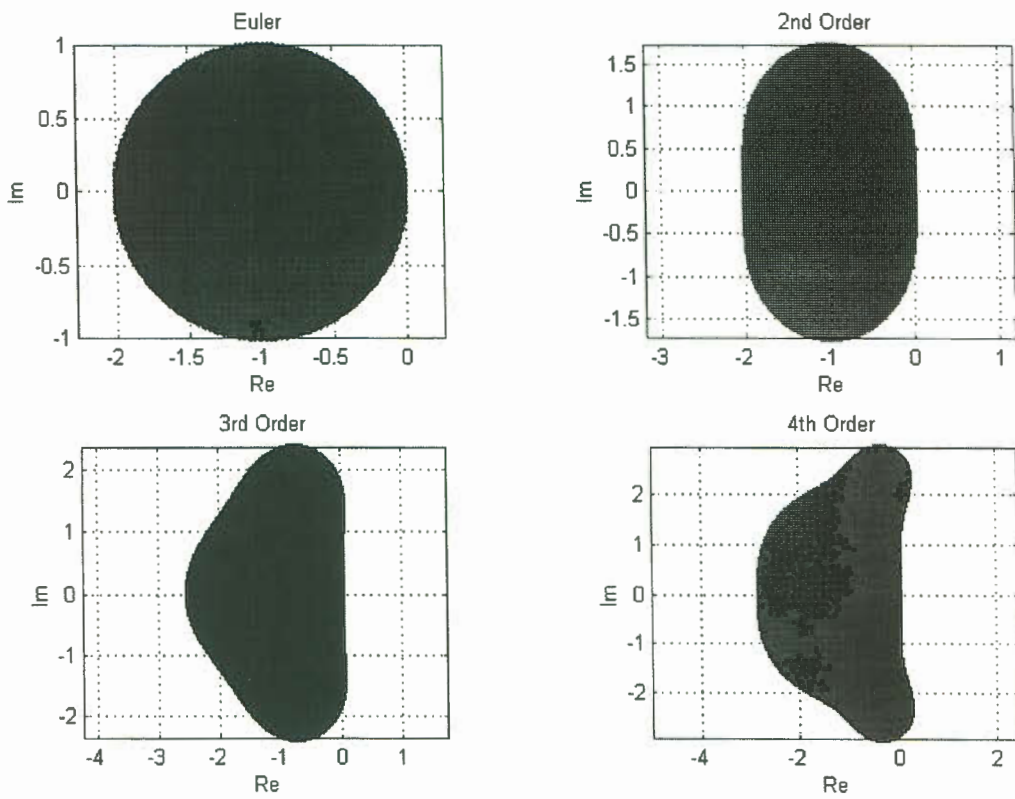
Figure C.1   *The absolute stability regions of different Runge-Kutta orders for the test equation.*

<div align="right">

APPENDIX D

MODEL VERIFICATION

</div>

D.1 Double Pendulum

Consider the double pendulum shown in Figure (D.1). The two masses m_1 and m_2 are connected with non-extendible, light strings of length l_1 and l_2 respectively.
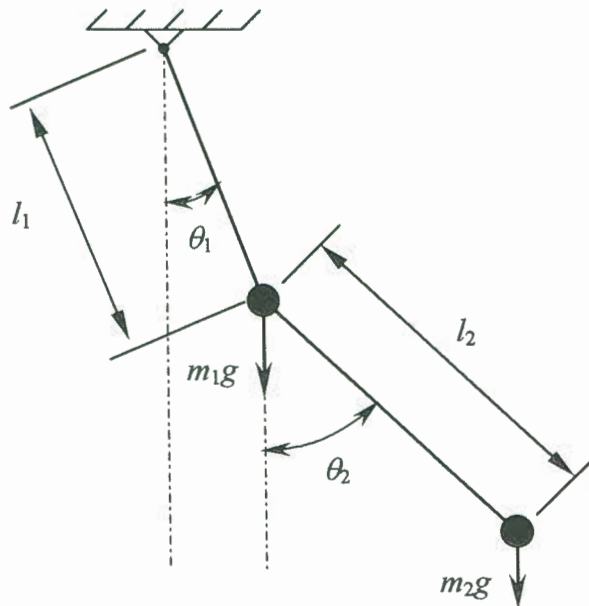

Figure D.1 *Double Pendulum*

The Lagrange's equations of motion for a double pendulum can be obtained as (See Meirovitch (1970), Example 2.4)

$$\frac{d}{dt}\left(\frac{\partial L}{\partial \dot{\theta}_1}\right) - \frac{\partial L}{\partial \theta_1} = (m_1 + m_2)l_1^2\ddot{\theta}_1 + m_2 l_1 l_2 \ddot{\theta}_2 \cos(\theta_2 - \theta_1)$$
$$- m_2 l_1 l_2 \dot{\theta}_1^2 \sin(\theta_2 - \theta_1) + (m_1 + m_2)l_1 g \sin(\theta_1) = 0$$

(D.1)

$$\frac{d}{dt}\left(\frac{\partial L}{\partial \dot{\theta}_2}\right) - \frac{\partial L}{\partial \theta_2} = m_2 l_1 l_2 \ddot{\theta}_1 \cos(\theta_1 - \theta_2) + m_2 l_2^{\,2} \ddot{\theta}_2$$
$$+ m_2 l_1 l_2 \dot{\theta}_1^2 \sin(\theta_2 - \theta_1) + m_2 l_2 g \sin \theta_2 = 0 \qquad (D.2)$$

These equations can be written in the form

$$a\ddot{\theta}_1 + b\ddot{\theta}_2 + c = 0 \qquad (D.3)$$

$$d\ddot{\theta}_1 + e\ddot{\theta}_2 + f = 0 \qquad (D.4)$$

where

$$a = (m_1 + m_2)l_l^2$$

$$b = m_2 l_1 l_2 \cos(\theta_2 - \theta_1)$$

$$c = -m_2 l_1 l_2 \dot{\theta}_1^2 \sin(\theta_2 - \theta_1) + (m_1 + m_2)l_1 g \sin(\theta_1)$$

$$d = m_2 l_1 l_2 \cos(\theta_2 - \theta_1)$$

$$e = m_2 l_l^2$$

$$f = m_2 l_1 l_2 \dot{\theta}_2 \sin(\theta_2 - \theta_1) + m_2 l_2 g \sin(\theta_2)$$

from which we can obtain the equations for the angular acceleration

$$\ddot{\theta}_1 = \left(a - \frac{d}{e}\right)^{-1}\left(\frac{f}{e} - c\right) \qquad (D.5)$$

$$\ddot{\theta}_2 = -\frac{1}{e}\left(d\ddot{\theta}_1 + f\right) \qquad (D.6)$$

These equations form a set of non-linear differential equations and no closed-form solution exists. They must be solved with a numeric method.

Comparison

The system that was modelled to verify the multibody description had the following properties:

132

$m_1 = 10 \text{ kg}$

$m_2 = 5 \text{ kg}$

$l_1 = 0.5 \text{ m}$

$l_2 = 1 \text{ m}$

With the following initial conditions

$\theta_1 = 30°$

$\theta_2 = 10°$

The analytic solution was obtained using the MATLAB ode45 integration routine. The values of the two angular displacements for the first 5 seconds of motion are compared in Figure (D.2). Figure (D.3) compares the angular displacement between the fifteenth and twentieth seconds of the motion.
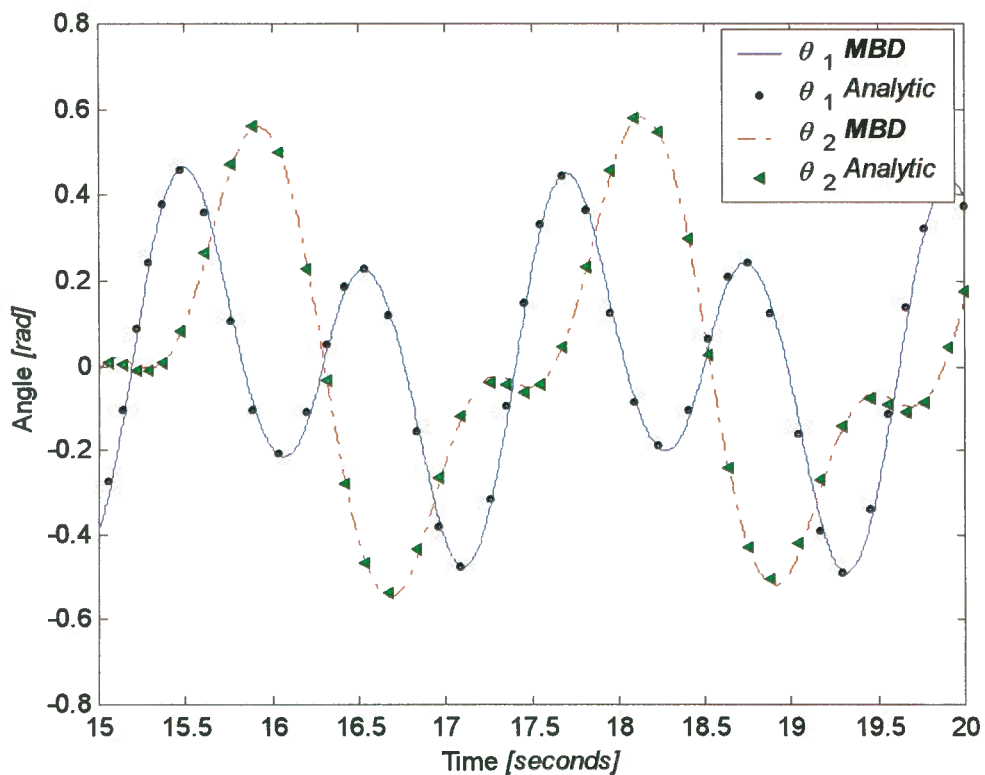

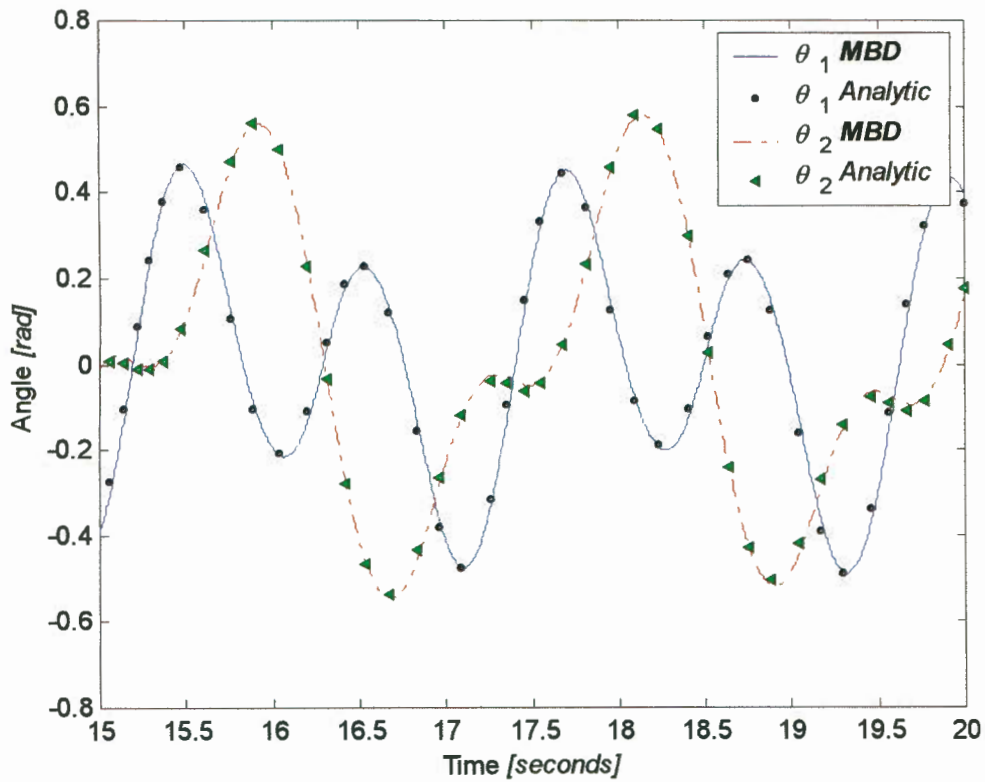**Figure D.2**   *Comparison of the angular displacement for the first 5 seconds of motion.*

Figure D.3   *Comparison of the angular displacement between the 15ᵗʰ and 20ᵗʰ second of motion.*

It can be seen that a very good comparison is obtained at the beginning of the time solution (Figure D.2), but that a slight difference developed later (Figure (D.3)). This difference is caused by errors in the numeric integration of both solutions. Using smaller time steps (or stricter error control) in the numeric integration process will reduce this difference.

D.2   Simple Rope and Pulley Model

Consider the simple rope and pulley system as shown in Figure (D.4). The rope has a length of l metre and a mass of ρ per unit length. The pulley has a moment of inertial of J_p about its rotation axis and it has a radius of r.
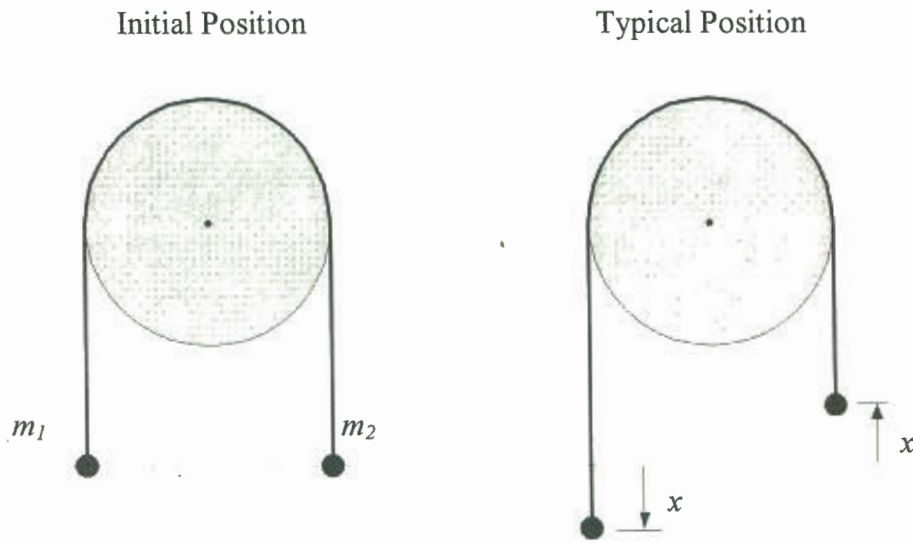
Initial Position   Typical Position

Figure D.4   *Simple rope and pulley model used for the verification.*

Analytic Solution (Energy Principles)

Kinetic energy (at time t)

$$T = \tfrac{1}{2}m_1\dot{x}^2 + \tfrac{1}{2}m_2\dot{x}^2 + \tfrac{1}{2}m_p\dot{x}^2 + \tfrac{1}{2}J_p(\dot{x}/r)^2 \tag{D.7}$$

The change in potential energy

$$V = -m_1 gx - m_2 gx + \rho gx^2 \tag{D.8}$$

The energy equation of the system

$$\left(\tfrac{1}{2}m_1 + \tfrac{1}{2}m_2 + \tfrac{1}{2}m_p + \tfrac{1}{2}J_p r^{-2}\right)\dot{x}^2 = \rho g x^2 + \left(m_1 - m_2\right)gx \tag{D.9}$$

and can be simplified to

$$a\dot{x}^2 = bx^2 + cx \tag{D.10}$$

where

$$a = \tfrac{1}{2}m_1 + \tfrac{1}{2}m_2 + \tfrac{1}{2}m_p + \tfrac{1}{2}J_p r^{-2}$$

$$b = \rho g$$

$$c = \left(m_1 - m_2\right)g$$

The solution of equation (D.10) is

$$t = \alpha \ln\left|x + \tfrac{1}{2}\beta + \sqrt{x^2 + \beta x}\right| - \alpha \ln\left|\tfrac{1}{2}\beta\right|$$

where

$$\alpha = \sqrt{\frac{a}{b}} \quad \text{and} \quad \beta = \frac{c}{b}$$

Comparison

To compare the solution of the time analysis obtained with a multibody method with the analytic solution, the following system was studied:

The rope had a length of 9.747 m (*l*) and a mass of 7.695 kg/m (*ρ*). The pulley had a diameter of 4 m (*r*) and a mass moment of inertia of 1.6 kg m². Two masses of 6 kg (*m₁*) and 5 kg (*m₂*) respectively were connected to the ends of the rope.

In the multibody simulation the rope was modeled with 15 rigid segments that had a mass of 5 kg and a length of 0.6498 m each. The principle moments of inertial (refer to Figure D.5) of each body are $J_{xx} = 0$ and $J_{yy} = J_{zz} = 0.17593$ *kg* m^2 each. The pulley-rope contact interaction was enforced with force elements that had a stiffness of 50000 N/m and a damping constant of $500\text{Nm}^{-1}\text{s}$. The three friction cases were solved in the multibody approach. Dynamic friction coefficients of $\mu = 0$, $\mu = 0.5$ and $\mu = 0.8$ respectively, were used.
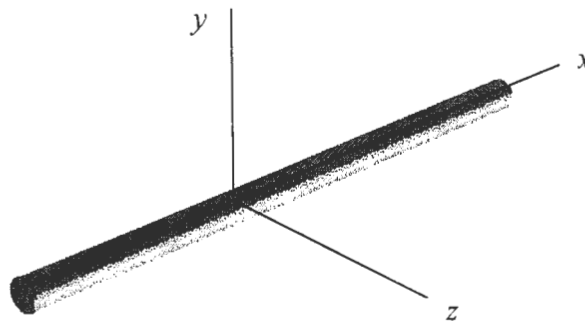

Figure D.5   *Definition of the principle axis of rigid segments.*

The vertical displacement (x) of the 6-kg mass is compared in Figure (D.6) and Figure (D.7).

In the multibody results, the acceleration of the mass is larger than in the analytic solution (the effect of the inertia of the pulley is smaller) and the larger friction coefficient gives a solution closer to the analytic solution.

For the frictionless case, the multibody method and the analytic solution are nearly the same. The multibody method has a small disturbance at the beginning, because the contact spring force was not in equilibrium.
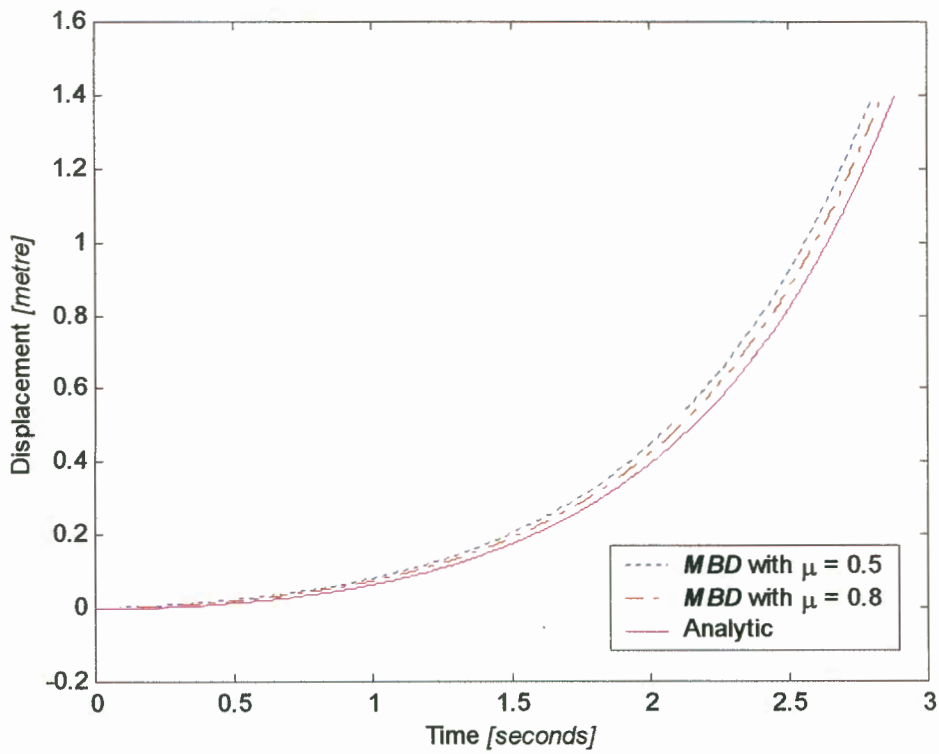
Figure D.6   *Comparison of multibody results with analytic solution that does not permit slip between the rope and the pulley.*
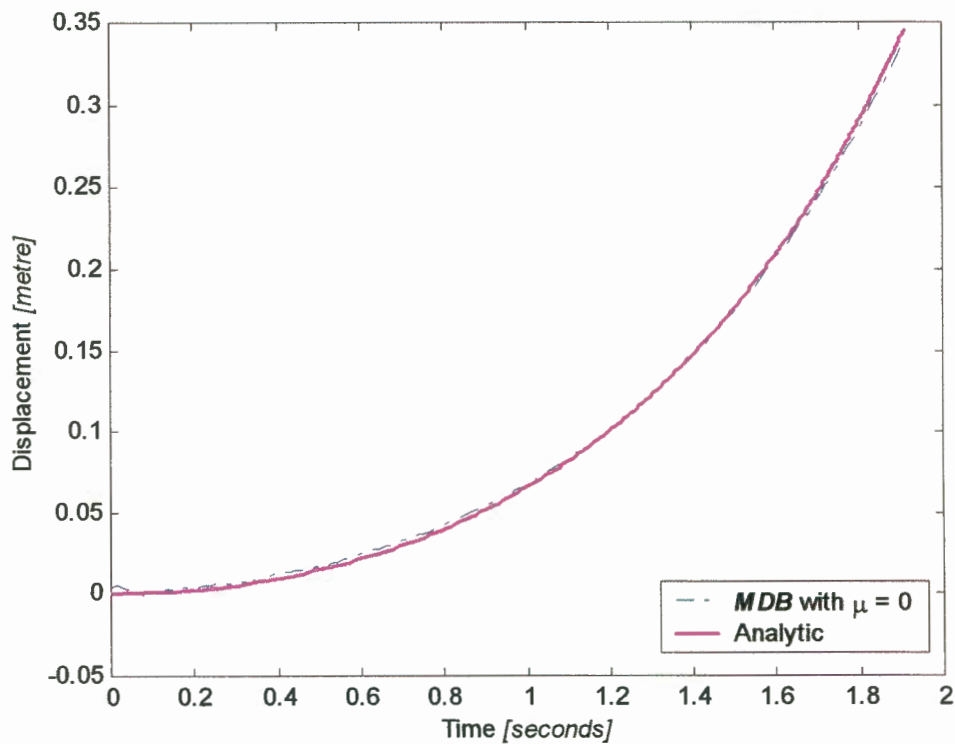

Figure D.7   *Comparison of multibody results with an analytic solution for a smooth cylinder ($J_p = 0$).*

REFERENCES

Adams, J.N., 1990, "UK opencast mining equipment in the 1980's," *International Journal of Surface Mining and Reclamation*, Vol. 4, No. 3, pp. 115-118.

Baafi, E.Y., and Mirabediny, H., 1997, "Computer Simulation of Complex Dragline Operations," *International Journal of Surface Mining, Reclamation and Environment*, Vol. 11, pp. 7-13.

Boresi, A.P., Sidebottom, O.M., Seely, F.B., and Smith, J.O., 1978, *Advanced Mechanics of Materials*, Third Edition, John Wiley and Sons, New York.

Brach, R.M., 1989, "Rigid Body Collisions," *Journal of Applied Mechanics*, Vol. 56, March, pp. 133-138.

Brown, P.N., Byrne, G.D., and Hindmarsh, A.C., 1989, "VODE: A Variable Coefficient ODE Solver," *SIAM Journal of Scientific Computing*, Vol. 10, No. 5, September 1989, pp. 1038-1051.

Chatterjee, A., and Ruina, A., 1998, "Two Interpretations of Rigidity in Rigid-Body Collisions," *Journal of Applied Mechanics*, Vol. 65, December 1998, pp. 894-900.

Choi J.H., Lee, H.C., and Shabana, A.A., 1998a, "Spatial Dynamics of Multibody Tracked Vehicles. Part 1: Spatial Equation of Motion," *Vehicle System Dynamics*, Vol. 29, pp. 27-49.

Choi J.H., Lee, H.C., and Shabana, A.A., 1998b, "Spatial Dynamics of Multibody Tracked Vehicles. Part 2: Contact Forces and Simulation Results," *Vehicle System Dynamics*, Vol. 29, pp. 113-137.

Chung, S., and Haug, E.J., 1993, "A Hybrid Variational Method for Multibody Dynamics," *International Journal for Numerical Methods in Engineering*, Vol. 36, pp. 87-109.

Cundall, P.A., and Strack, O.D.L., 1979, "A Discrete Numerical Model for Granular Assemblies," *Géotechnique*, Vol. 29, No. 1, pp.47-65.

Esterhuyse, S.W.P, 1997, "The Influence of Geometry on Dragline Bucket Filling Performance," Masters Degree thesis, University of Stellenbosch.

Gear, C.W., 1971, *Numerical Initial Value Problems in Ordinary Differential Equations*, Prentice-Hall, Inc., Englewood Cliffs, New Jersey.

Gerald, C.F., and Wheatley, P.O., 1994, *Applied Numerical Analysis*, Fifth Edition, Addison-Wesley Publishing Company, Reading, Massachusetts.

Golosinski, T.S., 1994, "Performance of Dragline Hoist and Drag Ropes," *Mining Engineering*, November, pp 1285-1288.

Greenwood, D.T., 1988, *Principles of Dynamics*, Second Edition, Prentice Hall Inc, New Jersey.

Hall, G., and Watt, J.M., 1976, *Modern Numerical Methods for Ordinary Differential Equations*, Clarendon Press, Oxford.

Hassenpflug, W.C., 1993, "Matrix Tensor Notation Part I: Rectilinear Orthogonal Coordinates," *Computers and Mathematics with Applications*, Vol. 26, No. 3, pp. 55-93.

Hassenpflug, W.C., 1995, "Matrix Tensor Notation Part II: Skew and Curved Coordinates," *Computers and Mathematics with Applications*, Vol. 29, No. 11, pp. 1-103.

Huston, R.L., *Multibody Dynamics*, Butterworth-Heinemann, Boston, 1990.

Huston, R.L., and Kamman, J.W., 1982, "Validation of Finite Segment Cable Models," *Computer and Structures*, Vol. 15, No. 6, pp. 653-660.

Huston, R.L., and Passerello, C., 1979, "On Multi-Rigid-Body System Dynamics," *Computers and Structures*, Vol. 10, pp. 439-446.

Huston, R.L., Liu, Y.S. and Liu, C., 1994, "Use of Absolute Coordinates in Computational Multibody Dynamics," *Computers and Structures*, Vol. 52, No. 1, pp. 17-25.

Kang, N.K., 1993, "Nonlinear Multibody Formulation for Rotorcraft Analysis," Ph.D. thesis, Rensselaer Polytechnic Institute, Troy, New York.

Kim, S.S., and Vanderploeg, M.J., 1986, "A General and Efficient Method for Dynamics Analysis of Mechanical Systems Using Velocity Transformations," *Journal of Mechanisms, Transmissions and Automation in Design*, Vol. 108, June 1986, pp. 176-182.

Knights, P., and Shanks, D., 1992, "Bucket Rigging Influence on Dragline Productivity," *The Australian Coal Journal*, No. 36, pp. 27-34.

Krinke, D.C., and Huston, R.L., 1980, "An Analysis of Algorithms for Solving Differential Equations," *Computers and Structures*, Vol. 11, pp. 69-74.

Lumley, G., and O'Beirne, T., 1997, "Improved Dragline Productivity Through Rigging Design," ACIRL, Report to ACARP.

McPhee, J.J. and Dubey, R.N., 1991, "Dynamic Analysis and Computer Simulation of Variable-Mass Multi-Rigid-Body Systems," *International Journal for Numerical Methods in Engineering*, Vol. 32, pp. 1711-1725.

Meirovitch, L., 1970, *Methods of Analytical Dynamics*, McGraw-Hill, Inc., New York.

Moon, F.C., 1987, *Chaotic Vibrations: An Introduction for Applied Scientist and Engineers*, John Wiley and Sons, New York.

Nikravesh, P.E., and Ambrosion, J.A.C., 1991, "Systematic Construction of the Equations of Motion for Rigid-Flexible Multibody Systems Containing Open and Closed Kinematic Loops," *International Journal for Numerical Methods in Engineering*, Vol. 32, pp. 1749-1766.

Pheiffer, F., and Glocker, C.,1996, *Multibody Dynamics with Unilateral Contacts*, John Wiley and Sons, Inc., New York.

Rismantab-Sany, J., and Shabana, A.A., 1989, "On the Numerical Solution of Differential/Algebraic Equations of Motion of Deformable Mechanical Systems with Nonholonomic Constraints," *Computers and Structures*, Vol. 33, No. 4, pp. 1017–1029.

Robertson, R.E., Schawertassek, R., 1988, *Dynamics of Multibody Systems*, Springer-Verlag, Berlin.

Rowlands, J.C., 1992, "Dragline Bucket Filling," PhD thesis, University of Queensland.

Rutten, O.W.J.S., Bornebroek, H., and Rossouw, P.A., 1994, "Opencast operations at Optimum Colliery, South Africa," *Colliery Guardian*, Vol. 242, No. 3, 3 May 1994, pp. 92-110.

Schäfer, J., Dippel, S., Wolf, D.E., 1996, "Force Schemes in the Simulation of Granular Materials," *Journal de Physique I*, Vol 6, January 1996, pp. 5-20.

Shabana, A.A., 1994, *Computational Dynamics*, John Wiley and Sons, Inc., New York.

Shampine, L.F. and Gear, C.W., 1979, "A User's View of Solving Stiff Ordinary Differential Equations," *SIAM Review*, Vol. 21, No. 1, January 1979, pp. 1-17.

Shampine, L.F. and Reichelt, M.W., 1997, "The MATLAB ODE Suite," *SIAM Journal of Scientific Computing*, Vol. 18, No. 1, January 1997, pp. 1-22.

Shampine, L.F., Watts, H.A., and Davenport, S.M., 1976, "Solving Nonstiff Ordinary Differential Equations – The state of the art", *SIAM Review*, Vol. 18, No. 3, July 1976, pp. 376-411.

Shand, A. N., 1970, "The Basic Principles of Equipment Selection for Surface Mining," *Proceedings of the Symposium on the Theoretical Background to the Planning of Open Pit Mines with Special Reference to Slope Stability*, Johannesburg, South Africa.

Steinhaug, T., and Wolfbrandt, A., "An Attempt to Avoid Exact Jacobian and Nonlinear Equations in the Numerical Solution of Stiff Differential Equations," *Mathematics of Computation*, Vol. 33, No. 146, April 1979, pp. 521-534.

Thompson, J.M.T., and Stewart, H.B., 1988, *Nonlinear Dynamics and Chaos: Geometric Methods for Engineers and Scientist*, John Wiley and Sons, Chischester.

Van Leyen, H., 1991, "Development of Surface Mining Technology in the Last Decade, *Bulk Solids Handling*, Vol. 11, No. 1, March 1991, pp. 169-182.

Wehage, R.A., 1980, "Generalized Coordinate Partitioning in Dynamic Analysis of Mechanical Systems," Ph.D. thesis, University of Iowa.

Wertz, J.R., *et al.*, 1978, *Spacecraft Attitude Determination and Control*, Kluwer Academic, Dordrecht, Nederlands, 1978.

Winget, J.M., and Huston, R.L., 1976, "Cable Dynamics – A Finite Segment Approach," *Computers and Structures*, Vol. 6, pp. 475-480.

Yen, J., and Chou, C.C., 1993, "Automatic Generation and Numerical Integration of Differential-Algebraic Equations of Multibody Dynamics," *Computer Methods in Applied Mechanics and Engineering*, Vol. 104, pp. 317-331.